

Large-area imaging reveals biologically driven non-random spatial patterns of corals at a remote reef

Edwards, Clinton; Eynaud, Yoan; Williams, Gareth; Pedersen, Nicole; Zgliczynski, Brian; Gleason, Arthur; Smith, Jennifer; Sandin, Stuart

Coral Reefs

DOI:
[10.1007/s00338-017-1624-3](https://doi.org/10.1007/s00338-017-1624-3)

Published: 01/12/2017

Peer reviewed version

[Cyswllt i'r cyhoeddiad / Link to publication](#)

Dyfyniad o'r fersiwn a gyhoeddwyd / Citation for published version (APA):
Edwards, C., Eynaud, Y., Williams, G., Pedersen, N., Zgliczynski, B., Gleason, A., Smith, J., & Sandin, S. (2017). Large-area imaging reveals biologically driven non-random spatial patterns of corals at a remote reef. *Coral Reefs*, 36(4), 1291-1305. <https://doi.org/10.1007/s00338-017-1624-3>

Hawliau Cyffredinol / General rights

Copyright and moral rights for the publications made accessible in the public portal are retained by the authors and/or other copyright owners and it is a condition of accessing publications that users recognise and abide by the legal requirements associated with these rights.

- Users may download and print one copy of any publication from the public portal for the purpose of private study or research.
- You may not further distribute the material or use it for any profit-making activity or commercial gain
- You may freely distribute the URL identifying the publication in the public portal ?

Take down policy

If you believe that this document breaches copyright please contact us providing details, and we will remove access to the work immediately and investigate your claim.

Large-area imaging reveals biologically-driven non-random spatial patterns of corals at a remote reef

Clinton B. Edwards^{1†}, Yoan Eynaud^{1†}, Gareth J. Williams^{1,2}, Nicole E. Pedersen¹, Brian J. Zgliczynski¹, Arthur C.R. Gleason³, Jennifer E. Smith¹, Stuart A. Sandin¹

¹Center for Marine Biodiversity and Conservation, Scripps Institution of Oceanography, University of California, San Diego, La Jolla, CA 92093-0202, USA

²School of Ocean Sciences, Bangor University, Menai Bridge, Anglesey, LL59 5AB, UK

³ Physics Department, University of Miami, 1320 Campo Sano Ave., Coral Gables, FL 33146

*Corresponding Author: Clinton Edwards, Email: clint@ucsd.edu, Center for Marine Biodiversity and Conservation, Scripps Institution of Oceanography, University of California, San Diego, 9500 Gilman Dr., La Jolla, CA 92093-0202, USA

† Authors contributed equally to this study

Keywords

Coral reefs, community structure, landscape ecology, spatial dispersion, photomosaics, Palmyra Atoll

ABSTRACT

For sessile organisms, such as reef building corals, differences in the degree of dispersion of individuals across a landscape may result from important differences in life history strategies or may reflect patterns of habitat availability. Descriptions of spatial patterns can thus be useful not only for the identification of key biological and physical mechanisms structuring a given ecosystem, but also by providing the data necessary to generate and test ecological theory. Here, we used an *in situ* imaging technique to create large-area photomosaics of 16 plots at Palmyra Atoll, central Pacific, each covering 100 m² of benthic habitat. We mapped the location of 44,007 coral colonies and identified each to the lowest taxonomic level possible. Using metrics of spatial dispersion, we tested for departures from spatial randomness and also used targeted model fitting to explore candidate processes leading to differences in spatial patterns among taxa. Most taxa were clustered and the degree of clustering varied by taxon. A small number of taxa did not significantly depart from randomness and none revealed evidence of spatial uniformity. Importantly, taxa which readily fragment or tolerate stress through partial mortality were found to be more clustered. With little exception, clustering patterns were consistent with models of fragmentation and dispersal limitation. For some taxa, dispersion levels were related linearly to abundance, suggesting density dependence of spatial patterning. The spatial patterns of stony corals are non-random and reflect fundamental life historical characteristics of the taxa, suggesting that the reef landscape may, in many cases, have important elements of spatial predictability.

Introduction

The modern paradigm in coral reef ecology suggests that coral communities reflect a history of disturbance and subsequent decline (Bellwood et al. 2004). Despite this, some coral communities also reflect histories of remarkable survival and recovery following mortality events (Diaz-Pulido et al. 2009; Roff et al. 2014; Furby 2017). The colonial growth form, for example, allows corals to sustain the loss of individual clones while maintaining overall colony function (Jackson and Coates 1986) and in some communities, fragmentation and colony regrowth can result in persistence of extremely long-lived corals (Highsmith et al. 1980; Edmunds 2015). The potential of colonies to shrink, grow, and fragment is complemented by the fundamental importance of new colony creation through sexual reproduction that supports long-term population genetic viability. Importantly, the breadth of demographic strategies within colonial corals, including recruitment, survival, fragmentation and recovery, provide a comparable breadth of spatial distributional processes. Investigation of spatial distributions in corals thus provides insights into the likely relative contribution of demographic mechanisms governing population dynamics across taxa.

The inferences that can be gained through the study of spatial patterns at the scale of individual organisms have been of interest to geographers, naturalists and biologists for more than a century (Turner 1989). In the last 40 years, renewed interest in spatial processes and patterns by terrestrial ecologists has led to the development of a suite of analytical tools to predict and describe spatial structure in nature (Wu 2013; Velázquez et al. 2016). To address spatial ecological questions, terrestrial landscape ecologists have taken advantage of comprehensive large-area sampling, often collected in the context of long-term study sites, including Barro Colorado Island (Hubbell and Foster 1992), the Hubbard Brook Experimental forest (Bormann

and Likens 2012) and various other locations (Condit et al. 2000). This work has identified a spectrum of dispersion patterns across ecosystems (Hubbell 1979, Lieberman et al. 1985, Condit et al. 2000) linked to a variety of key structuring mechanisms (e.g., recruitment patterns, habitat preference and availability, dispersal probabilities, resource limitation; Hubbell 1979; Connell 1985; Turner 1989; Condit et al. 2000; Rietkerk and van de Koppel 2008). Importantly, such work has been used to evaluate theoretical expectations of space use and to test candidate mechanisms generating the observed patterns, including the processes predicted by the Janzen-Connell Hypothesis (Janzen 1970; Connell 1978) which has been shown to influence diversity in both tropical rainforests (Harms et al. 2000) and coral reefs (Marhaver et al. 2013).

To date, the study of spatial variability in coral communities has focused largely on site (Goreau 1959; Kenyon et al. 2010), reef/island (Newman et al. 2006; Sandin et al. 2008) or regional level (Smith et al. 2016) patterns. Percent cover data has formed the basis of this substantial body of work, with more limited efforts tracking spatial and demographic processes affecting individual colonies, such as fragmentation and partial survival (Hughes and Tanner 2000; Edmunds 2015). Importantly, such demographic insights require spatially explicit data at the level of the individual organism. Application of data individual-level demographic data has been limited in subtidal marine environments largely due to the logistical constraints of obtaining data at the appropriate scale. Despite these difficulties, a number of studies have used individual-level data to study coral demography (Hughes 1984; Hughes and Tanner 2000; Edmunds 2015), to quantify competitive interactions (Bak et al. 1982; Bradbury and Young 1983; Reichelt and Bradbury 1984), or to describe habitat structure (Bak and Engel 1979; Bradbury and Young 1981), with comparably intense field campaigns tracking spatial disease patterns across populations (Jolles et al. 2002; Zvuloni et al. 2009). Less frequently collected are species-specific descriptions of

spatial patterning of coral reef benthic organisms which rely upon extremely labor-intensive *in situ* mapping (Lewis 1970; Stimson 1974; Dana 1976; Carlon and Olson 1993; Karlson et al. 2007; Deignan and Pawlik 2015). The value of such spatially explicit distributional data is clear, but the costs in terms of subtidal labor has limited the proliferation of these approaches in the broader marine scientific community.

Advances over the past decade in digital imaging, computing and data science now enable the straightforward collection and creation of composite large-area (hundreds to thousands of square meters) highly detailed orthorectified *photomosaics* of subtidal benthic marine environments (Gracias et al. 2003; Lirman et al. 2007) (Figure 1). Like other image-based underwater survey methods, such as video-transects or photoquadrats, field-based image collections for photomosaicing are complemented by lab-based data extraction. A variety of metrics, including percent cover, species composition, and disease or bleaching incidence can be extracted from photomosaics using point counts, polygon digitization, or other methods commonly used to analyze underwater imagery. Importantly, the high detail and large spatial extent of photomosaic surveys can capture thousands of individual coral colonies identifiable to the species level, enabling the extraction of spatially explicit information of benthic communities previously only available through intense field campaigns.

This study used a large-area imaging approach and spatial analytical techniques to describe spatial patterns of coral communities at a remote Pacific Atoll. Information from digitized photomosaics was used to enumerate and map individual corals at 16 plots representing 1600 m² of benthic habitat. We assessed the dispersion patterns of adult corals and investigated whether variability in measures of spatial dispersion are indicative of taxonomic differences or functional morphology. Further, we used targeted model fitting to test whether candidate habitat and

biologically driven mechanisms might have generated the observed patterns. We also considered whether observed levels of dispersion were influenced by relative density of each group.

Methods

Study location

All work was conducted on Palmyra Atoll, a U.S Fish and Wildlife National Wildlife Refuge and part of the Pacific Remote Island Areas Marine National Monument, located approximately 1600 km south of Oahu, HI. Aside from alterations made to the lagoon (e.g., dredging and construction of causeways, docks, and runways) during the brief military occupation in the mid-20th century, Palmyra's reef ecosystems have remained largely undisturbed by local human impacts (Sandin et al. 2008). In 2013, 16 plots were established on fore reef habitats along the 10 meter isobath and positioned for maximum spatial coverage across the atoll (Figure 2).

Although photomosaics can be collected at a variety of spatial scales, for the purposes of this study we analyzed imagery from 100 m² plots. Plots of this size were chosen as raw imagery can be collected easily during a single SCUBA dive, and are manageable in the time-intensive step of ecological post-processing (see: *Ecological post-processing*, below), while also capturing data at a sufficient scale to include 1000's of coral colonies per plot (Table 1). All plots were established with two geo-referenced steel pins to facilitate repeat surveys.

Collection of mosaic imagery

Images used for the creation of photomosaics were collected using two Nikon D7000 16.2 megapixel DSLR still cameras mounted to a custom frame. The camera used to generate

processed photomosaics is equipped with a wide-angle 18 mm focal length lens to ensure high overlap among adjacent images. The second camera is equipped with a 55 mm focal length lens to capture images with ≤ 1 mm resolution. To obtain continuous coverage of the reef floor within a plot, the diver operating the camera system swims a gridded pattern approximately 1.5 m above the average depth of the plot at speeds ($5-7 \text{ m min}^{-1}$) sufficient to maintain maximum overlap between adjacent images. Images are captured every second from each still camera using the built-in intervalometers. Depending on conditions, a single mosaic can be collected in 45-60 min, and consists of approximately 2500 individual images per still camera.

Technical processing of mosaic imagery

The details of the technical processing software implemented to generate the photomosaics used in this study will not be addressed in detail here, as it has been documented in several previous publications (Gracias et al. 2003; Lirman et al. 2007). Briefly, photomosaics are created from raw imagery using image processing and numerical optimization modules that work with little user intervention. The output is an orthorectified photomosaic generated by fusing the registered images together. Measurements collected in the field between ground control points (Electronic Supplementary Material, ESM, Figure 1) are used to calibrate the composite rendering.

Ecological post-processing of mosaic imagery

Photomosaics were ecologically post-processed through a manual digitization process adapted from previous work (Lirman et al. 2007). Imagery was first uploaded to Adobe Photoshop CC and the boundaries of all corals $>9 \text{ cm}^2$ were digitized by hand using a Wacom pen-tablet (model # CTH-470). Linked high resolution imagery was used to separate adjacent colonies of the same species (Figure 1). We follow the operational definition of a colony as a contiguous patch of live tissue

(Highsmith 1982). Using the best available species lists (ESM Table 1) we designated corals to the highest taxonomic level possible. When the species could not be determined, taxa were grouped within genera based on functional morphology (ESM Table 1). To determine whether spatial patterns also varied at the functional level, corals were grouped by functional morphology. Corals were classified as branching, corymbose, encrusting, free-living, massive, plating, sub-massive or tabular using the best available sources (ESM Table 1). Taxonomic and functional morphology designations were confirmed with high resolution imagery (Figure 1). Different taxonomic groups were then represented as separate image ‘layers’ in Photoshop and exported as individual .PNG image files.

Analytical processing of mosaic imagery

Exported image files (.PNG) were processed analytically using custom algorithms designed by the authors using R 2.15.1 (R Core Team 2016). The algorithm reads RGB pixel values from the individual digitized .PNG image files to identify and enumerate individual coral colonies and calculate percent cover/surface area. Distance between ground control point markers (in cm) was measured in the field (ESM Figure 1) and compared to the distances in the photomosaics (in pixels) to establish the ratio of pixels-to-cm, scale and internally georeference and calibrate photomosaics, in turn creating a spatially explicit map of each plot. Previous evaluations of geometric accuracy in photomosaic imagery have shown maximum distance errors ranging from 10.7-13.5 cm, while evaluations of abundance, diversity and percent cover were statistically indistinguishable from standard methodologies (Lirman et al. 2007). The count based metrics used here are robust to distance errors, especially at high sample sizes. However, to evaluate potential bias in abundance estimates we performed a sensitivity analysis. Drawing from a normal probability distribution of offset values ranging from 0 to the maximum error distance, we randomly assigned

coral colonies spatial offset values and found no significant difference in abundance or aggregation metrics.

Quantitative processing of mosaic imagery

After corals were enumerated and mapped in each photomosaic (ESM Figure 2a-p), we described the spatial patterns of corals at the finest taxonomic resolution possible to determine how individual species or taxonomic groups of corals drive the observed patterns. We then quantified patterns using a functional morphology-based approach to explore how shared morphological and life history strategies might contribute to common spatial patterning.

Dispersion Patterns

One of the oldest and most frequently applied measures of spatial patterning, the variance-to-mean ratio (VMR) (Dale 1999; Dale et al. 2002) allows identification of departures from complete spatial randomness (CSR), with potential alternatives being increased uniformity (i.e., individuals are more evenly spaced than expected) or increased clustering (i.e., individuals more aggregated than expected) (sensu Hutchinson 1953, Dale 1999).

Our calculation of VMR uses a simulated quadrat sampling approach commensurate in scale to the imagery collected by most benthic monitoring and research programs. Using a bootstrapping approach, we estimate the mean and variation of VMR across each of the 16 plots for each of the taxonomic and functional morphological groups considered here. For each group, i , and each plot, j , we sampled $Q=25$ non-overlapping 1 m^2 quadrats and enumerated all colony centroids in each quadrat, n_q . We then calculated the mean ($\mu_{i,j,k}$) and VMR ($v_{i,j,k}$) of the number of colony centroids from the $N=25$ quadrats for each bootstrapped replicate, k . Summary statistics were calculated as follows:

$$v_{i,j,k} = \frac{\sigma_{i,j,k}^2}{\mu_{i,j,k}} \text{ with } \mu_{i,j,k} = \frac{1}{Q} \sum_{q=1}^Q n_{i,j,k,q} \text{ and } \sigma_{i,j,k}^2 = \frac{1}{Q} \sum_{q=1}^Q (n_{i,j,k,q} - \mu_{i,j,k})^2$$

By repeating this process B times for each plot, setting $B=1000$, we obtained a distribution of VMR values for each taxonomic and functional morphological group composing the set, $(v_{i,j,1}, \dots, v_{i,j,k}, \dots, v_{i,j,B})$. Next, we calculated the mean VMR for each replicate (k) across the j plots to obtain a distribution of means, $(\bar{v}_{i,1}, \dots, \bar{v}_{i,k}, \dots, \bar{v}_{i,B})$ for each group, expressed as:

$$\bar{v}_{i,k} = \frac{1}{M} \sum_{j=1}^M v_{i,j,k}$$

where M is the total number of plots. From this distribution we then estimate the bootstrapped-mean VMR for each group:

$$\bar{\bar{v}}_i = \frac{1}{B} \sum_{k=1}^B \bar{v}_{i,k}$$

Finally, we estimate the 95% confidence interval of this distribution, $\bar{\bar{v}}_{i,0.025}$ and $\bar{\bar{v}}_{i,0.975}$ for each group i , where $\bar{\bar{v}}_{i,\alpha}$ is the α^{th} quartile of the vector of bootstrapped mean VMRs for each i . For values of $\bar{\bar{v}}_{i,0.025} > 1$, the dispersion pattern is *clustered*, if $\bar{\bar{v}}_{i,0.025} < 1$ and $\bar{\bar{v}}_{i,0.975} > 1$, the dispersion pattern is *random* and when $\bar{\bar{v}}_{i,0.975} < 1$, the spatial distribution is *over-dispersed*.

For further explanation of the bootstrapping and estimation procedures please refer to ESM Appendix 1, *Dispersion Patterns*.

Model Comparison

To explore potential processes contributing to the observed spatial patterns, we used a goodness-of-fit approach to compare four hypothesized null models of spatial patterning for each group, as follows: (i) a homogenous Poisson process, where all points (e.g., colony centroids) are randomly and independently distributed across the landscape (e.g. CSR) and which is analogous to the VMR approach; (ii) a non-homogenous Poisson (NHP) process which models patterns created by availability of open space or habitat preferences, defined here as habitat filtering; (iii) a homogeneous clustering processes (HC) which represents biotic mechanisms such as spatially constrained dispersal and fragmentation; and (iv) a non-homogeneous clustering (NHC) process which combines both habitat filtering and biotic clustering and processes.

For each taxonomic and functional morphology group in each plot, we used a simulation procedure to compare the observed spatial patterns against each of the null models outlined above using the pair correlation function (PCF), a non-cumulative second order summary statistic (Baddeley et al. 2015). The PCF represents the expected density of colony centroids within rings of radius r centered on the centroid of the focal colony divided by the intensity of the spatial pattern. We then compared the difference between the mean values from the simulations and the observed values for each group, allowing us to test the fit of the null the hypothesis that the observed pattern is similar to the model it is being tested against. Note that the analyses were conducted only on those groups with sufficient statistical power, defined here as groups with at least 20 colonies present in at least 4 plots, i.e., 25% of our plots.

For a detailed explanation of the model comparison approach, please see ESM Appendix 1, *Model Comparison* and references therein.

Density Dependence

To identify potential density dependence in the observed levels of dispersion, we used linear regression to describe relationships between the colony density (# 100 m⁻²) and the mean VMR value of each bootstrapped sample at each plot for each group., expressed as:

$$\bar{v}_{i,j} = \frac{1}{B} \sum_{k=1}^B v_{i,j,k} .$$
 For many groups, there was a large range in colony density across plots, hence

colony density data and mean VMR values, $\bar{v}_{i,j}$, were log transformed for all groups. Regressions were conducted for both taxonomic and functional morphology analyses.

To maximize the power of the VMR and linear regression analyses, we only considered groups with at least 10 colonies present in at least 4 plots (25% of our sample). Further, plots with less than 10 colonies for a given group were dropped from the analysis as this is the minimum number of colonies required to make inferences about dispersion patterns.

Development of models and all analyses we completed using R 3.2 and the package *spatstat* was used for the model comparison section (R Core Team 2016).

Results

Abundance and Percent Cover Patterns

We identified 44,008 individual coral colonies (>9 cm²) from 33 different taxonomic groups (ESM Table 1) belonging to 8 different functional morphology groups in the 1600 m² of fore reef habitat that was surveyed (16 plots, each 100 m²) (Table 1, ESM Figure 2a-p). Abundance values ranged from a maximum of 4980 coral colonies 100 m⁻² to a minimum of 1572 colonies 100 m⁻²

with an average of 2750 ± 256 (mean \pm SE) colonies 100 m^{-2} across all 16 plots (Table 1). The number of colonies per taxonomic and functional group was variable between plots. *Porites superfusa* was the most abundant taxonomic group in 9 of the 16 plots, with an average of 696 ± 108 (mean \pm SE) colonies 100 m^{-2} . The next most abundant group, the genus *Fungia*, was nearly half as abundant, 383 ± 131 (mean \pm SE) colonies 100 m^{-2} . However, *Fungia* also displayed the highest variability, with abundance values ranging from 22 to 1752 colonies 100 m^{-2} , and had the highest single plot abundance. The third most abundant group, the genus *Pocillopora*, demonstrated much less variability across plots with abundance values ranging from 166 to 565 colonies 100 m^{-2} with an average of 330 ± 26 (mean \pm SE) colonies 100 m^{-2} . At the other end of the spectrum, 9 of 33 observed taxonomic groups were represented by less than 100 colonies across all 16 plots (Table 1).

Coral cover ranged from 12.0% (Table 2) to 31.3%, with an average of $22.7\% \pm 1.3$ (mean \pm SE). As with numerical abundance, percent cover values for the various taxonomic and functional groups were variable between plots. Massive corals from the genus *Porites* had the highest percent cover in 8 of 16 plots, with an average cover of $3.8\% \pm 0.5$ (mean \pm SE) across the 16 plots. The group with the second highest mean percent cover values, *Pocillopora* $3.3\% \pm 0.3$ (mean \pm SE), was also the third most numerically abundant group. The group with the third highest mean percent cover values, encrusting *Montipora*, demonstrated the greatest variability across plots with percent cover values ranging from 0.7% to 8.0%, and was also the group with the highest single plot percent cover value (Table 2).

Dispersion Patterns

Of the 32 taxonomic groups that were observed in the 16 plots, 23 groups had sufficient sample sizes to investigate dispersion patterns, while all 8 functional morphologies had sufficient sample

sizes for the analysis. Overall, we found the dispersion patterns of adult hard corals to be highly clustered at both the taxonomic and functional morphology levels (Figure 3a,b, respectively), with little or no evidence for randomness or uniformity, respectively.

The results of the taxonomic analysis show that the degree of dispersion was variable within and among groups, however there was a strong tendency for clustering. Of the 23 coral groups considered, we found evidence (i.e., $\bar{v}_{i,0.025} > 1$) of spatial clustering in 21 of them (Figure 3b).

Corals of the genus *Fungia* displayed the greatest median VMR as well as the greatest variability across the 16 plots. Other groups with high levels of clustering, (branching *Acropora*, *Favia stelligera* and *Turbinaria reniformis*) also showed similar levels of variability. *Porites superfusa* on the other hand, displayed the second highest median VMR, but with much lower variability than other highly clustered groups. Although still significantly clustered, the lowest levels of VMR were found in sub-massive corals of the genus *Favites* and the fast-growing table *Acropora* and corymbose *Pocillopora* groups. We found non-significant departures from randomness (i.e., $\bar{v}_{i,0.025} < 1$ and $\bar{v}_{i,0.975} > 1$) in only 2 groups of corals, massive colonies of the genus *Platygyra* and the species *Pocillopora eydouxi* (Figure 3b).

At the functional morphology level there was also variability in the level of spatial dispersion among groups. Despite this variability, all 8 of the observed functional morphology groups showed clustered dispersion patterns (Figure 3a). Overall, the free-living functional morphology showed the greatest degree of clustering. These results strongly reflect the pattern of the numerically dominant genus *Fungia*, as other free-living groups were rare. Other morphologies exhibiting high levels of clustering were the encrusting and branching morphologies. As the branching functional morphology was comprised of only a single taxonomic group (*Acropora*), caution should be used in generalizing the results.

Model Comparison

Results of the null model comparisons show striking patterns of non-randomness, with the CSR model (model (i)) being rejected for all observed taxonomic and functional morphology groups (Figure 4). These results are consistent with the VMR analysis, with two notable differences – *Pocillopora eydouxi*, did not significantly depart from randomness in the VMR analysis despite rejection from model (i) and *Platygyra sp.* was not included in model comparisons due to limited sample sizes. The goodness-of-fit for NHP model (model (ii)) was rejected for all but 4 of the 21 taxonomic groups examined – branching and corymbose *Acropora* species, *Hydnophora exesa*, and *Pocillopora eydouxi*. The only functional morphology group comparison for which the NHP model could not be rejected was the branching corals group (Figure 4). Given that this group is made up exclusively of branching *Acropora* species, these results are unsurprising.

We found little support to reject the clustering models (either model (iii) or (iv)) as an underlying cause leading to the observed distributions for the taxa examined (Figure 4). Both clustering models were rejected for only two coral species, *Hydnophora microconos* and *Favia stelligera*. We did not find evidence to reject HC model (model (iii)) for *Favites sp.* (sub-massive) *Pocillopora eydouxi* or *Stylophora pistillata*, however, there was support to reject NHC model (model (iv)) for these three groups. On the other hand, while we rejected the HC model for *Montipora sp.* (encrusting), *Pocillopora sp.* and *Porites superfusa* we did not find support to reject the NHC model for these groups (Figure 4).

In the functional group comparisons, both clustering models (models (iii) and (iv)) were rejected only for sub-massive corals. However, as this group is numerically dominated by *Favia stelligera* (46% of colonies), generalization of these results should be done with caution.

Similarly, we rejected the HC model (model (iii)) for encrusting corals, however this group is

heavily dominated by *Porites superfusa* (65% of colonies) for which the HC model was also rejected.

Density Dependence

While only a limited number of groups showed significant relationships, there was an overall tendency for a positive density dependence in VMR values (Table 3). Of the 23 groups with adequate sample sizes, only *Fungia*, encrusting *Montipora*, *Pocillopora*, and *Porites superfusa* showed significant positive relationships in the linear regressions between colony abundance and the VMR (Table 3). At the functional group level while the free living, corymbose and encrusting groups showed significant density dependence, these results reflect the influence of the hyper abundant *Fungia*, *Pocillopora* and *Porites superfusa* groups.

We did not observe any negative relationships between colony abundance and the VMR. Across all groups the lack of density dependence does not appear to be related to truncated abundance ranges, as many coral groups showing non-significant relationships between abundance and VMR exhibited large differences in colony abundance across the 16 plots (Tables 1 & 3).

Discussion

Using methodological and quantitative approaches developed to address spatial ecological questions in terrestrial systems, we described the spatial distribution of scleractinian corals across 16 plots at the remote coral reef, Palmyra Atoll. In our exploration of spatial dispersion, we found an overall tendency for individual corals within taxonomic groups to be clustered across the landscape but the degree to which they aggregated varied by taxon. Similarly, at the functional morphology level all groups displayed clustered distributions, indicating spatial co-

occurrence within functional morphological groups. Next, using a goodness-of-fit model fitting procedure, we explored whether the observed spatial distributions matched simulated distributions based on hypothesized mechanisms of habitat filtering and biotic clustering process such as dispersal limitation and fragmentation. We did not find support for the random spatial (i.e., CSR) model in any of the observed functional or taxonomic groups. Overwhelmingly, our observed distributions were most consistent with models of biotic clustering (models (iii) and (iv)), with little support for habitat filtering (model (ii)) alone as a putative mechanism for the observed patterns. While levels of clustering were variable within taxonomic and functional groups, we found an overall tendency for the degree of clustering to be positively related to abundance.

Previous work investigating the spatial patterns of corals have found similar, but more equivocal, results (Lewis 1970; Carlon and Olson 1993; Karlson et al. 2007). Similarly, authors working in terrestrial plant communities have found support for a range of dispersion patterns including overdispersion, random and clustered spatial patterns at a variety of intensities (Anderson et al. 1982; Lieberman et al. 1985; Taylor and Woiwod 1982; Condit et al. 2000). This work and the spatial patterns revealed here, along with our targeted model fitting, suggest that multiple mechanisms are likely working in concert to produce emergent spatial patterns in communities of reef-building corals.

Spatial Dispersion Patterns: Abiotic factors

A variety of abiotic factors can affect the distribution and spatial patterns of corals across the landscape. For example, the degree of fragmentation in branching corals has been shown to be positively related to the intensity and frequency of disturbance. Previous work has shown significant and complicated patterns of variation in the physical environment around Palmyra

(Williams et al. 2013) that may partially explain the observed high degree of variability in dispersion patterns for some of our coral groups. For instance, while corals from the free-living genus *Fungia* and branching species from the genus *Acropora* were consistently clustered, they also displayed the highest variability in dispersion values. The observed clustering in *Fungia* may also be the result of large scale physical factors such as the direction of predominant wave energy and currents which may transport these free-living corals to particular locations on the reef. The clustering of adults across the landscape may also be the result of larval preferences for, and availability of, suitable habitat (e.g. habitat filtering). If the distribution of suitable habitat is heterogeneous, or uniform, recruitment patterns should also be expected to be clustered (Figure 4).

Spatial Dispersion Patterns: Biotic Factors

Important differences in growth strategies may in part explain the observed levels of clustering. Many invertebrates, particularly colonial organisms such as corals, have the unique ability to grow almost without limit and sustain fluctuations in body size in response to stress (Jackson and Coates 1986; Sebens 1987). The ability of colonial organisms to tolerate stress via loss of individual clones without suffering total colony mortality allows corals to grow indeterminately (Jackson and Hughes 1985; Hughes et al. 1992) which is reflected in many corals through high rates of partial survival and regrowth following fragmentation (Hughes and Jackson 1980; Highsmith 1982; Furby 2017). The formation of multiple daughter colonies from a single parent colony occurs through fission, fragmentation and budding (Highsmith 1982; Hughes and Connell 1987). Differences in these processes may produce fundamentally different spatial patterns as new colonies formed from fragmentation arise via skeletal fracturing and have some limited dispersal capabilities. On the other hand, colonies formed via fission of tissues alone will

necessarily be unable to disperse and may later fuse to reform a single colony following regrowth, resulting in necessarily more restricted spatial distributions.

Encrusting corals, particularly *Pavona varians*, *Porites superfusa*, and those from the genera *Favites* and *Montipora* showed strong clustering with low levels of variation. These corals, and *Porites superfusa* in particular, have been found to have remarkable regenerative capabilities, with colony fragments readily surviving post fusion and new growth readily originating from these surviving fragments (Furby et al. 2017). Visual inspection of imagery also suggests that individuals from these genera are frequently highly fragmented via fission, likely producing the observed clustering. It is perhaps not surprising that there is repeated support for models of clustering (models (iii) and (iv)) given that fission and regrowth of large coral colonies typically is constrained to areas of the colony's original footprint, namely the limestone previously accreted by the colony which is inherently spatially constrained.

We also found moderate clustering in sub-massive corals from the genus *Pavona*, and the species *Favia stelligera*. The distribution of sub-massive *Pavona* fit null clustering models, comparable to the patterns observed for the encrusting corals. In contrast, none of the null models consistently fit data for *Favia stelligera*, suggesting that the distribution of this species is structured by a complex collection of mechanisms. Interestingly, while both of these species readily fragment via fission, fusion is more common in *Favia stelligera*.

The distributions of both branching and corymbose *Acropora* species were clustered, with the pattern consistent with models of both habitat filtering and biotic clustering mechanisms (Figure 4). Many *Acropora* species are known to have impressive regenerative capabilities and readily produce viable fragments (Highsmith 1982; Wallace 1985; Riegl and Piller 2001; Diaz-Pulido et al. 2009). Branching *Acropora* displayed strong clustering but the level of clustering was much

more variable, perhaps reflecting plot specific differences in habitat patterning. Levels of clustering in corymbose *Acropora* were lower and showed much less variability. Interestingly, as the distributions of both groups fit all of the null spatial models tested here (except for the CSR model), the effects of habitat filtering may be equally important drivers of clustering patterns in addition to fragmentation. Another readily fragmenting group *Lobophyllia*, which lives colonially, yet without tissue connections between adjacent polyps (Brickner et al. 2006), also showed high levels of clustering with moderate levels of variability and was supported by both clustering null models. The spatial patterns reported here represent the first records for the majority of the central Pacific coral groups examined, and are consistent with the hypothesis that fragmentation plays a key role in determining the spatial patterns of coral communities.

When examining results at the functional morphology level, we see that the increase in clustering largely follows a gradient from determinate to indeterminate growth, e.g. from taxa known to grow more or less linearly to bounded maximum sizes to taxa with fluid growth capabilities and without clear size limits, respectively (Highsmith 1982; Hughes 1987; Sebens 1987).

Determinate growth in corals is frequently associated with corymbose and plating taxa with small maximum size, high growth rates and fecundity and low stress tolerance (Szmant 1986).

The lower levels of clustering found in these groups (e.g., *Pocillopora*, *Montipora*) is likely the result of the relatively lower survivorship and regenerative capabilities of both adult colonies and fragments. This is contrasted with indeterminate growth in corals which is generally associated with slower growing, stress tolerant sub-massive and massive forms (Highsmith 1982; Szmant 1986; Hughes et al. 1992). Fragmentation and regrowth are known functions of indeterminate growth and have been positively linked to increasing size and inherent morphological

characteristics in massive and other corals (Hughes and Connell 1987; DeVantier and Endean 1989; Pisapia and Pratchett 2014).

At the other extreme, free-living corals exhibit unique growth traits that are associated with indeterminism, likely contributing to their high degree of clustering. Remnant tissue in injured adult colonies, and even seemingly dead ones, has the potential to produce large numbers of buds (Kramarsky-Winter and Loya 1996). Despite potential limited facultative dispersal and habitat selectivity, this movement is highly spatially constrained due to habitat effects. The results of the model fitting procedure strongly support the conclusion that budding processes have produced the highly-clustered patterns observed here (Figure 4). The final group considered, encrusting corals, showed the second highest median level of clustering. While generally considered less stress tolerant, some encrusting corals have a remarkable ability to undergo fission and regrowth (Furby et al. 2017), likely leading to the high level of clustering found here. As some coral taxa have a mix of these traits, the patterns observed here are likely the result of interactions among traits.

Dispersal in sessile organisms such as plants, algae, fungi, bryozoans and reef building corals occurs via a limited number of processes. Though some free-living corals have limited facultative dispersal (Chadwick 1988), as a whole, adult coral dispersal will only occur following dislodgement or fragmentation as a result of biophysical forcing (e.g., storms, waves).

Consequently, the dispersive pattern of early life stages (e.g., larvae) will drive recruitment patterns and ultimately the spatial structure of sessile communities (Hubbell 1979; Condit et al. 2000). The various reproductive strategies of corals can largely be categorized as spawners and brooders. Brooding corals produce fully competent larvae that can settle and metamorphose in the immediate vicinity of parent colonies following release of planula (Carlson and Olson 1993).

On the other hand, gametes released via broadcast spawning are released into the water column where they are subject to mixing and must be transported to settlement locations. Variation in these reproductive modes may therefore be expected to lead to differences in the spatial distributions of adult corals. Previous evidence has shown large scale spatial structuring of coral communities related to reproductive mode (Stimson 1978), however spatial variation at the inter-colony scale due to differences in reproductive mode has seldom been explicitly considered (*though see* Carlon and Olson 1993). Here we found the brooding coral, *Stylophora pistillata*, to exhibit moderate levels of clustering, while broadcasting corals, *Pocillopora* in particular, showed levels of dispersion much closer to randomness, perhaps resulting from the differences outlined above.

Spatial Dispersion Patterns: Density dependence

Several of the functional and taxonomic groups showed significant positive relationships between plot specific VMR and colony abundance (Table 3). These relationships may arise from fundamental processes of reproduction, aggregation and repulsion. Taylor's law (Taylor 1961; Taylor and Woiwod 1982) asserts that log-log relationships between variance and mean abundance can be expected to have positive slopes of 1-2, which is equivalent to slopes between 0 and 1 when relating VMR and mean, (ESM Appendix 2). We found significant relationships with slopes ranging from $\beta=0.225$ to $\beta=0.650$ for taxonomic groups, and $\beta=0.411$ to $\beta=0.761$ for functional morphology groups (Table 3). Moreover, while only a handful of the taxonomic and functional groups had significant VMR-abundance relationships, the general trend of positive relationships across all taxonomic groups occurred significantly more frequently than expected by chance alone (21 of 23 groups, binomial test, $p < 0.01$), following the predictions of Taylor's law. This relationship, however, was not significant at the functional morphology level

(3 of 8 groups, binomial test, $p=0.07$), suggesting species specific traits may be an important determinant of density dependent processes.

The value of these slopes should correlate positively with fragmentation/reproduction rates, however, inferring relationships between ecological processes should be treated with caution (Anderson et al. 1982; Routledge and Swartz 1991). Interestingly, however, species with high reproduction/fragmentation rates living in heterogeneous environments can exhibit steeper slopes than species with a lower reproduction/fragmentation rate in more homogeneous environments (Anderson et al. 1982). Here the strongest relationship was found for *Fungia* (Table 3), perhaps reflecting the comparatively high reproductive rates and constraints imposed on the free-living morphology in more topographically and hydrodynamically heterogeneous areas. For other groups, the strength of relationship between the level of clustering and abundance appears to arise from the capacity of a given group to use fragmentation as a survival/reproductive mechanism, as seen in the significant positive relationships found for encrusting *Porites superfusa* and *Montipora*. We also saw a significant relationship for *Pocillopora*, which dominates juvenile coral ($<9\text{cm}^2$) abundances across the majority of our plots. This suggests that interactions between habitat heterogeneity and reproduction may be contributing strongly to the results found here.

ACKNOWLEDGEMENTS

This work was made possible through funding provided by the Gordon and Betty Moore Foundation, grant #3420, and the UC San Diego Frontiers of Innovations Scholarship Program. We are grateful to Gideon Butler and Sho Kodera who contributed to image digitization. This is

Palmyra Atoll Research Consortium contribution ## PARC-0125. Thank you to The Nature Conservancy and the Palmyra Atoll Research Consortium for logistical support, and the United States Fish Wildlife Service for special use permit # 12533-13025 and access to the refuge.

References

- Anderson RM, Gordon DM, Crawley MJ, Hassell MP (1982) Variability in the abundance of animal and plant species. *Nature* 296:245-248
- Baddeley A, Rubak E, Turner R (2015) *Spatial point patterns: methodology and applications with R*. Chapman & Hall/CRC Press
- Bak R, Engel M (1979) Distribution, abundance and survival of juvenile hermatypic corals (Scleractinia) and the importance of life history strategies in the parent coral community. *Mar Biol* 54:341-352
- Bak R, Termaat R, Dekker R (1982) Complexity of coral interactions: influence of time, location of interaction and epifauna. *Mar Biol* 69:215-222
- Bellwood DR, Hughes TP, Folke C, Nystrom M (2004) Confronting the coral reef crisis. *Nature* 429:827-833
- Bormann FH, Likens G (2012) *Pattern and process in a forested ecosystem: disturbance, development and the steady state based on the Hubbard Brook ecosystem study*. Springer-Verlag, New York
- Bradbury R, Young P (1983) Coral interactions and community structure: an analysis of spatial pattern. *Mar Ecol Prog Ser* 11:265-271
- Bradbury RR, Young PP (1981) The effects of major forcing function, wave energy, on a coral reef ecosystem. *Mar Ecol Prog Ser* 5:229-241

- Brickner I, Oren U, Frank U, Loya Y (2006) Energy integration between the solitary polyps of the clonal coral *Lobophyllia corymbosa*. *Journal of Experimental Biology* 209:1690-1695
- Carlson DB, Olson RR (1993) Larval dispersal distance as an explanation for adult spatial pattern in two Caribbean reef corals. *J Exp Mar Biol Ecol* 173:247-263
- Chadwick NE (1988) Competition and locomotion in a free-living fungiid coral. *J Exp Mar Biol Ecol* 123:189-200
- Condit R, Ashton PS, Baker P, Bunyavejchewin S, Gunatilleke S, Gunatilleke N, Hubbell SP, Foster RB, Itoh A, LaFrankie JV, Lee HS, Losos E, Manokaran N, Sukumar R, Yamakura T (2000) Spatial patterns in the distribution of tropical tree species. *Science* 288:1414-1418
- Connell JH (1978) Diversity in tropical rain forests and coral reefs. *Science* 199:1302-1310
- Connell JH (1985) The consequences of variation in initial settlement vs. post-settlement mortality in rocky intertidal communities. *J Exp Mar Biol Ecol* 93:11-45
- Dale MRT (1999) Spatial pattern analysis in plant ecology. *Ecology* 88:366-370
- Dale MRT, Dixon P, Fortin M-J, Legendre P, Myers DE, Rosenberg MS (2002) Conceptual and mathematical relationships among methods for spatial analysis. *Ecography* 25:558-577
- Dana TF (1976) Reef-coral dispersion patterns and environmental variables on a Caribbean coral reef. *Bull Mar Sci* 26:1-13
- Deignan L, Pawlik J (2015) Perilous proximity: Does the Janzen–Connell hypothesis explain the distribution of giant barrel sponges on a Florida coral reef? *Coral Reefs* 34:561-567
- DeVantier L, Endean R (1989) Observations of colony fission following ledge formation in massive reef corals of the genus *Porites*. *Mar Ecol Prog Ser* 58:191-195

- Diaz-Pulido G, McCook LaJ, Dove S, Berkelmans R, Roff G, Kline DI, Weeks S, Evans RD, Williamson DH, Hoegh-Guldberg O (2009) Doom and boom on a resilient reef: climate change, algal overgrowth and coral recovery. PLoS ONE 4:e5239
- Edmunds PJ (2015) A quarter-century demographic analysis of the Caribbean coral, *Orbicella annularis*, and projections of population size over the next century. Limnol and Oceanogr 60:840-855
- Furby, KA, Smith JE, Sandin SA (2017) *Porites superfusa* mortality and recovery from a bleaching event at Palmyra Atoll, USA. PeerJ 1:e3204
- Goreau TF (1959) The Ecology of Jamaican coral reefs I. Species composition and zonation. Ecology 40:67-90
- Gracias NR, Van Der Zwaan S, Bernardino A, Santos-Victor J (2003) Mosaic-based navigation for autonomous underwater vehicles. IEEE Journal of Oceanic Engineering 28:609-624
- Harms KE, Wright SJ, Calderon O, Hernandez A, Herre EA (2000) Pervasive density-dependent recruitment enhances seedling diversity in a tropical forest. Nature 404:493-495
- Highsmith RC (1982) Reproduction by fragmentation in corals. Mar Ecol Prog Ser 7:207-226
- Highsmith RC, Riggs AC, D'Antonio CM (1980) Survival of hurricane-generated coral fragments and a disturbance model of reef calcification/growth rates. Oecologia 46:322-329
- Hubbell SP (1979) Tree dispersion, abundance, and diversity in a tropical dry forest. Science 203:1299-1309
- Hubbell SP, Foster RB (1992) Short-term dynamics of a neotropical forest: why ecological research matters to tropical conservation and management. Oikos 63:48-61
- Hughes R (1987) The functional ecology of clonal animals. Funct Ecol 1:63-69

- Hughes T, Jackson J (1980) Do corals lie about their age? Some demographic consequences of partial mortality, fission, and fusion. *Science* 209:713-715
- Hughes TP (1984) Population dynamics based on individual size rather than age: a general model with a reef coral example. *Am Nat* 123:778-795
- Hughes TP, Connell JH (1987) Population dynamics based on size or age? A reef-coral analysis. *Am Nat* 129:818-829
- Hughes TP, Tanner JE (2000) Recruitment failure, life histories, and long-term decline of Caribbean corals. *Ecology* 81:2250-2263
- Hughes TP, Ayre D, Connell JH (1992) The evolutionary ecology of corals. *Trends Ecol Evol* 7:292-295
- Hutchinson GE (1953) The concept of pattern in ecology. *Proc Acad Nat Sci Philadelphia* 105:1-12
- Jackson JBC, Hughes TP (1985) Adaptive strategies of coral-reef invertebrates: coral-reef environments that are regularly disturbed by storms and by predation often favor the very organisms most susceptible to damage by these processes. *Am Sci* 73:265-274
- Jackson JBC, Coates AG (1986) Life cycles and evolution of clonal (modular) animals. *Proc R Soc Lond B Biol Sci* 313:7-22
- Janzen DH (1970) Herbivores and the number of tree species in tropical forests. *The Am Nat* 104:501-528
- Jolles AE, Sullivan P, Alker AP, Harvell CD (2002) Disease transmission of *aspergillosis* in sea fans: inferring process from spatial pattern. *Ecology* 83:2373-2378
- Karlson RH, Cornell HV, Hughes TP (2007) Aggregation influences coral species richness at multiple spatial scales. *Ecology* 88:170-177

- Kenyon JC, Maragos JE, Cooper S (2010) Characterization of coral communities at Rose Atoll, American Samoa. *Atoll Res Bull* 586:1-28
- Kramarsky-Winter E, Loya Y (1996) Regeneration versus budding in fungiid corals: a trade-off. *Mar Ecol Prog Ser* 134:179-185
- Lewis JB (1970) Spatial distribution and pattern of some Atlantic reef corals. *Nature* 227:1158-1159
- Lieberman D, Lieberman M, Peralta R, Hartshorn GS (1985) Mortality patterns and stand turnover rates in a wet tropical forest in Costa Rica. *Journal of Ecology* 73:915-924
- Lirman D, Gracias NR, Gintert BE, Gleason ACR, Reid RP, Negahdaripour S, Kramer P (2007) Development and application of a video-mosaic survey technology to document the status of coral reef communities. *Environ Monit Assess* 125:59-73
- Marhaver K, Vermeij M, Rohwer F, Sandin S (2013) Janzen-Connell effects in a broadcast-spawning Caribbean coral: distance-dependent survival of larvae and settlers. *Ecology* 94:146-160
- Newman MJH, Paredes GA, Sala E, Jackson JBC (2006) Structure of Caribbean coral reef communities across a large gradient of fish biomass. *Ecol Lett* 9:1216-1227
- Pisapia C, Pratchett MS (2014) Spatial variation in background mortality among dominant coral taxa on Australia's Great Barrier Reef. *PLoS ONE* 9:e100969
- R Core Team (2016) R: A language and environment for statistical computing. R Foundation for Statistical Computing, Vienna, Austria URL <https://www.R-project.org/>
- Reichelt R, Bradbury R (1984) Spatial patterns in coral reef benthos: multiscale analysis of sites from three oceans. *Mar Ecol Prog Ser* 17:251-257

- Riegl B, Piller W (2001) Cryptic tissues inside *Acropora* frameworks (Indonesia): a mechanism to enhance tissue survival in hard times while also increasing framework density. *Coral Reefs* 20:67-68
- Rietkerk M, van de Koppel J (2008) Regular pattern formation in real ecosystems. *Trends Ecol Evol* 23:169-175
- Roff G, Bejarano S, Bozec Y-M, Nugues M, Steneck RS, Mumby PJ (2014) Porites and the Phoenix effect: unprecedented recovery after a mass coral bleaching event at Rangiroa Atoll, French Polynesia. *Mar Biol* 161:1385-1393
- Routledge RD, Swartz TB (1991) Taylor's power law re-examined. *Oikos* 60:107-112
- Sandin SA, Smith JE, DeMartini EE, Dinsdale EA, Donner SD, Friedlander AM, Konotchick T, Malay M, Maragos JE, Obura D (2008) Baselines and degradation of coral reefs in the northern Line Islands. *PLoS ONE* 3:e1548
- Sebens KP (1987) The ecology of indeterminate growth in animals. *Annu Rev Ecol Evol Syst* 18:371-407
- Smith JE, Brainard R, Carter A, Grillo S, Edwards C, Harris J, Lewis L, Obura D, Rohwer F, Sala E, Vroom PS, Sandin S (2016) Re-evaluating the health of coral reef communities: baselines and evidence for human impacts across the central Pacific. *Proc R Soc Lond B Biol Sci* 283:20151985
- Stimson J (1974) An analysis of the pattern of dispersion of the hermatypic coral *Pocillopora meandrina var. nobilis* Verril. *Ecology*:445-449
- Stimson JS (1978) Mode and timing of reproduction in some common hermatypic corals of Hawaii and Enewetak. *Mar Biol* 48:173-184
- Szmant AM (1986) Reproductive ecology of Caribbean reef corals. *Coral Reefs* 5:43-53

- Taylor L (1961) Aggregation, variance and the mean. *Nature* 189:732-735
- Taylor L, Woiwod I (1982) Comparative synoptic dynamics. I. Relationships between inter-and intra-specific spatial and temporal variance/mean population parameters. *Journal Anim Ecol* 51:879-906
- Turner MG (1989) Landscape ecology: the effect of pattern on process. *Annu Rev Ecol Evol Syst* 20:171-197
- Velázquez E, Martínez I, Getzin S, Moloney KA, Wiegand T (2016) An evaluation of the state of spatial point pattern analysis in ecology. *Ecography* 39:1042-1055
- Wallace CC (1985) Reproduction, recruitment and fragmentation in nine sympatric species of the coral genus *Acropora*. *Mar Biol* 88:217-233
- Williams GJ, Smith JE, Conklin EJ, Gove JM, Sala E, Sandin SA (2013) Benthic communities at two remote Pacific coral reefs: effects of reef habitat, depth, and wave energy gradients on spatial patterns. *PeerJ* 1:e81
- Wu J (2013) Landscape sustainability science: ecosystem services and human well-being in changing landscapes. *Landsc Ecol* 28:999-1023
- Zvuloni A, Artzy-Randrup Y, Stone L, Kramarsky-Winter E, Barkan R, Loya Y (2009) Spatio-Temporal Transmission Patterns of Black-Band Disease in a Coral Community. *PLOS ONE* 4:e4993

Electronic Supplemental Figure Captions

ESM Figure 1. Visual schematic of plot setup. Permanent markers (P1, P2) were installed in 2013. Four additional temporary markers (C1-C4) are placed at the corners of the plots during mosaic surveys. A series of measurements (dotted black lines) are then taken between all plot markers to be used for mosaic calibration. Weighted floats are placed approx. 1m outside the plot margins to aid in navigation during imaging (R1-R4). Distances were measured underwater using standard underwater meter-tapes.

ESM Figure 2. Raw and digitized photomosaics of all 16 plots (a-p). Colors in the digitized images correspond to the 32 observed taxa (q). Photomosaics were cropped to the 100 m² area used in the analysis. All images were hand digitized in Adobe Photoshop CC. Raw and digitized images have been compressed for viewing.

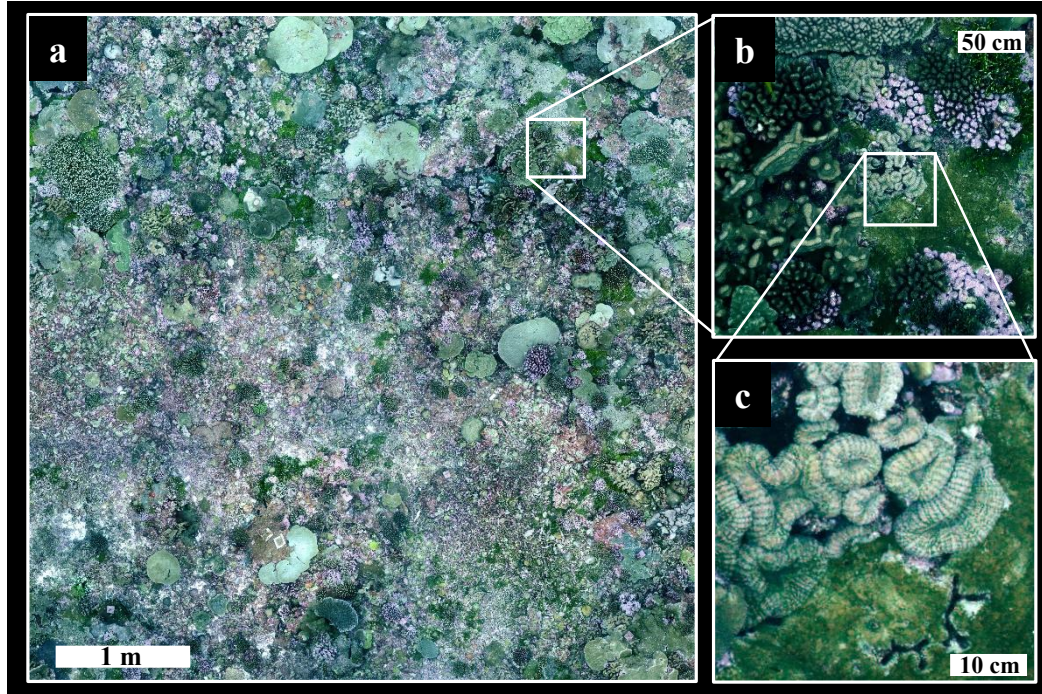


Figure 1. 25 m² subsection of raw landscape mosaic imagery (a) and embedded high-resolution composite images (b) taken with the 55 mm focal length camera enable which highly detailed analysis of individual processes at multiple scales (c). The image in panel B is roughly commensurate in scale with imagery collected for standard point count percent cover based analyses. Please see ESM Figure 2 for full size imagery.

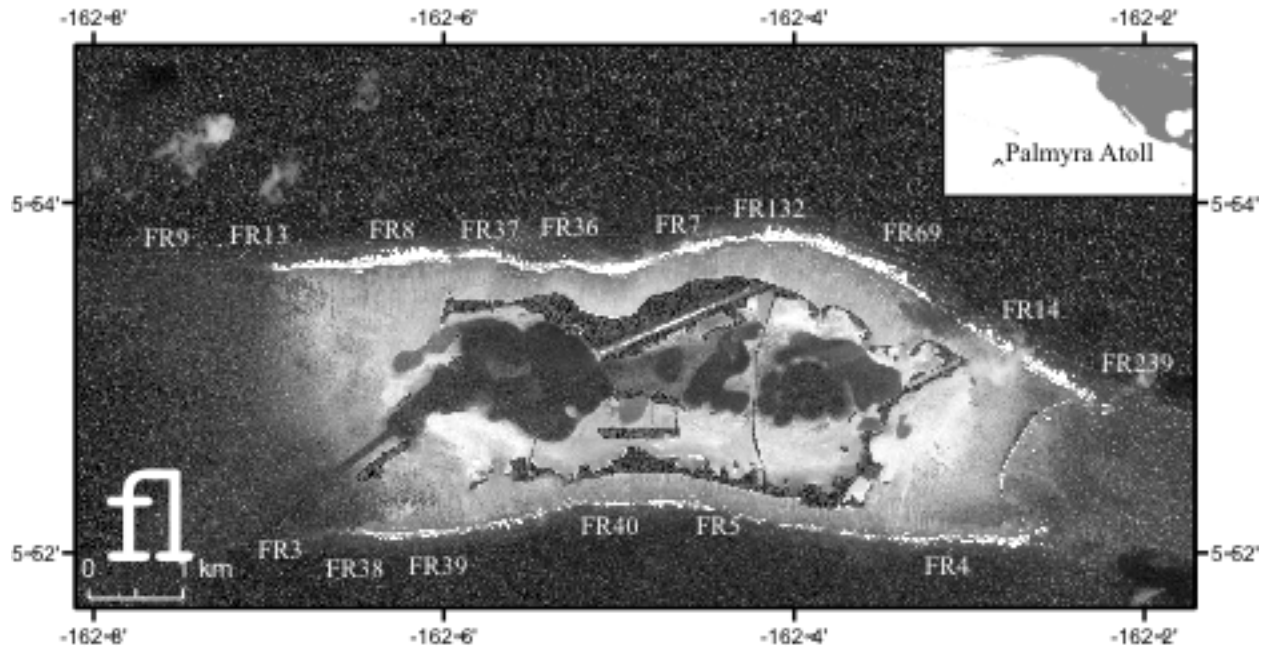


Figure 2. Satellite imagery showing the location of study plots at Palmyra Atoll, a remote uninhabited atoll and National Wildlife Refuge located approx. 1600 km south of the Hawaiian Islands (Inset). Replicate plots were established at 16 locations on fore reef habitats along the 10 m isobath, and positioned to obtain maximum spatial coverage across the atoll.

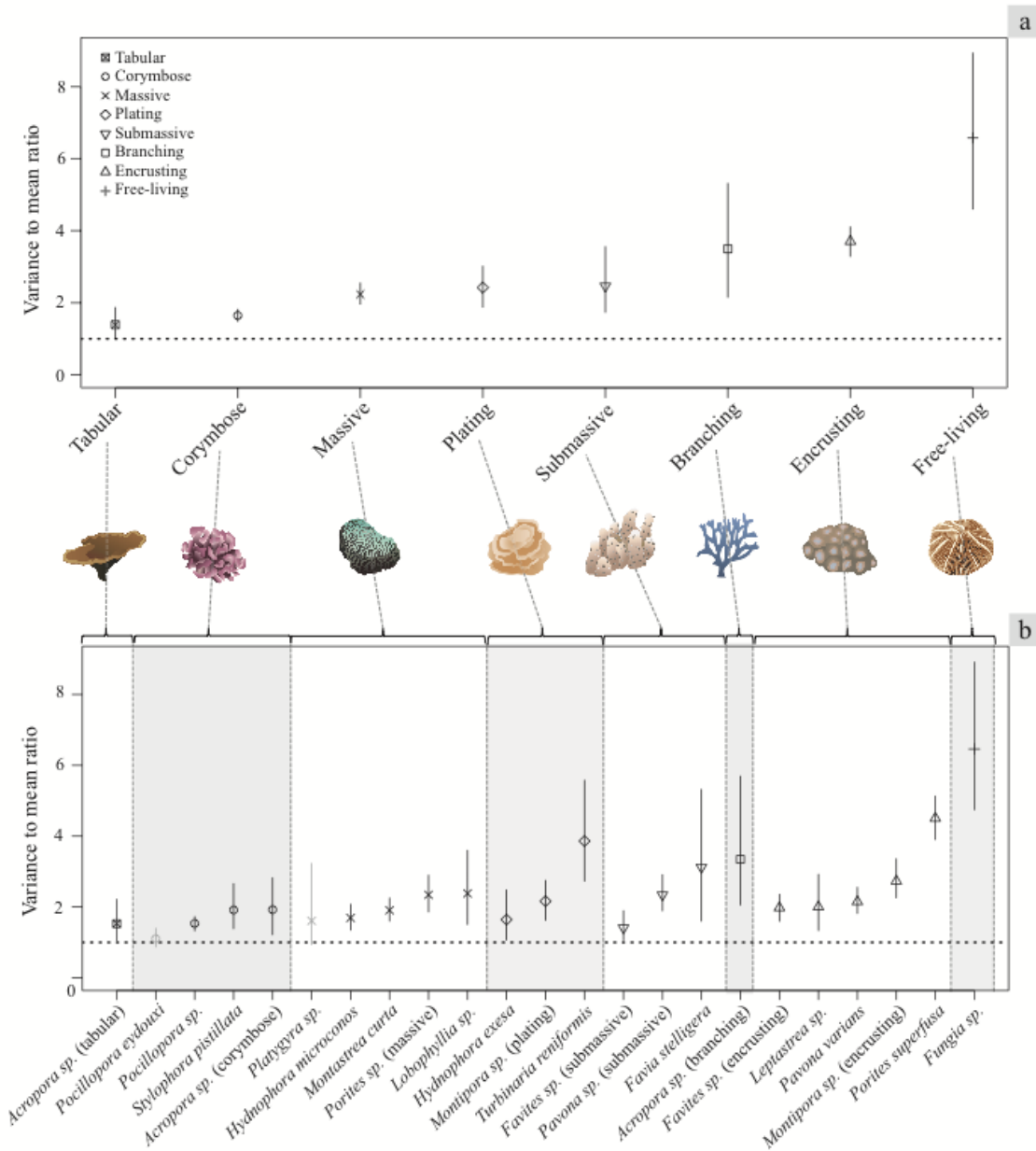


Figure 3. Dispersion results by species and functional group. Using a bootstrapping procedure, we calculated the variance to mean ratio (VMR) of numerical abundance of all coral taxa and functional groups in each of our 16 plots. Boxplots of simulated VMR distributions are presented with medians (symbols) and 95% quantile ranges (lines) displayed. The dotted line indicates a VMR=1 (e.g., randomness) and 95% quantile ranges not overlapping 1 are indicative of significant departures from randomness. Box colors and symbols in b correspond to the functional morphology groups in a.

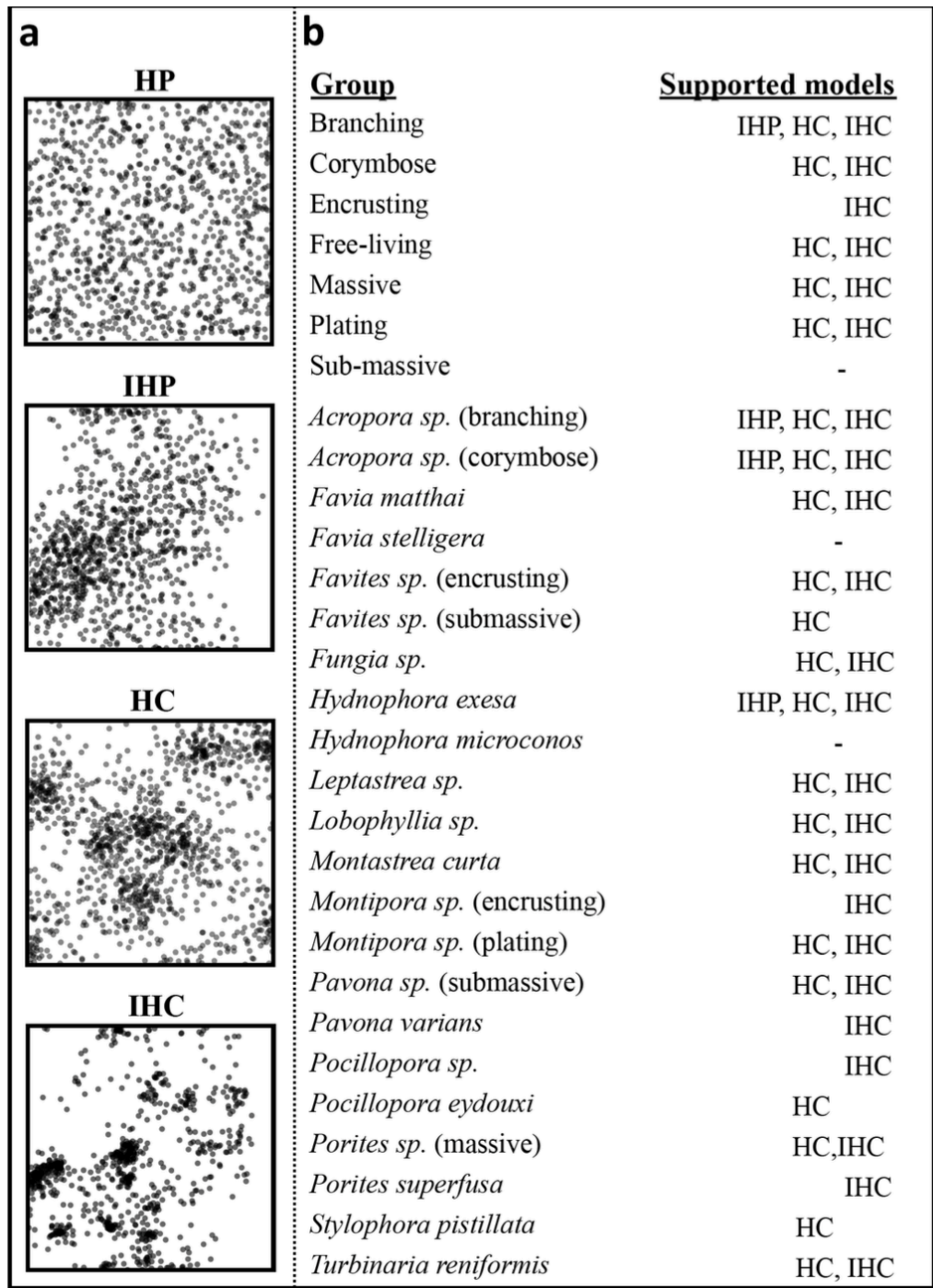


Figure 4. Icons (a) representing stereotypical examples of each of the simulated distributions: (i) Homogeneous Poisson (HP), (ii) non-homogeneous Poisson (NHP), (iii) homogeneous clustering process (HC) and (iv) non-homogeneous clustering process (NHC). Model comparison results (b) by functional and taxonomic group for each of the simulated null models of spatial dispersion showing only the models fitting each group. As the HP model did not fit any of the groups here it has been omitted, and those groups with no model fits are designated with a ‘-’.

Table 1. The total number of coral colonies observed in the 32 taxonomic and 8 functional morphology groups at each of the 16 sites (sites are arranged counterclockwise starting with FR3, Figure 1). In total, we digitized over 44k coral colonies in a combined area of 1600m². Abundance values exclude juveniles (< 9cm²) and colonies which could not be reliably identified (n=3000). Overall, 49% of all observed coral colonies were identified to the species-level. However, when excluding corals from the genus *Fungia* and *Pocillopora* this fraction increased to 67%.

Group	Morphology	FR3	FR38	FR39	FR40	FR5	FR4	FR239	FR14	FR69	FR132	FR7	FR36	FR8	FR37	FR13	FR9	Total
<i>Acropora sp.</i>	Branching	0	161	18	73	0	0	0	49	0	3	0	71	0	11	0	0	386
<i>Acropora sp.</i>	Corymbose	0	35	5	36	1	11	66	2	5	10	1	11	1	9	2	25	220
<i>Pocillopora eydouxi</i>	-	4	4	11	13	0	0	12	8	10	27	0	11	0	29	29	0	158
<i>Pocillopora sp.</i>	-	244	457	277	290	450	406	365	166	239	359	236	309	219	372	329	565	5283
<i>Sylophora pistillata</i>	-	82	0	0	6	72	167	0	0	0	0	4	0	0	0	122	390	843
Group Total	-	330	496	293	345	523	584	443	176	254	396	241	331	220	410	482	980	6504
<i>Favites sp.</i>	Encrusting	18	48	49	59	9	21	23	51	35	118	47	85	59	125	119	0	866
<i>Leptastrea sp.</i>	-	0	32	17	71	0	0	7	8	6	86	9	13	27	25	10	6	317
<i>Leptoseria sp.</i>	-	0	1	0	5	0	4	2	5	3	3	0	4	0	3	5	0	35
<i>Montipora sp.</i>	-	100	328	114	260	58	103	175	43	46	251	64	397	217	284	124	132	2696
<i>Pasmocora sp.</i>	-	1	1	0	1	0	0	5	7	4	5	0	1	0	0	13	0	38
<i>Pavona varians</i>	-	125	132	102	230	42	141	91	93	64	354	103	156	110	102	174	77	2096
<i>Porites superfusca</i>	-	529	849	557	406	320	1760	878	501	959	443	198	347	270	939	1449	726	11131
Group Total	-	773	1391	836	1032	429	2029	1181	708	1117	1260	421	1003	683	1478	1894	941	17179
<i>Fungia sp.</i>	Free-living	1032	68	83	57	360	1112	119	68	61	37	176	22	47	200	1752	940	6134
<i>Halomitra pileus</i>	-	0	0	0	0	0	0	0	0	0	0	0	0	0	0	12	0	12
<i>Herpolitha sp.</i>	-	0	0	0	1	0	0	0	2	0	1	0	0	0	0	0	0	4
<i>Sandalolitha dentata</i>	-	0	1	1	0	0	0	0	0	0	0	0	0	0	0	0	0	2
Group Total	-	1032	69	84	58	360	1112	119	70	61	38	176	22	47	200	1764	940	6152
<i>Favia matthai</i>	Massive	0	1	2	2	0	239	1	1	0	7	0	0	0	0	1	95	349
<i>Hydnophora microconos</i>	-	16	151	131	178	0	12	68	39	42	217	57	184	125	182	14	21	1437
<i>Lobophyllia sp.</i>	-	16	0	0	0	257	7	0	0	0	0	4	0	0	2	68	54	408
<i>Montastrea curta</i>	-	12	85	55	128	0	20	132	128	113	452	51	332	169	345	35	19	2076
<i>Platygyra sp.</i>	-	9	20	11	17	2	2	6	24	7	53	14	40	26	13	7	11	262
<i>Porites rus</i>	-	0	0	0	1	0	0	0	0	0	0	0	0	0	7	0	0	8
<i>Porites sp.</i>	-	88	217	164	203	66	92	200	162	85	336	242	182	148	280	95	70	2630
Group Total	-	141	474	363	529	325	372	407	354	247	1065	368	738	468	829	220	270	7170
<i>Hydnophora exesa</i>	Plating	26	4	1	0	3	12	13	1	0	0	0	0	3	14	12	23	112
<i>Montipora sp.</i>	-	10	65	64	59	1	16	2	9	1	11	0	88	49	70	67	3	515
<i>Turbinaria reniformis</i>	-	0	42	167	0	0	0	99	1	137	175	127	90	126	85	124	317	1490
Group Total	-	36	111	232	59	4	28	114	11	138	186	127	178	178	169	203	343	2117
<i>Astreopora myriophthalma</i>	Sub-Massive	0	0	1	0	0	0	0	0	0	0	3	1	0	0	0	0	5
<i>Favia stelligera</i>	-	118	310	244	188	20	0	160	134	84	174	127	187	0	198	89	0	2033
<i>Favites sp.</i>	-	7	21	32	53	0	20	12	7	2	18	38	14	31	20	5	0	280
<i>Gardineroseris planulata</i>	-	0	0	0	0	1	0	0	0	0	0	0	0	0	0	0	0	1
<i>Goniastrea pectinata</i>	-	0	0	0	5	0	0	1	0	1	2	0	0	0	0	0	0	9
<i>Pavona sp.</i>	-	79	58	65	101	13	474	88	99	62	179	71	104	247	103	307	17	2067
Group Total	-	204	389	342	347	33	494	261	240	149	373	239	306	278	321	401	17	4394
<i>Acropora sp.</i>	Tabular	12	10	1	15	0	2	2	0	4	13	0	7	12	10	16	1	105
Total	ALL	2528	3101	2172	2458	1674	4621	2527	1608	1970	3334	1572	2656	1886	3428	4980	3492	44008

ESM Table 2: Cover (in % of benthic substrate 100m⁻²) observed at the highest taxonomic resolution and functional morphology levels for each of the 16 sites. Percent cover values were variable (16.2-31.2%), and across all sites average coral cover was 22.71% ± 0.2 (mean ± SE). These values do not differ from previous estimates of coral cover at this location determined via quadrat sampling methods (Smith 2016).

Group	Morphology	FR3	FR38	FR39	FR40	FR5	FR4	FR239	FR14	FR69	FR132	FR7	FR36	FR8	FR37	FR13	FR9	Average
<i>Acropora sp.</i> (branching)	Branching	0.0	3.8	0.4	0.6	0.0	0.0	0.0	1.2	0.0	0.1	0.0	0.9	0.0	0.3	0.0	0.0	0.4
<i>Acropora sp.</i> (corymbose)	Corymbose	0.0	0.2	0.0	0.6	0.0	0.1	0.9	0.2	0.1	0.0	0.0	0.1	0.1	0.1	0.0	0.1	0.2
<i>Pocillopora eydouxi</i>	-	0.1	0.0	0.1	0.3	0.0	0.0	0.3	0.3	0.3	0.7	0.0	0.3	0.0	1.0	0.4	0.0	0.2
<i>Pocillopora sp.</i>	-	3.4	3.5	3.1	2.7	4.4	3.1	3.5	1.9	2.9	3.2	3.0	2.5	2.8	3.7	2.6	6.7	3.3
<i>Stylophora pistillata</i>	-	1.1	0.0	0.0	0.0	0.9	1.8	0.0	0.0	0.0	0.0	0.0	0.0	0.0	0.0	1.1	5.9	0.7
Group Total	-	4.5	3.7	3.3	3.7	5.3	5.0	4.7	2.3	3.2	3.9	3.0	2.9	2.9	4.7	4.0	12.8	4.4
<i>Favites sp.</i> (encrusting)	Encrusting	0.4	0.2	0.3	0.3	0.1	0.2	0.1	0.3	0.2	1.0	0.3	0.5	0.3	0.8	0.6	0.0	0.3
<i>Leptastrea sp.</i>	-	0.0	0.2	0.1	0.5	0.0	0.0	0.0	0.1	0.0	0.6	0.1	0.1	0.2	0.1	0.1	0.1	0.1
<i>Leptoseris sp.</i>	-	0.0	0.0	0.0	0.0	0.0	0.0	0.0	0.0	0.0	0.0	0.0	0.0	0.0	0.0	0.0	0.0	0.0
<i>Montipora sp.</i> (encrusting)	-	3.7	5.1	1.9	3.2	1.1	1.6	2.9	0.8	1.0	2.9	0.7	8.0	3.2	3.8	2.1	3.5	2.8
<i>Pasmocora sp.</i>	-	0.0	0.0	0.0	0.0	0.0	0.0	0.1	0.1	0.0	0.0	0.0	0.0	0.0	0.1	0.0	0.0	0.0
<i>Pavona varians</i>	-	0.6	0.6	0.6	1.3	0.3	0.6	0.7	0.6	0.3	1.8	0.5	0.5	0.5	0.4	0.4	0.3	0.6
<i>Porites superfusa</i>	-	1.2	1.4	1.1	0.6	1.0	3.1	3.2	1.5	2.4	0.6	0.4	0.7	0.4	1.9	2.7	2.4	1.5
Group Total	-	5.9	7.4	4.0	5.9	2.4	5.4	6.9	3.4	3.9	6.9	2.0	9.6	4.6	7.0	5.8	6.3	5.5
<i>Fungia sp.</i>	Free-living	3.9	0.2	0.3	0.2	0.8	1.9	0.4	0.2	0.1	0.1	0.6	0.0	0.1	0.2	2.6	3.4	0.9
<i>Halomitra pileus</i>	-	0.0	0.0	0.0	0.0	0.0	0.0	0.0	0.0	0.0	0.0	0.0	0.0	0.0	0.0	0.2	0.0	0.0
<i>Herpolitha sp.</i>	-	0.0	0.0	0.0	0.0	0.0	0.0	0.0	0.0	0.0	0.0	0.0	0.0	0.0	0.0	0.0	0.0	0.0
<i>Sandalolitha dentata</i>	-	0.0	0.1	0.0	0.0	0.0	0.0	0.0	0.0	0.0	0.0	0.0	0.0	0.0	0.0	0.0	0.0	0.0
Group Total	-	3.9	0.2	0.3	0.2	0.8	1.9	0.4	0.2	0.1	0.1	0.6	0.0	0.1	0.2	2.8	3.4	1.0
<i>Favia matthai</i>	Massive	0.0	0.1	0.3	0.1	0.0	4.2	0.0	0.0	0.0	0.2	0.0	0.0	0.0	0.0	0.1	1.8	0.4
<i>Hydnophora microconos</i>	-	0.6	0.8	1.5	1.5	0.0	0.3	0.5	0.4	0.5	1.9	1.0	2.0	2.0	2.0	0.3	0.4	1.0
<i>Lobophyllia sp.</i>	-	1.3	0.0	0.0	0.0	5.6	0.1	0.0	0.0	0.0	0.0	0.0	0.0	0.0	0.6	0.7	0.5	0.5
<i>Montastrea curta</i>	-	0.1	0.3	0.4	0.7	0.0	0.1	0.5	0.7	0.6	1.7	0.3	1.2	1.0	1.7	0.2	0.1	0.6
<i>Platygyra sp.</i>	-	0.2	0.1	0.1	0.2	0.2	0.1	0.1	0.2	0.1	0.6	0.2	0.4	0.3	0.2	0.1	0.5	0.2
<i>Porites rus</i>	-	0.0	0.0	0.0	0.0	0.0	0.0	0.0	0.0	0.0	0.0	0.0	0.0	0.0	0.2	0.0	0.0	0.0
<i>Porites sp.</i> (massive)	-	7.8	5.0	5.5	3.3	1.2	3.2	3.9	5.0	1.4	4.4	6.5	3.0	3.2	4.3	2.2	1.4	3.8
Group Total	-	10.0	6.3	7.8	5.8	6.9	8.0	5.0	6.3	2.6	8.8	7.9	6.6	6.4	8.3	3.4	4.9	6.6
<i>Hydnophora exesa</i>	Plating	1.4	0.1	0.0	0.0	0.0	0.2	0.3	0.0	0.0	0.0	0.0	0.0	0.2	0.3	0.3	0.6	0.2
<i>Montipora sp.</i> (plating)	-	0.7	1.6	2.5	1.5	0.0	0.7	0.0	0.3	0.0	0.4	0.0	2.7	1.6	2.7	1.8	0.3	1.0
<i>Turbinaria reniformis</i>	-	0.0	0.4	1.9	0.0	0.0	0.0	0.5	0.0	0.9	0.9	1.4	0.6	2.1	0.3	0.3	2.2	0.7
Group Total	-	2.1	2.1	4.4	1.5	0.0	0.9	0.9	0.3	0.9	1.2	1.4	3.4	3.8	3.3	2.4	3.1	2.0
<i>Astreopora myriophthalma</i>	Sub-Massive	0.0	0.0	0.3	0.0	0.0	0.0	0.0	0.0	0.0	0.0	0.3	0.0	0.0	0.0	0.0	0.0	0.0
<i>Favia stelligera</i>	-	3.2	1.3	2.9	1.5	0.6	0.0	0.9	1.1	0.8	1.9	1.4	1.6	0.0	2.1	1.2	0.0	1.3
<i>Favites sp.</i> (submassive)	-	0.5	0.1	0.5	1.0	0.0	0.4	0.3	0.2	0.0	0.2	0.7	0.1	0.5	0.3	0.1	0.0	0.3
<i>Gardineroseris planulata</i>	-	0.0	0.0	0.0	0.0	0.0	0.0	0.0	0.0	0.0	0.0	0.0	0.0	0.0	0.0	0.0	0.0	0.0
<i>Goniastrea pectinata</i>	-	0.0	0.0	0.0	0.0	0.0	0.0	0.0	0.0	0.0	0.0	0.0	0.0	0.0	0.0	0.0	0.0	0.0
<i>Pavona sp.</i> (submassive)	-	0.8	0.6	0.5	0.9	0.1	2.3	0.6	0.9	0.4	1.4	0.7	0.9	2.4	0.6	1.4	0.2	0.9
Group Total	-	4.6	2.1	4.2	3.4	0.7	2.7	1.9	2.1	1.2	3.5	3.1	2.7	3.0	3.0	2.7	0.2	2.6
<i>Acropora sp.</i> (tabular)	Tabular	0.3	2.0	0.1	1.0	0.0	0.0	0.1	0.0	0.2	0.2	0.0	0.3	0.6	0.2	1.3	0.0	0.4
Total		31.3	27.5	24.4	22.0	16.2	23.7	19.8	15.8	12.0	24.8	17.9	26.5	21.3	27.0	22.4	30.7	22.7

Table 2. Results of linear regressions of VMR and colony abundance. Significant relationships (*) were observed for 4 of the 23 taxonomic and 3 of the 8 functional groups. The number of plots with sufficient abundance (>10 colonies per plot) is also shown.

Group	Morphology	Beta	R2	p-value	n
Acropora	Branching	0.12	0.07	0.61	6.00
Acropora	Corymbose	0.36	0.41	0.12	7.00
*Pocillopora	-	0.32	0.29	0.03	16.00
Pocillopora eydouxi	-	0.01	0.00	0.93	8.00
Stylophora pistillata	-	0.26	0.16	0.51	5.00
*Group Total	-	0.41	0.67	0.00	16.00
Favites	Encrusting	0.17	0.19	0.12	14.00
Leptastrea	-	0.15	0.20	0.27	8.00
*Montipora	-	0.23	0.31	0.03	16.00
Pavona varians	-	0.09	0.03	0.51	16.00
*Porites superfusa	-	0.49	0.68	0.00	16.00
*Group Total	-	0.76	0.48	0.00	16.00
*Fungia	Free-living	0.65	0.74	0.00	16.00
Favia stelligera	Massive	0.24	0.06	0.43	13.00
Hydnophora microconos	-	0.05	0.06	0.38	15.00
Lobophyllia	-	0.32	0.67	0.18	4.00
Montastrea curta	-	0.08	0.10	0.27	15.00
Platygyra	-	0.01	0.00	0.97	10.00
Porites	-	-0.20	0.12	0.18	16.00
Group Total	-	-0.04	0.01	0.73	16.00
Hydnophora exesa	Plating	-0.01	0.00	0.99	6.00
*Montipora	-	0.36	0.88	0.00	10.00
Turbinaria reniformis	-	0.12	0.02	0.71	11.00
Group Total	-	0.15	0.10	0.26	15.00
Favites	Submassive	0.16	0.10	0.37	10.00
Pavona	-	0.16	0.17	0.11	16.00
Group Total	-	0.18	0.02	0.58	16.00
Acropora	Tabular	0.78	0.30	0.20	7.00

1 **Investigating colony level spatial patterns of coral assemblages using** 2 **large-area imaging at a remote coral reef: Appendix 1**

3 Clinton B. Edwards^{1,†}, Yoan Eynaud^{1,†}, Gareth J. Williams^{1,2}, Nicole E. Pedersen¹, Brian J.
4 Zgliczynski¹, Arthur C.R. Gleason³, Jennifer E. Smith¹, Stuart A. Sandin¹

5 ¹Center for Marine Biodiversity and Conservation, Scripps Institution of Oceanography,
6 University of California, San Diego, La Jolla, CA 92093-0202, USA

7 ²School of Ocean Sciences, Bangor University, Menai Bridge, Anglesey, LL59 5AB, UK

8 ³Physics Department, University of Miami, 1320 Campo Sano Ave., Coral Gables, FL 33146

9

10 *Corresponding Author: Clinton Edwards, Email: clint@ucsd.edu, Center for Marine

11 Biodiversity and Conservation, Scripps Institution of Oceanography,

12 University of California, San Diego, 9500 Gilman Dr., La Jolla, CA

13 92093-0202, USA

14 † Authors contributed equally to this study

15

16 **Quantitative processing of mosaic imagery**

17 A variety of methods exist to explore spatial patterns which have various strengths and weaknesses

18 depending on the system and question of interest (Dale et al. 2002; Wiegand 2004). The analysis of

19 the spatial pattern observed for each group of coral was divided in two major steps. First, we

20 determined if a given spatial pattern exhibited a *dispersion pattern* significantly different from

21 complete randomness using the variance:mean ratio (VMR), a well-established method which is

22 robust to the questions of interest here, to determine if the dispersion pattern of a given group

23 exhibited a significant departure from complete spatial randomness (CSR). Then, we used null

24 spatial point pattern model comparisons to enlighten the likely drivers of the observed dispersion
25 patterns. In the following, we describe the quantitative approaches used to address those
26 complementary steps; the summarized results are presented and discussed in the main text. Note that
27 our approach as well as the presentation of the data builds from established approaches (Baddeley et
28 al. 2015, Velázquez et al. 2016). All analysis were done using R 2.15.1 with an emphasis on the
29 package *spatstat* for the *model comparison* section (R Core 2016).

30

31 ***Dispersion Patterns***

32 In the first part of this study, we test if spatial distributions of scleractinian corals are random or
33 if they follow a non-random pattern across our 16 plots. We investigated spatial patterns at two
34 biological scales – finest recognizable taxonomic level and functional group level. After corals were
35 enumerated and mapped in the individual mosaics we described the spatial patterns of corals at the
36 highest taxonomic resolution possible in order to determine how individual species (or genera) of
37 corals fit observed patterns, hereafter referred to as the ‘taxonomic analysis’. Based upon the most
38 resolved taxonomic data, we lumped taxa into functional groups based upon colony morphology and
39 repeated the spatial analyses, hereafter referred to as the ‘functional group analysis’.

40 A variety of methods exist to explore spatial patterns which have strengths and weaknesses
41 depending on the system and question of interest (Dale et al. 2002, Wiegand and A. Moloney 2004,
42 Velázquez et al. 2016). In order to describe first order spatial patterns of adult coral assemblages at
43 Palmyra we used the variance-to-mean ratio (VMR), a well-established method which is robust to
44 addressing core questions of deviations from spatial randomness in many contexts. One of the oldest
45 and most popular measures of spatial patterning (Dale et al. 2002), the VMR allows identification of

46 departure from complete spatial randomness (CSR) as uniformity (i.e., individuals are more evenly
 47 spaced than expected) or increased clustering (i.e., individuals more aggregated than expected).
 48 We used a bootstrapping approach to estimate the mean and variation of VMR across each of the
 49 16 plots for each of the taxonomic and functional morphological groups considered here. For
 50 each group, i , and for each plot, j , we sampled $Q=25$ non-overlapping 1 m^2 quadrats and
 51 enumerated all colonies with centroids in each quadrat, n_q . We then calculated the mean ($\mu_{i,j,k}$)
 52 and VMR ($v_{i,j,k}$) of the number of colony centroids from the $N=25$ quadrats for each
 53 bootstrapped replicate, k . Summary statistics were calculated using common relationships, as
 54 follows:

$$55 \quad v_{i,j,k} = \frac{\sigma_{i,j,k}^2}{\mu_{i,j,k}} \quad \text{with} \quad \mu_{i,j,k} = \frac{1}{Q} \sum_{q=1}^Q n_{i,j,k,q} \quad \text{and} \quad \sigma_{i,j,k}^2 = \frac{1}{Q} \sum_{q=1}^Q (n_{i,j,k,q} - \mu_{i,j,k})^2$$

56 By repeating this process B times for each plot, setting $B=1000$, we obtained a distribution of
 57 VMR values for each taxonomic and functional morphological group composing the set,
 58 $(v_{i,j,1}, \dots, v_{i,j,k}, \dots, v_{i,j,B})$. Next, we calculated the mean VMR for each replicate (k) across the j
 59 plots to obtain a distribution of means, $(\bar{v}_{i,1}, \dots, \bar{v}_{i,k}, \dots, \bar{v}_{i,B})$ for each group, expressed as:

$$60 \quad \bar{v}_{i,k} = \frac{1}{M} \sum_{j=1}^M v_{i,j,k}$$

61 with M the total number of plots. From this distribution we then estimate the bootstrapped-mean
 62 VMR for each group:

$$63 \quad \bar{\bar{v}}_i = \frac{1}{B} \sum_{k=1}^B \bar{v}_{i,k}$$

64 Finally, we estimate the 95% confidence interval of this distribution, $\bar{\bar{v}}_{i,0.025}$ and $\bar{\bar{v}}_{i,0.975}$ for each
 65 group, where $\bar{\bar{v}}_{i,\alpha}$ is the α^{th} quartile of the vector of bootstrapped mean VMRs for group i . For

66 values of $\bar{v}_{i,0.025} > 1$, the dispersion pattern is categorized as *clustered*. If $\bar{v}_{i,0.025} < 1$ and $\bar{v}_{i,0.975} > 1$
67, the dispersion pattern is *random* and when $\bar{v}_{i,0.975} < 1$, the spatial distribution is categorized as
68 *over-dispersed*.

69 To maximize the power of the VMR analyses, we only consider groups with at least 10 colonies
70 present in at least 4 plots (25% of our sample). Further, plots with less than 10 colonies for a given
71 group were dropped from the analysis as this is the minimum number of colonies required to make
72 inferences about dispersion patterns.

73 ***Model Comparison***

74 With the previous effort, we identified divergence from a random spatial distribution and
75 compare levels of aggregation at a given scale. However, this analysis does not allow for
76 consideration of putative processes creating the observed pattern. To tackle this question, we
77 compared the spatial pattern of each species across plots with a series of simulated spatial pattern
78 models following a given set of hypotheses. Namely we identified two types of processes driving
79 a given species spatial pattern: (i) a habitat filtering effect, in which spatial characteristics of the
80 landscape influence the probability of group-specific presence, and (ii) biotic processes, in which
81 endogenous mechanisms such as partial mortality, fragmentation and dispersal limitation
82 contribute to the creation of spatial patterns.

83 We used a replicated model-testing approach to test the effect of each process, alone and in
84 combination. Thus we compared the spatial pattern of a given species across plots with four
85 different models: (1) a set of null communities originating from a Poisson process, or Complete
86 Spatial Randomness (see Fig A1-A&F); (2) a set of null communities originating from
87 heterogeneous Poisson which are structured by habitat filtering ([i] only; see Fig A1-B&G); (3) a
88 set of null communities assembled with homogeneous cluster processes (Cauchy cluster process)

89 which are structured by putatively biotic processes only ([ii] only; see Fig A1-C&H); (4) a set of
 90 null communities assembled with heterogeneous cluster processes (Cauchy cluster process)
 91 which are simultaneously structured by habitat filtering and biotic processes (both [i] and [ii]; see
 92 Fig A1-D&I). For more information about the model comparison approach as well as model
 93 descriptions, see Baddeley et al. (2015) and Velasquez et al. (2016), and references therein.
 94 In summary, we conducted a repeated goodness-of-fit approach for each model across the
 95 collection of data. For each species at each plot, we generated a set of 200 null spatial
 96 distributions for each of the tested models. To compare the observed spatial pattern with the
 97 simulated null spatial distribution's pattern, we used a non-cumulative second order summary
 98 statistic, i.e., the pair correlation function, presented as $g(r)$. This function represents the
 99 expected density of colony centroids within rings of radius r centered on the centroid of the focal
 100 colony, divided by the intensity of the spatial pattern. This summary statistic allows for an
 101 intuitive assessment of scale dependent effects.

102 For each tested model, each group, i , and for each plot, j , we estimated $g_{i,j,k}(r)$ for
 103 $r \in [20cm, 250cm]$. While the lower bound is determined by the average size of coral colonies,
 104 the upper bound is determined by the size of photomosaics (10m*10m). By simulating $B=200$
 105 null communities for each plot, we obtained a distribution of $g(r)$ values for each taxonomic
 106 group: $(g_{i,j,1}(r), \dots, g_{i,j,k}(r), \dots, g_{i,j,B}(r))$. Next, we calculated the mean of $g_{i,j,k}$ for each replicate, k ,
 107 across the j plots to obtain a distribution of means, $(\bar{g}_{i,1}(r), \dots, \bar{g}_{i,k}(r), \dots, \bar{g}_{i,B}(r))$ for each group,
 108 expressed as:

$$109 \quad \bar{g}_{i,k}(r) = \frac{1}{M} \sum_{j=1}^M g_{i,j,k}(r)$$

110 Additionally, we defined the mean across simulations noted as:

111
$$\hat{g}_i(r) = \frac{1}{B} \sum_{k=1}^B \bar{g}_{i,k}(r)$$

112 Similarly, we calculated for each group, i , the mean across the j plots for the observed spatial
 113 pattern, expressed as:

114
$$\hat{g}_i^*(r) = \frac{1}{M} \sum_{j=1}^M g_{i,j}^*(r)$$

115 To compare the model against the observed pattern, we evaluated the distance between the mean
 116 across simulations for each group $\hat{g}_i(r)$ and each replicate k , $\bar{g}_{i,k}(r)$:

117
$$d_k = \int_{20}^{250} (\hat{g}_i(r) - \bar{g}_{i,k}(r))^2 dr$$

118 Similarly, we obtained the distance between the mean across simulations for each group $\hat{g}_i(r)$
 119 and the observed pattern $\hat{g}_i^*(r)$ presented as:

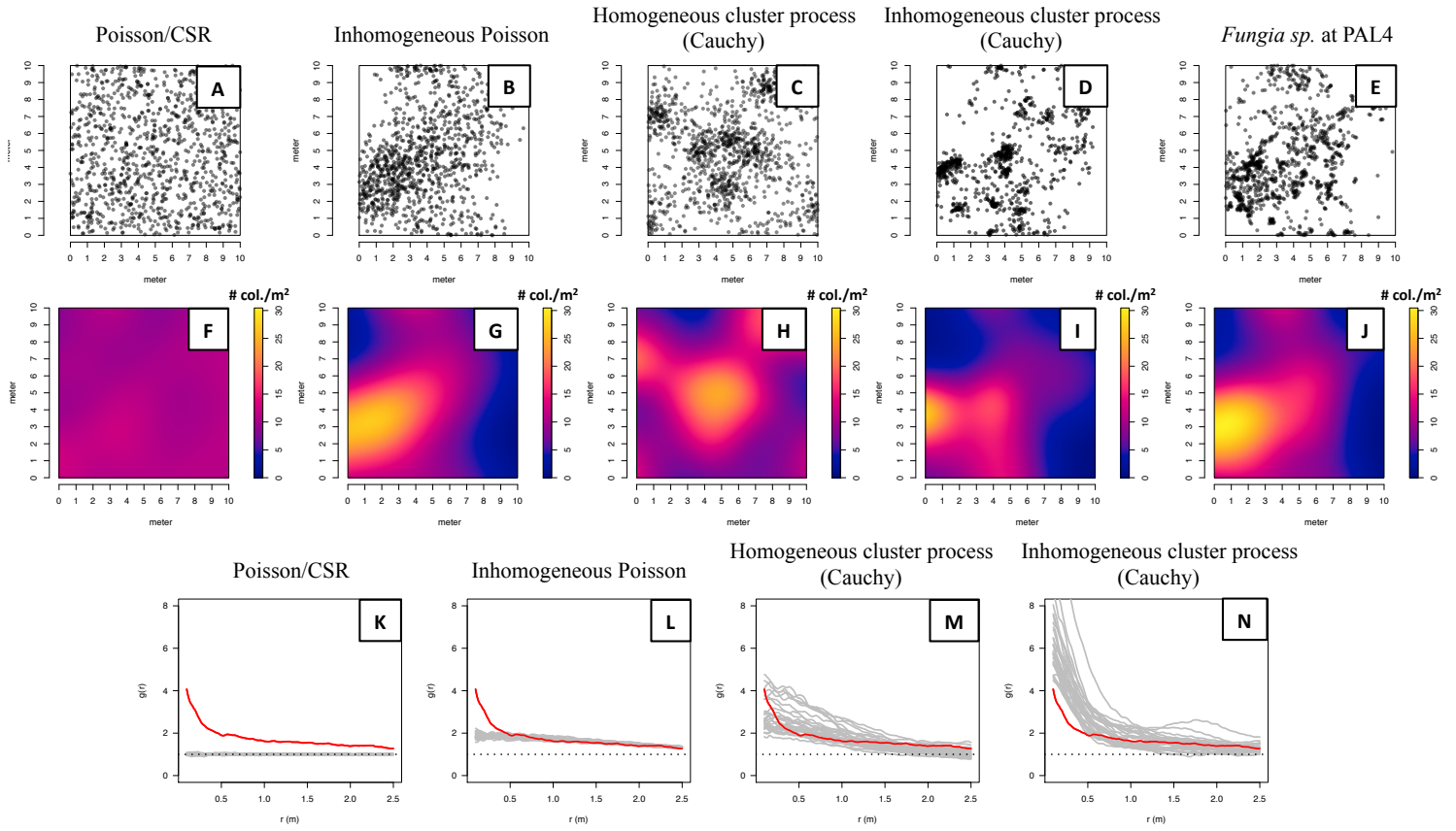
120
$$d^* = \int_{20}^{250} (\hat{g}_i^*(r) - \hat{g}_i(r))^2 dr$$

121 By comparing d^* to the distribution of distances, $(d_1, \dots, d_k, \dots, d_B)$, we estimated a probability
 122 allowing use to test the fit of the null hypothesis:

123 H_0 : *the observed pattern is similar to the one exhibited by the simulated communities.*

124 See table A1&A2 for the values obtained respectively at the morphological and taxonomical
 125 scale.

126 Comparable to the analysis of density dependent effects, we limited our analyses to groups with
 127 at least 20 colonies present in at least 4 plots (25% of our sample).



129 **Figure A1:** Example of a stereotypical set of null point process models using the data
 130 from *Fungia sp.* as a model from plot PAL4 (E). (A) Complete spatial randomness (CSR)
 131 or Poisson process, where the points of the pattern are randomly and independently
 132 distributed within the plot. (B) Inhomogeneous Poisson process where the points are
 133 randomly and independently placed within the plot following the estimated probability
 134 density function (J). (C) A homogeneous Cauchy cluster process, where the offspring
 135 points are distributed around the parent points according to a circular Cauchy distribution
 136 and where parent points follow a Poisson process (see Baddeley et. al. 2015). (D) An
 137 inhomogeneous Cauchy cluster process, where the offspring points are distributed around
 138 the parent points according to a circular Cauchy distribution and the parent points are
 139 distributed following an inhomogeneous Poisson process. (F)–(I) Probability density
 140 function estimated from the simulated spatial point pattern respectively described in (A)–
 141 (D). (K)–(N) Estimation of the observed pair correlation function (red line) along with the
 142 estimation of the pair correlation function for 200 realizations of the tested point process
 143 model. We used a bandwidth of 5mm for the estimation of the pair correlation functions.
 144

145 Table A1: Probability of incorrectly rejecting the following null: *the spatial pattern exhibited by a*
 146 *given morphology is following a process similar to* (respectively): (i) *Poisson/CSR*, (ii)
 147 *Inhomogeneous Poisson*, (iii) *Homogeneous cluster process (Cauchy)* and (iv) *Inhomogeneous*
 148 *cluster process (Cauchy)*.

Group	Poisson/CSR	Inhomogeneous Poisson	Homogeneous cluster process (Cauchy)	Inhomogeneous cluster process (Cauchy)
Branching	<0.001	0.12	0.44	0.28
Corymbose	<0.001	<0.001	0.08	0.08
Encrusting	<0.001	<0.001	<0.001	0.2
Free-living	<0.001	<0.001	0.44	0.12
Massive	<0.001	<0.001	0.08	0.32
Plating	<0.001	<0.001	0.12	0.4
Sub-massive	<0.001	<0.001	<0.001	<0.001

149

150 Table A2: Probability of incorrectly rejecting the following null: *the spatial pattern exhibited by a*
151 *given taxonomical group is following a process similar to (respectively): (i) Poisson/CSR, (ii)*
152 *Inhomogeneous Poisson, (iii) Homogeneous cluster process (Cauchy) and (iv) Inhomogeneous*
153 *cluster process (Cauchy).*

Group	Poisson/CSR	Inhomogeneous Poisson	Homogeneous cluster process (Cauchy)	Inhomogeneous cluster process (Cauchy)
<i>Acropora sp.</i> (branching)	<0.001	0.07	0.45	0.22
<i>Acropora sp.</i> (corymbose)	<0.001	0.19	0.7	0.77
<i>Favia matthai</i>	<0.001	0.01	0.2	0.31
<i>Favia stelligera</i>	<0.001	<0.001	0.03	<0.001
<i>Favites sp.</i> (encrusting)	<0.001	<0.001	0.11	0.08
<i>Favites sp.</i> (submassive)	<0.001	<0.001	0.58	<0.001
<i>Fungia sp.</i>	<0.001	<0.001	0.5	0.23
<i>Hydnophora exesa</i>	<0.001	0.19	0.81	0.7
<i>Hydnophora microconos</i>	<0.001	<0.001	0.02	0.01
<i>Leptastrea sp.</i>	<0.001	<0.001	0.66	0.28
<i>Lobophyllia sp.</i>	<0.001	<0.001	0.99	0.14
<i>Montastrea curta</i>	<0.001	<0.001	0.1	0.79
<i>Montipora sp.</i> (encrusting)	<0.001	<0.001	0.02	0.8
<i>Montipora sp.</i> (plating)	<0.001	<0.001	0.98	0.89
<i>Pavona sp.</i> (submassive)	<0.001	<0.001	0.99	0.18
<i>Pavona varians</i>	<0.001	<0.001	<0.001	0.14
<i>Pocillopora sp.</i>	<0.001	<0.001	0.01	0.17

<i>Pocillopora eydouxi</i>	0.03	0.05	0.15	0.02
<i>Porites sp. (massive)</i>	<0.001	<0.001	0.09	0.11
<i>Porites superfusa</i>	<0.001	<0.001	<0.001	0.1
<i>Stylophora pistillata</i>	<0.001	<0.001	0.42	<0.001
<i>Turbinaria reniformis</i>	<0.001	<0.001	0.67	0.52

154

155

156 **References**

157 Baddeley A, Rubak E, Turner R (2015). Spatial point patterns: methodology and applications

158 with R. – Chapman and Hall/CRC Press.

159 Dale MRT, Dixon P, Fortin M-J, Legendre P, Myers DE, Rosenberg MS (2002) Conceptual and

160 mathematical relationships among methods for spatial analysis. *Ecography* 25:558-577

161 R Core Team (2016). R: A language and environment for statistical computing. R Foundation for

162 Statistical Computing, Vienna, Austria URL <https://www.R-project.org/>

163 Velázquez E, Martínez I, Getzin S, Moloney KA, Wiegand T (2016) An evaluation of the state

164 of spatial point pattern analysis in ecology. *Ecography* 39:1042-1055

165 Wiegand T, A. Moloney K (2004) Rings, circles, and null-models for point pattern analysis in

166 ecology. *Oikos* 104:209-229

1 **Investigating colony level spatial patterns of coral assemblages using large-area imaging at**
2 **a remote coral reef: Appendix 2**

3 Clinton B. Edwards¹, Yoan Eynaud¹, Gareth J. Williams^{1,2}, Nicole E. Pedersen¹, Brian J.
4 Zgliczynski¹, Arthur C.R. Gleason³, Jennifer E. Smith¹, Stuart A. Sandin¹

5 ¹Center for Marine Biodiversity and Conservation, Scripps Institution of Oceanography,
6 University of California, San Diego, La Jolla, CA 92093-0202, USA

7 ²School of Ocean Sciences, Bangor University, Menai Bridge, Anglesey, LL59 5AB, UK

8 ³ Physics Department, University of Miami, 1320 Campo Sano Ave., Coral Gables, FL 33146

9

10 *Corresponding Author: Clinton Edwards, Email: clint@ucsd.edu, Center for Marine
11 Biodiversity and Conservation, Scripps Institution of Oceanography,
12 University of California, San Diego, 9500 Gilman Dr., La Jolla, CA
13 92093-0202, USA

14

15 A general trend of positive relationship is noticeable across all groups at the highest taxonomic
16 level (21 of 23 groups, binomial test with p-value<0.01). Such a relationship is expected
17 following Taylor's law (Taylor, 1961, 1982), which relates the variance of the number of
18 individuals of a species per unit area of habitat to the corresponding mean by a power law
19 relationship:

20
$$\sigma^2 = a * \chi^b$$

21 which is equivalent to:

$$22 \quad \frac{\sigma^2}{\chi} = a * \chi^{b-1} \quad (1)$$

23 where σ^2 is the variance of a distribution of sample of the population of mean χ . Here, we used
24 the mean over the bootstrapped sample of the variance to mean ratio ($\bar{v}_{i,j}$), defined as:

$$25 \quad \bar{v}_{i,j} = \frac{1}{B} \sum_{k=1}^B v_{i,j,k}$$

26 We then express $\bar{v}_{i,j}$ as a function of the density of the number of individual coral colonies $\cdot \text{m}^{-2}$
27 of a given group at given site ($X_{i,j}$):

$$28 \quad \ln(\bar{v}_{i,j}) = \alpha_i * \ln(X_{i,j}^\beta) + \beta_i + \varepsilon_i \quad (2)$$

29 Which can be derived from equation (2):

$$30 \quad \bar{v}_{i,j} = a_i * X_{i,j}^{\beta_i} \quad \text{with} \quad a_i = e^{\alpha_i + \varepsilon_i} \quad (3)$$

31 such that Eq.(3) is homologous to Eq.(1) with $b_i = \beta_i + 1$. Therefore, we see that the positive
32 relationships between colonies abundance per site and the variance to mean ratio follows
33 Taylor's law (Taylor 1961; Taylor and Woivod 1982).

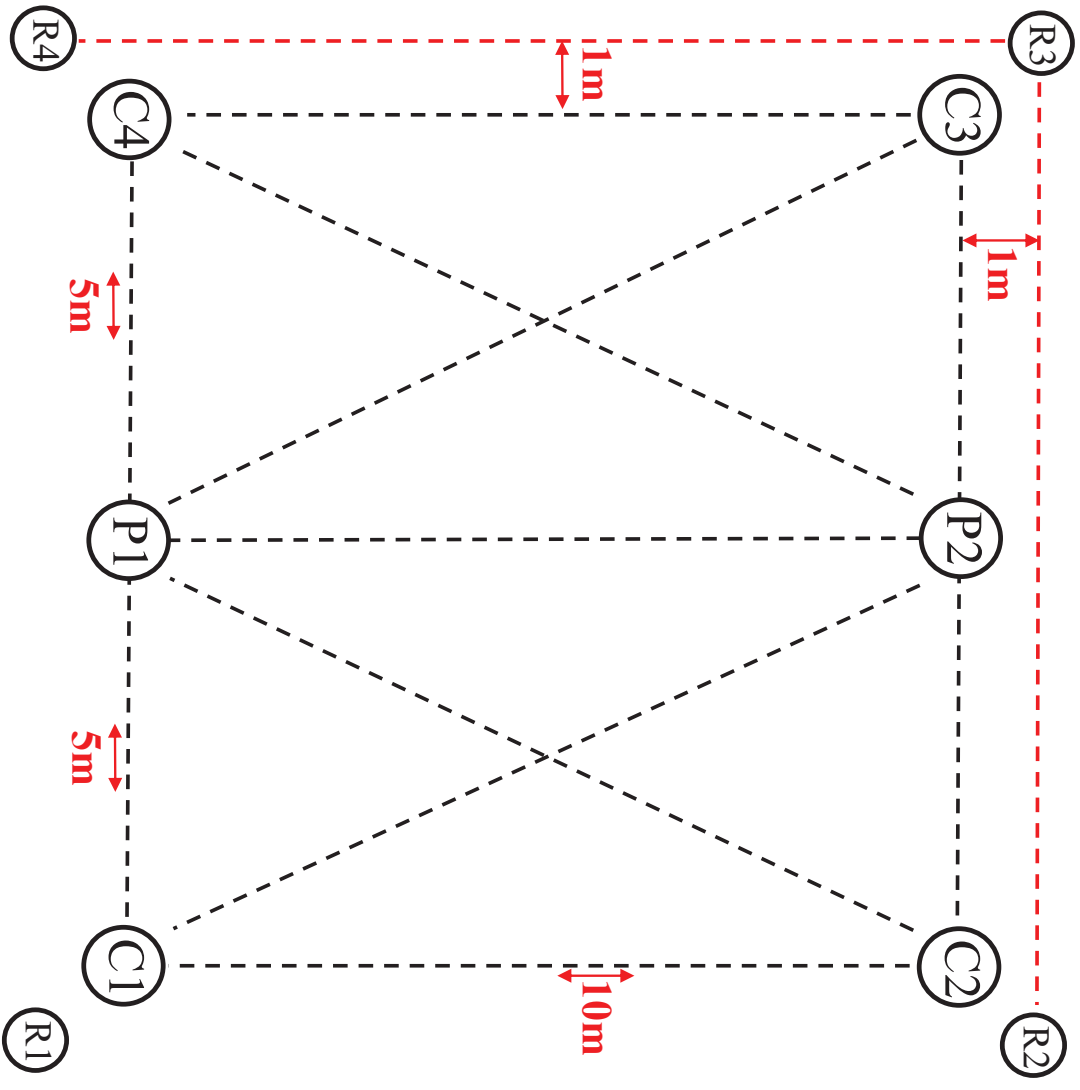
34

35 **References**







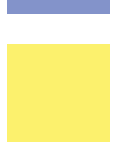

























36 Taylor L (1961) Aggregation, variance and the mean. Nature 189:732-735

37 Taylor L, Woiwod I (1982) Comparative synoptic dynamics. I. Relationships between inter-and
38 intra-specific spatial and temporal variance/mean population parameters. *Journal Anim Ecol*
39 51:879-906

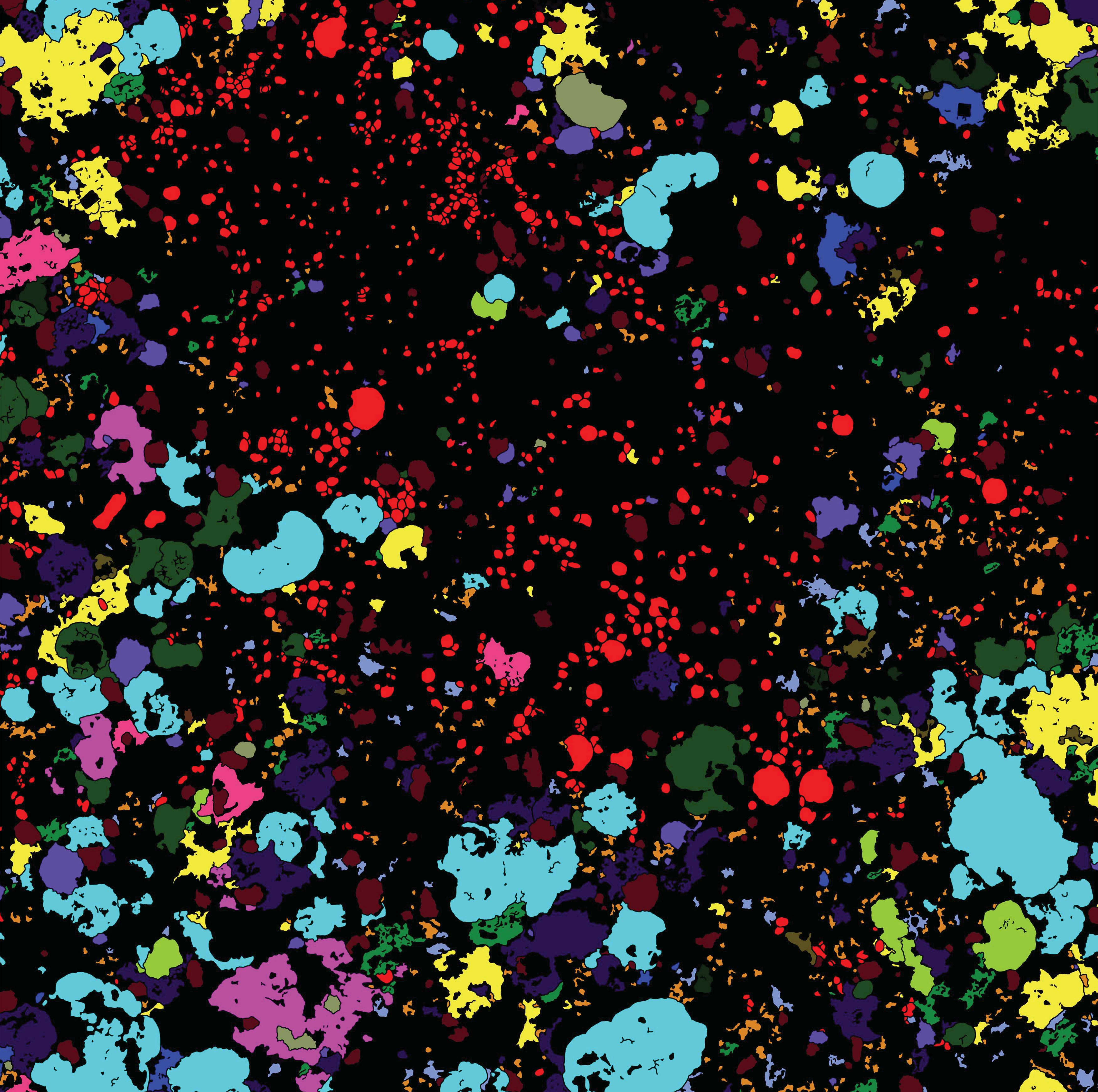
40



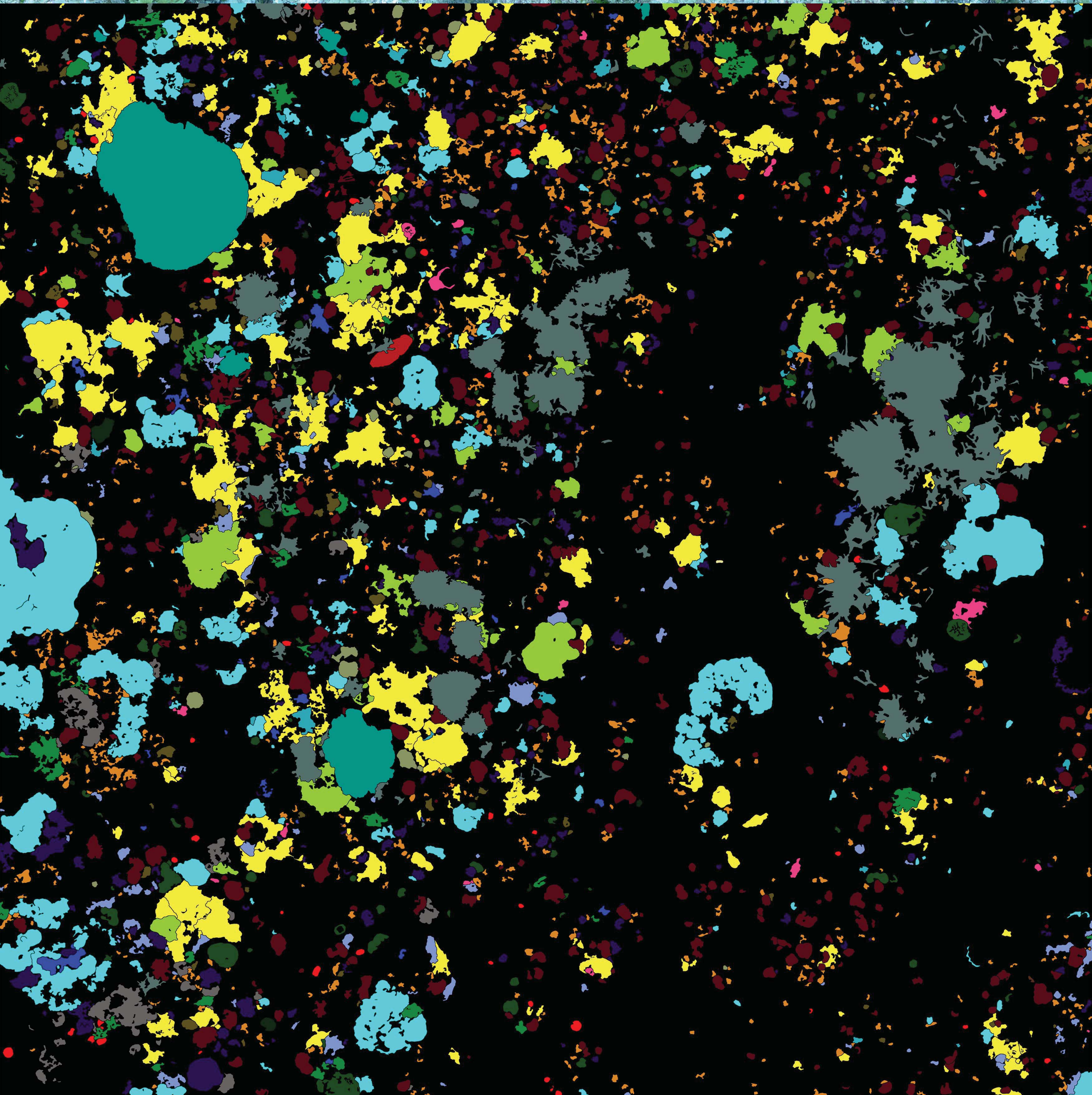
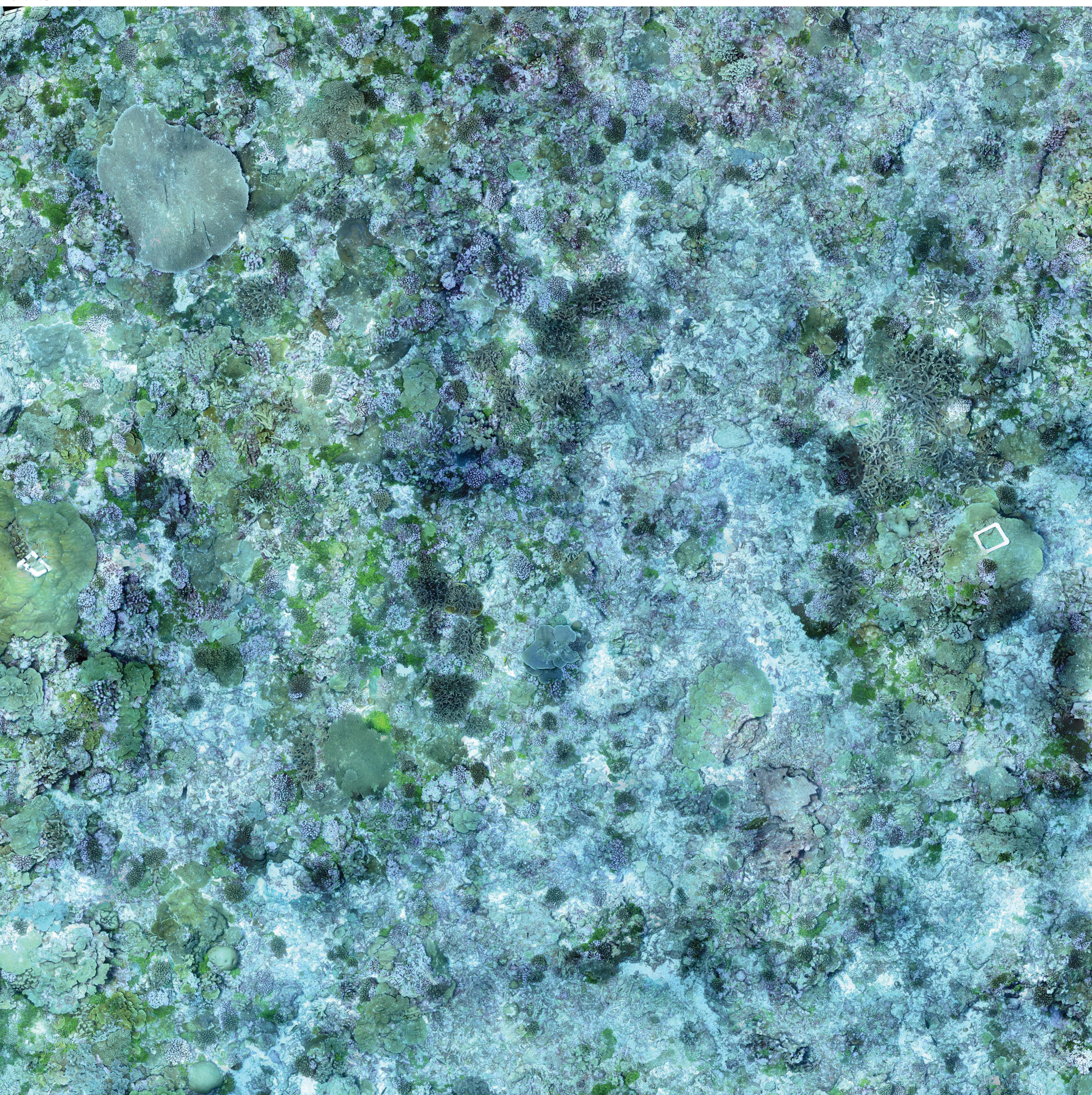
LEGEND

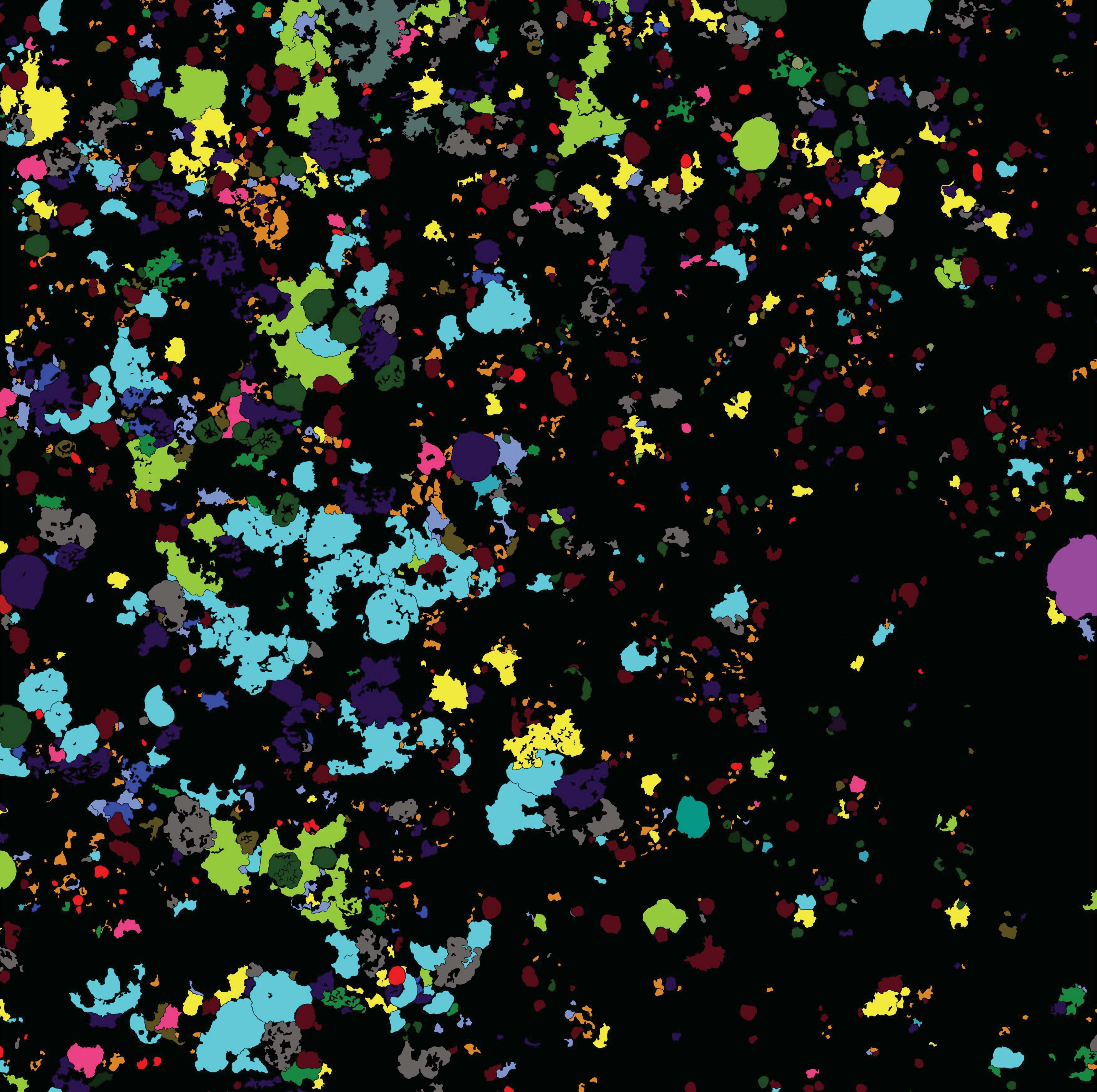
 Favites sp. (encrusting)	 Hydnothya exesa	 Montipora sp. (plating)	 Porites rus
 Acropora sp. (branching)	 Favites sp. (submassive)	 Hydnothya microconos	 Porites sp. (massive)
 Acropora sp. (coymbose)	 Fungia sp.	 Leptastrea sp.	 Porites superfusa
 Acropora sp. (tabular)	 Gardineroseris planulata	 Leptoseris sp.	 Sandalolitha dentata
 Astreopora myriophthalma	 Goniastrea pectinata	 Lobophyllia sp.	 Stylophora
 Favia matthai	 Halomitra pileus	 Montastrea curta	 Turbinaria reniformis
 Favia stelligera	 Herpolitha sp.	 Montipora sp. (encrusting)	 Pocillopora sp.
		 Pavona sp. (submassive)	
		 Pavona varians	
		 Platygyra sp.	
		 Pocillopora eydouxi	

a. Site: FR3

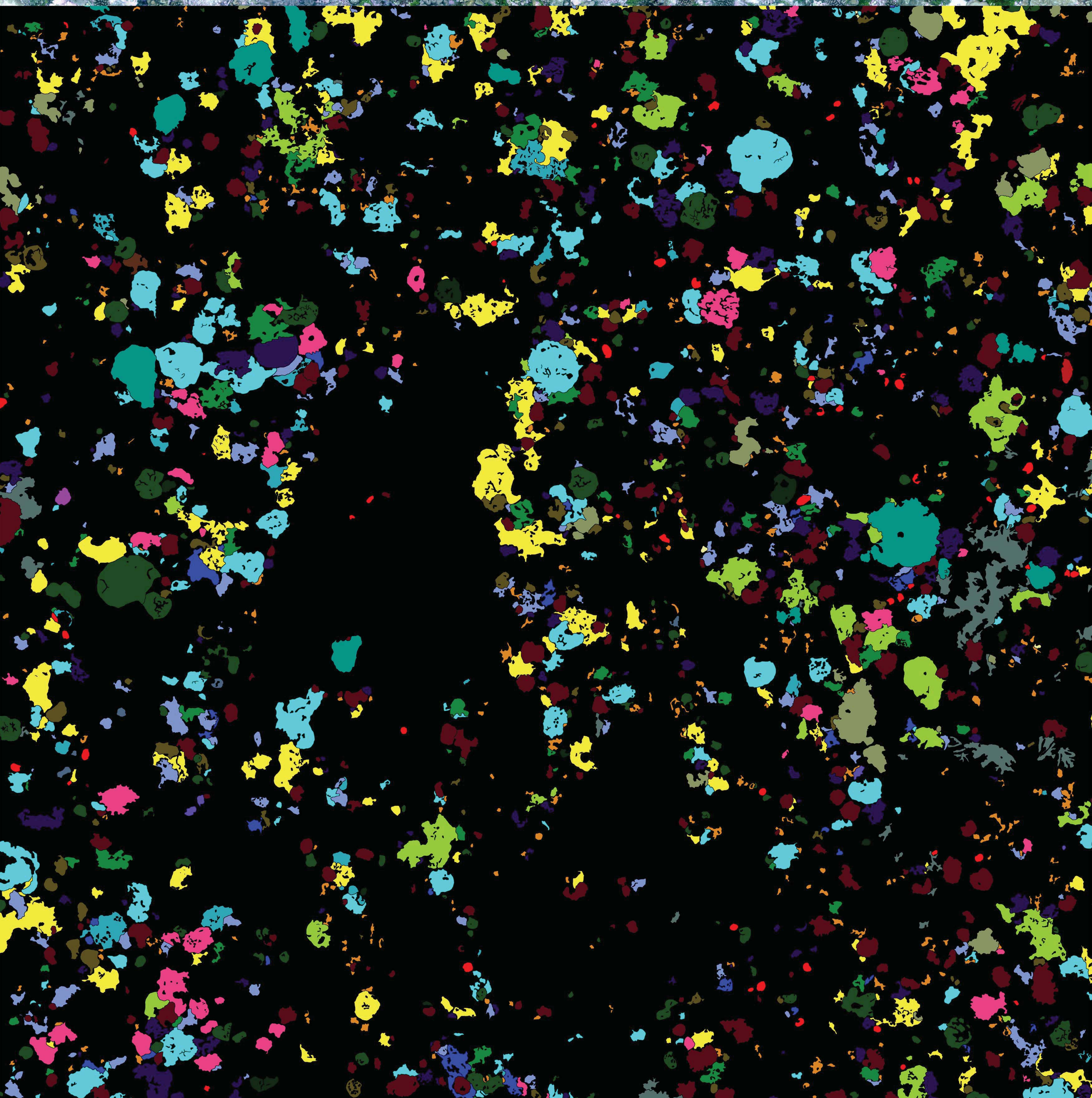


b. Site: FR38

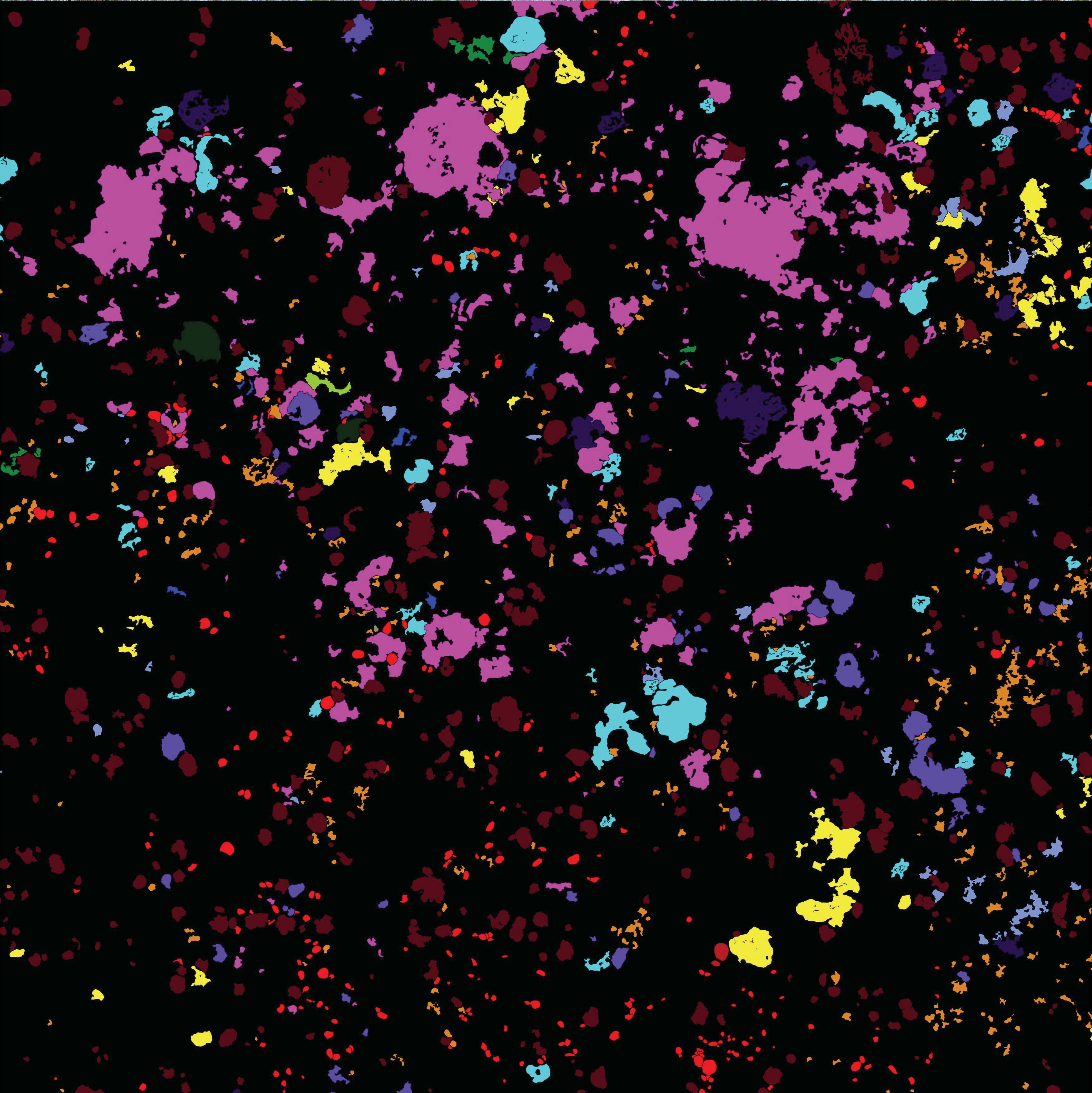
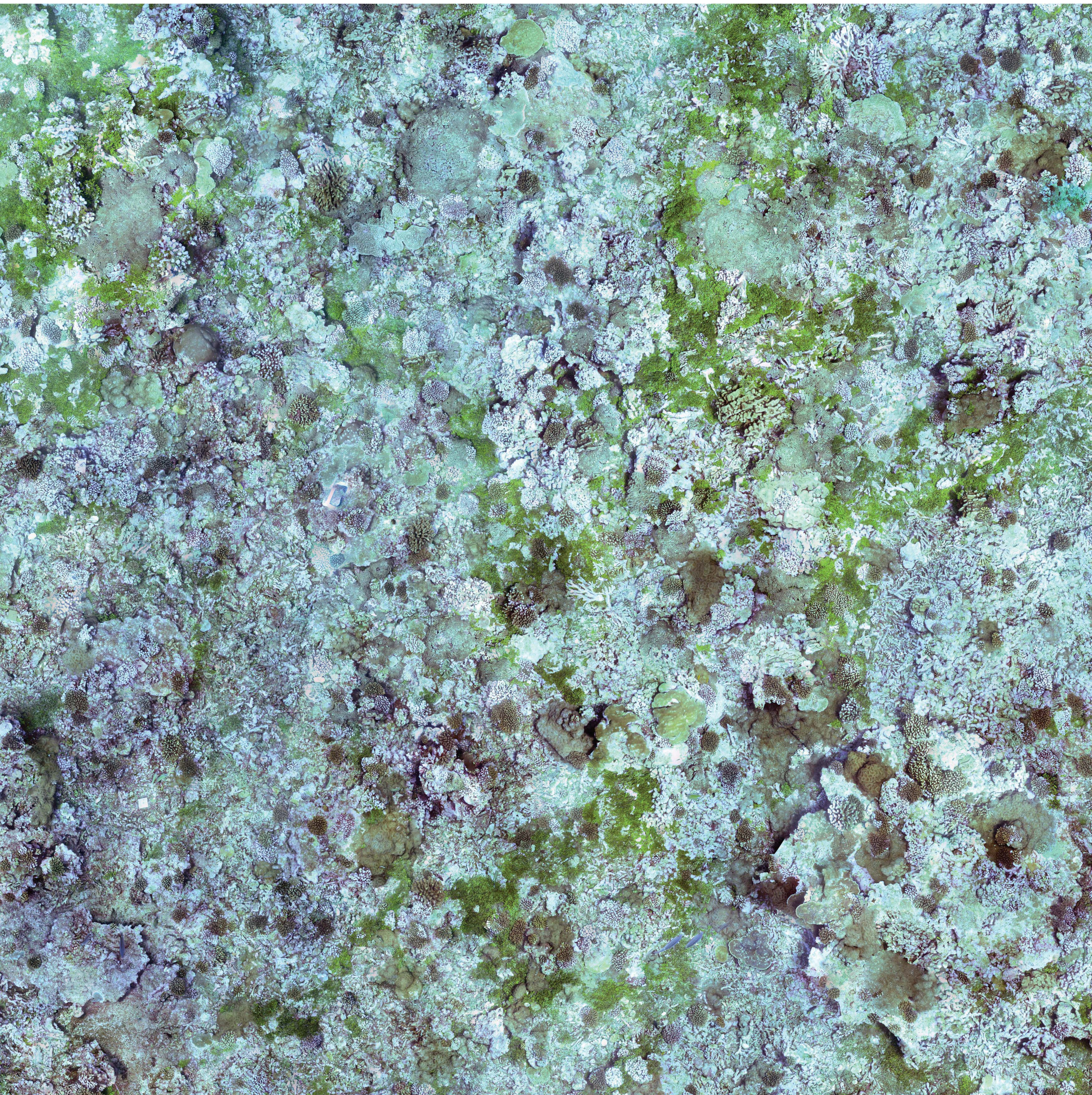


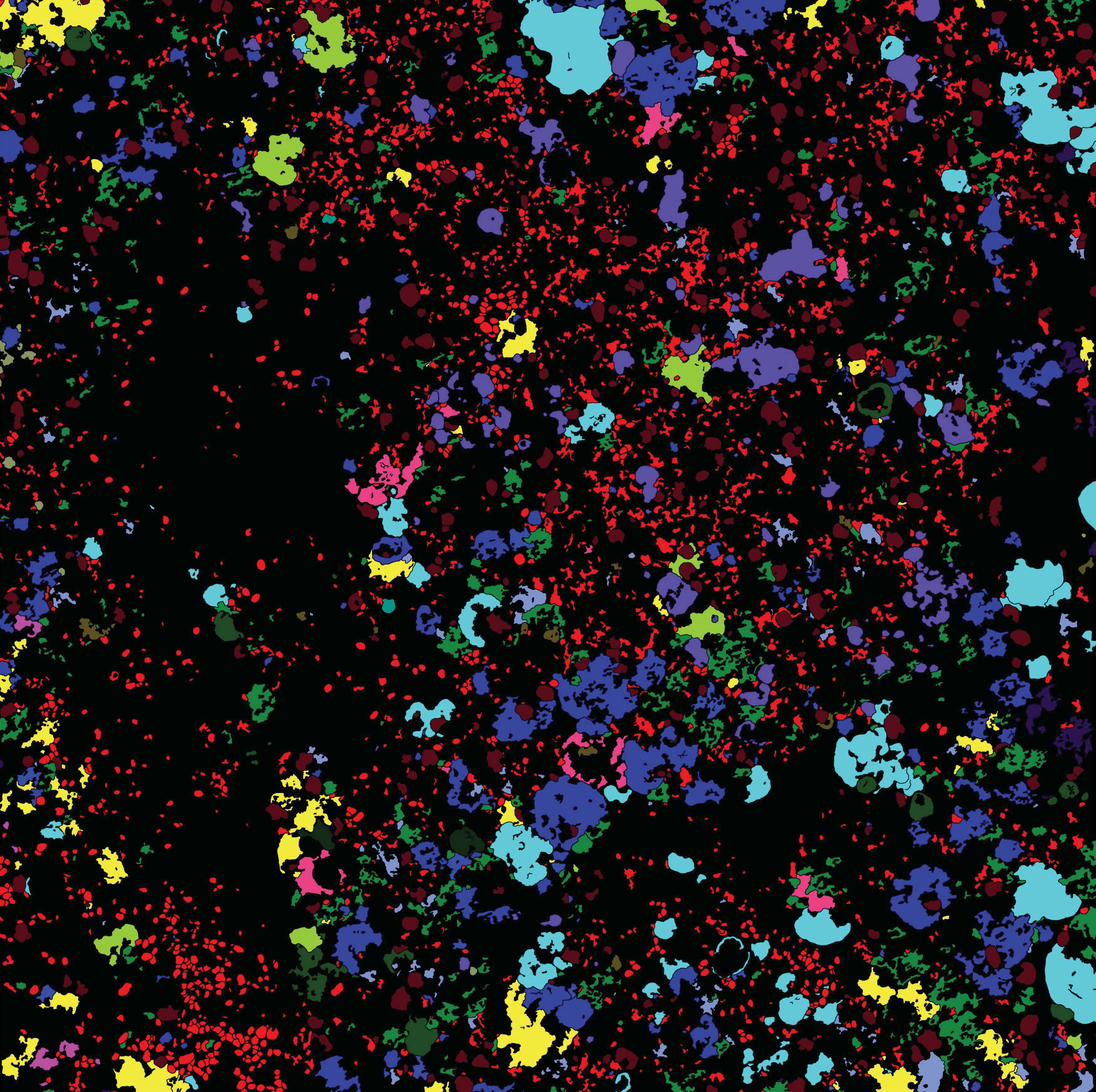
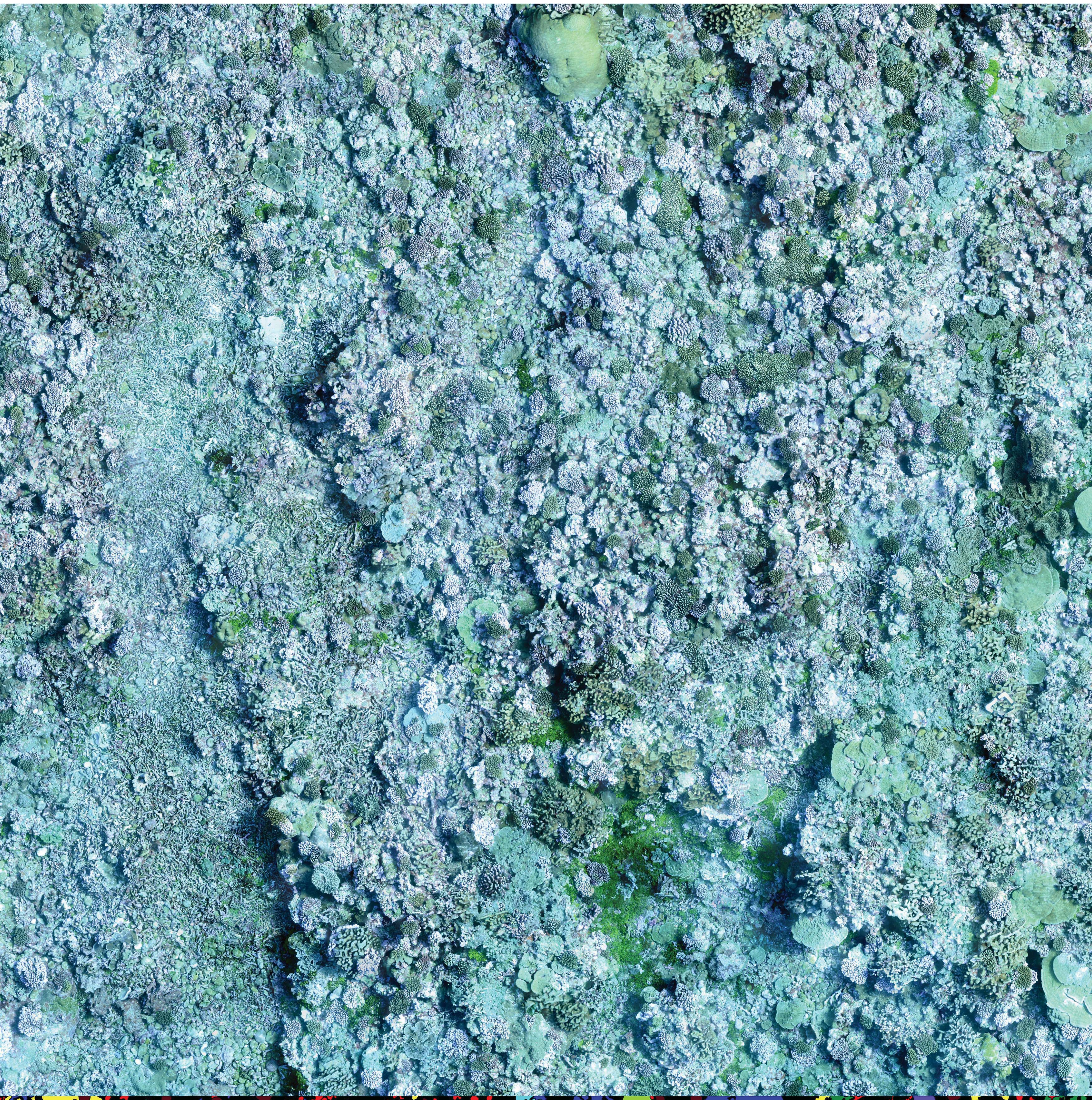


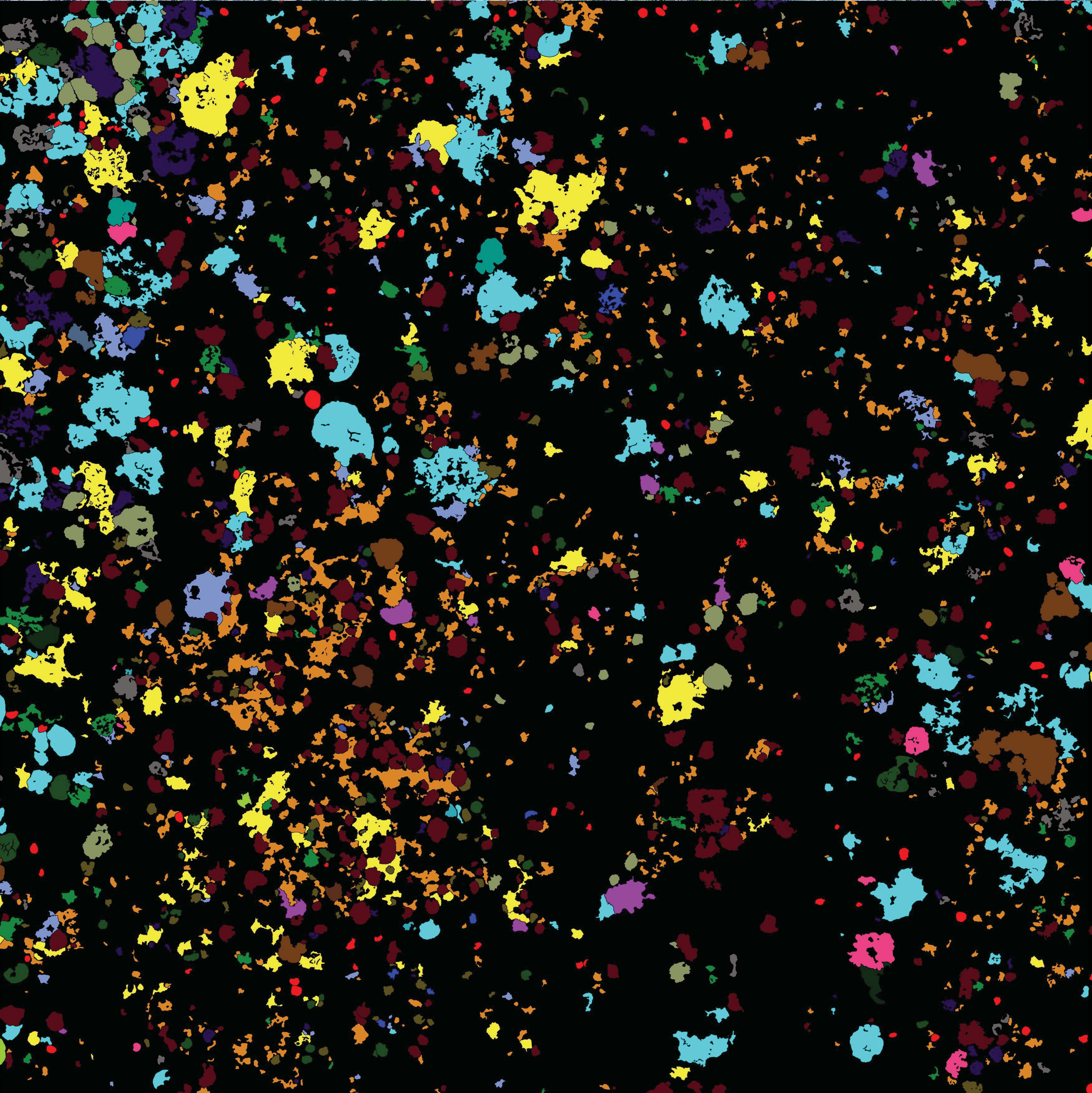
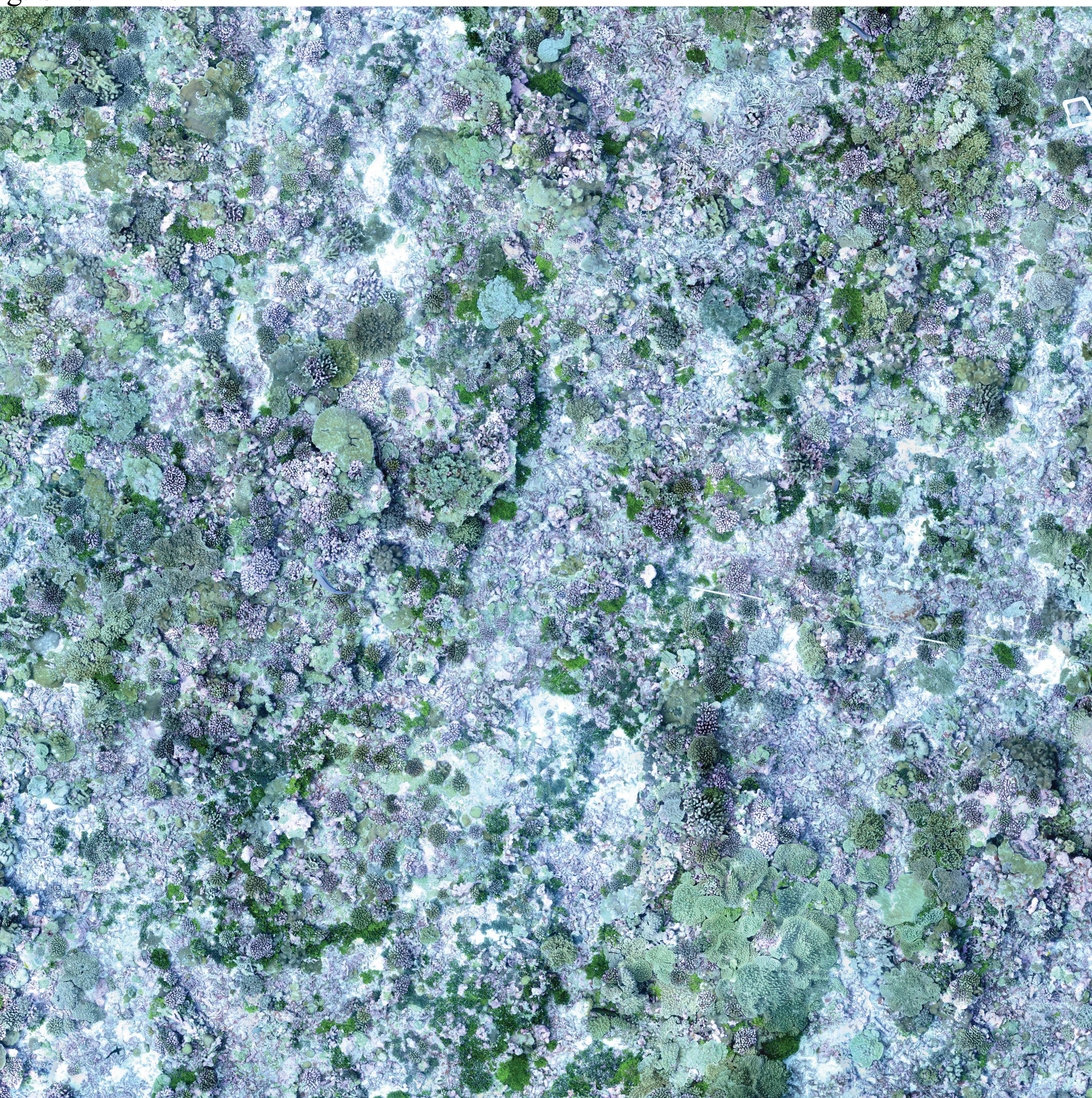
d. Site: FR40

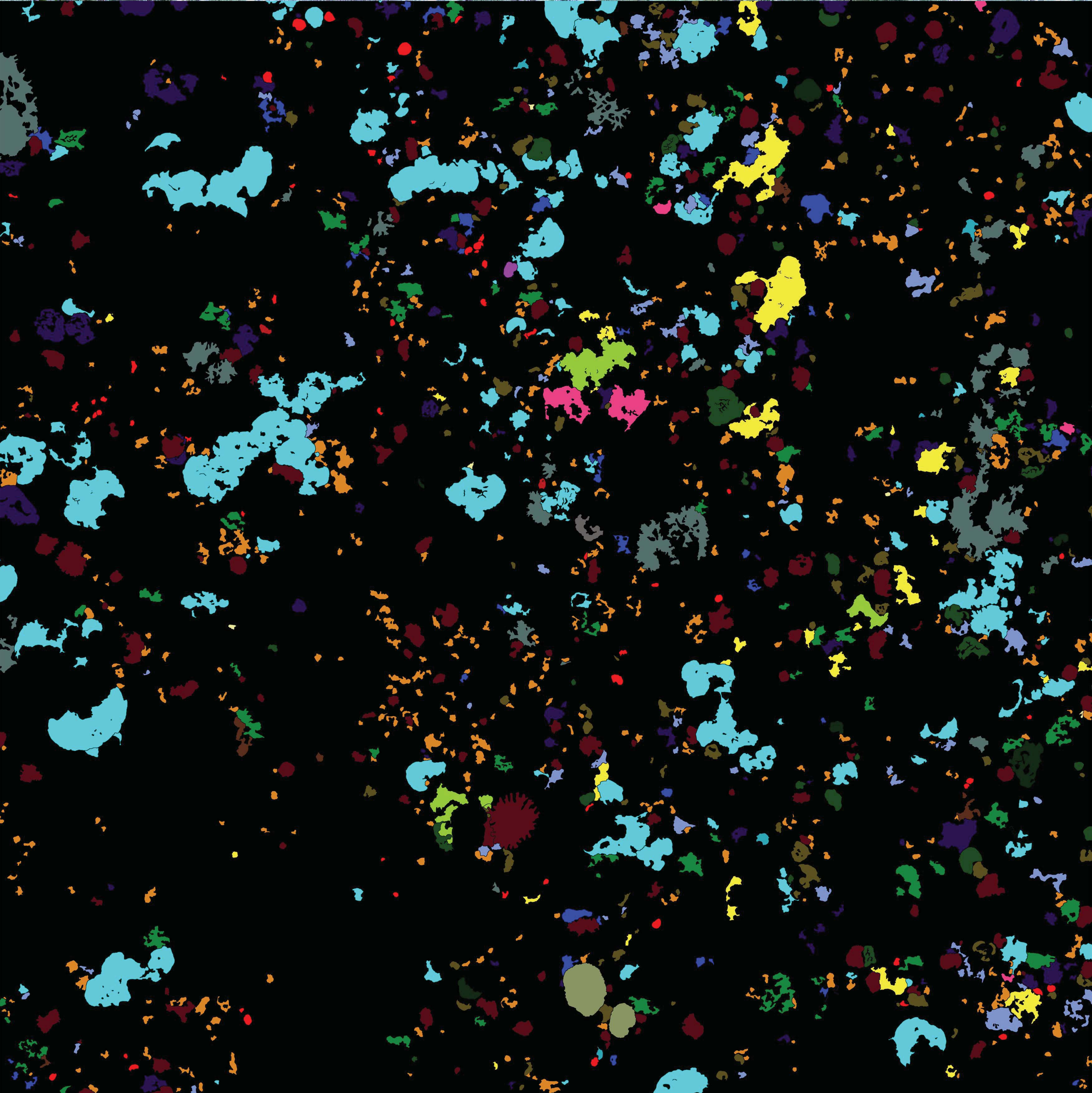
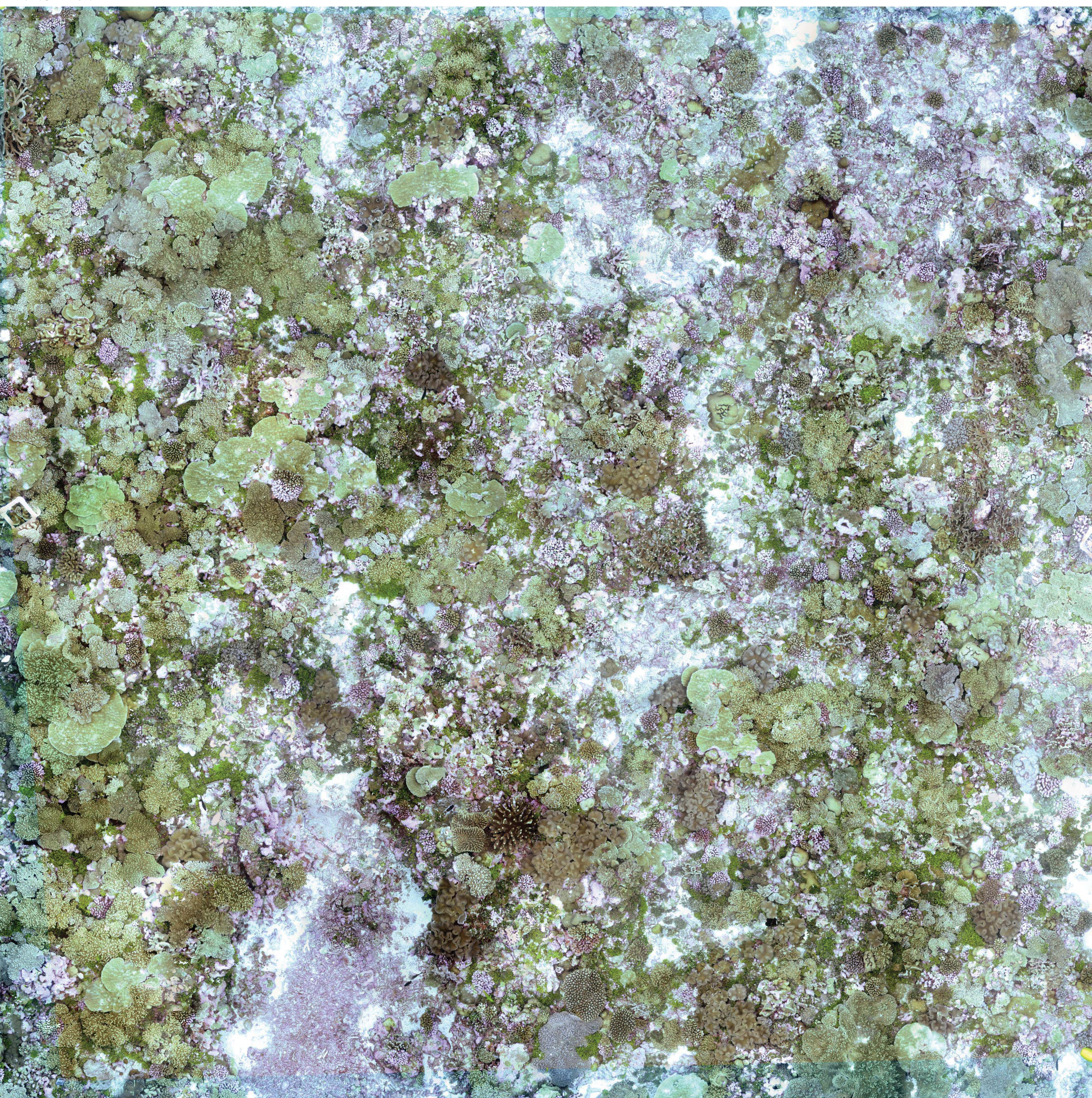


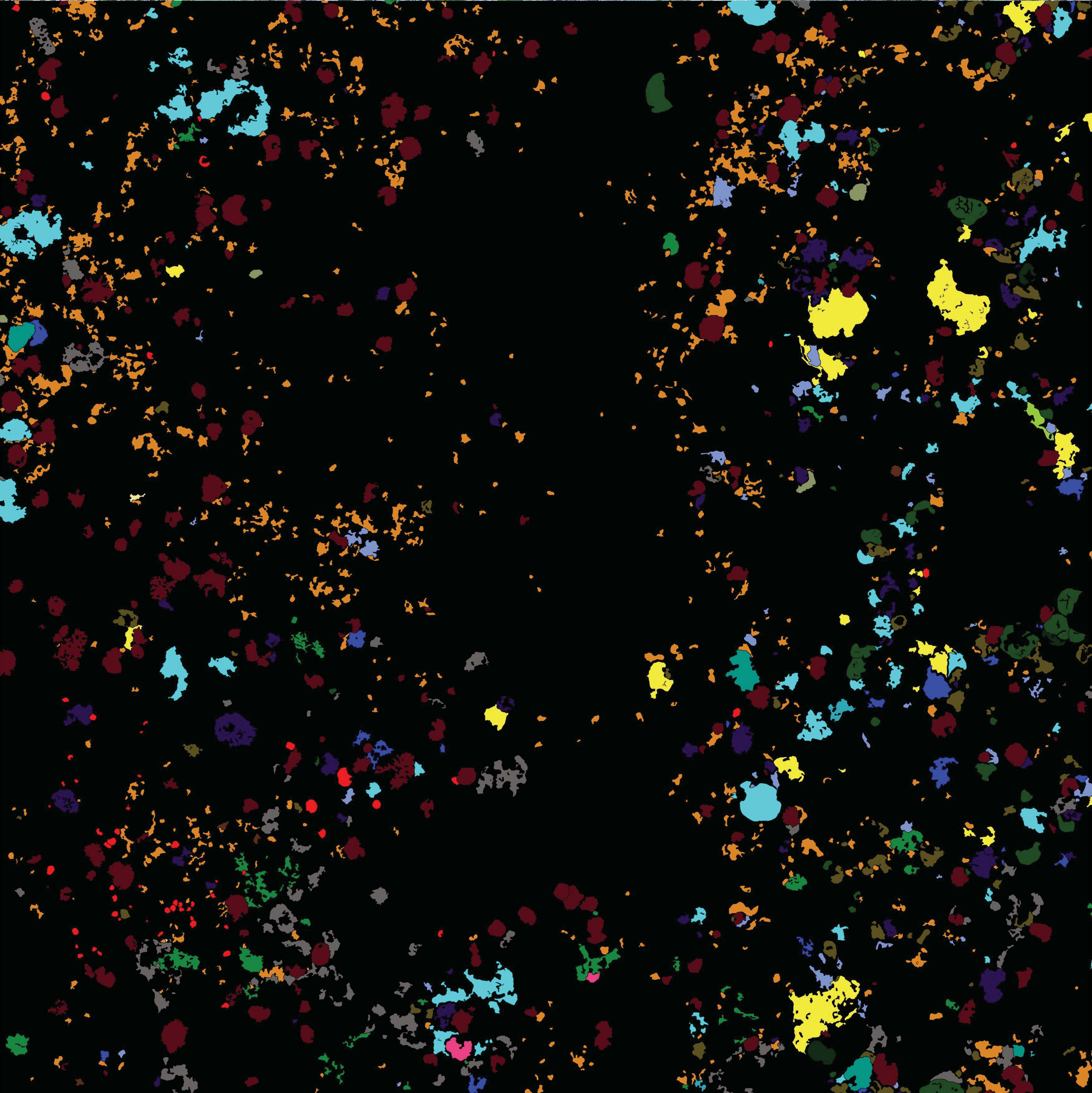
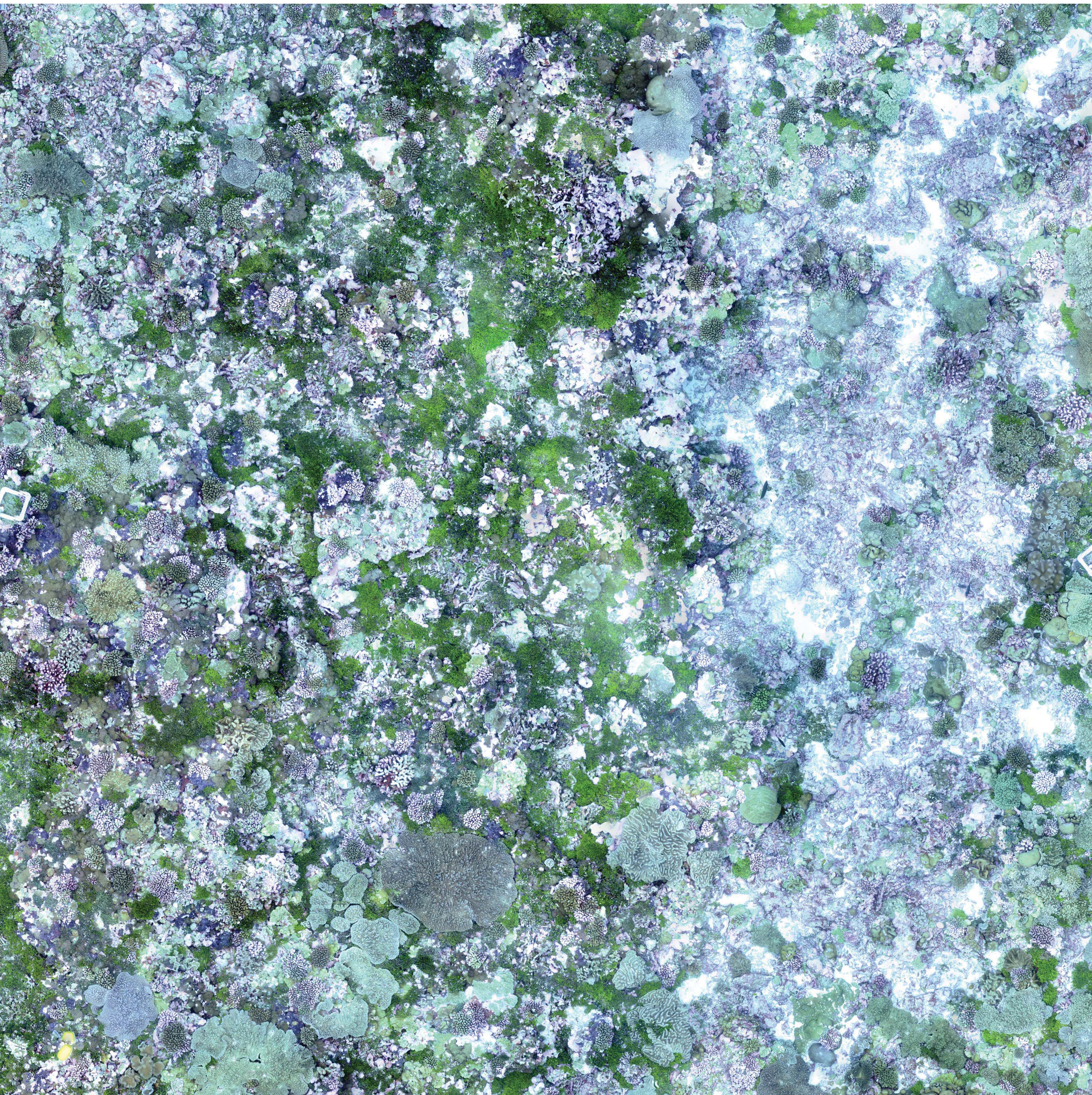
e. Site: FR5

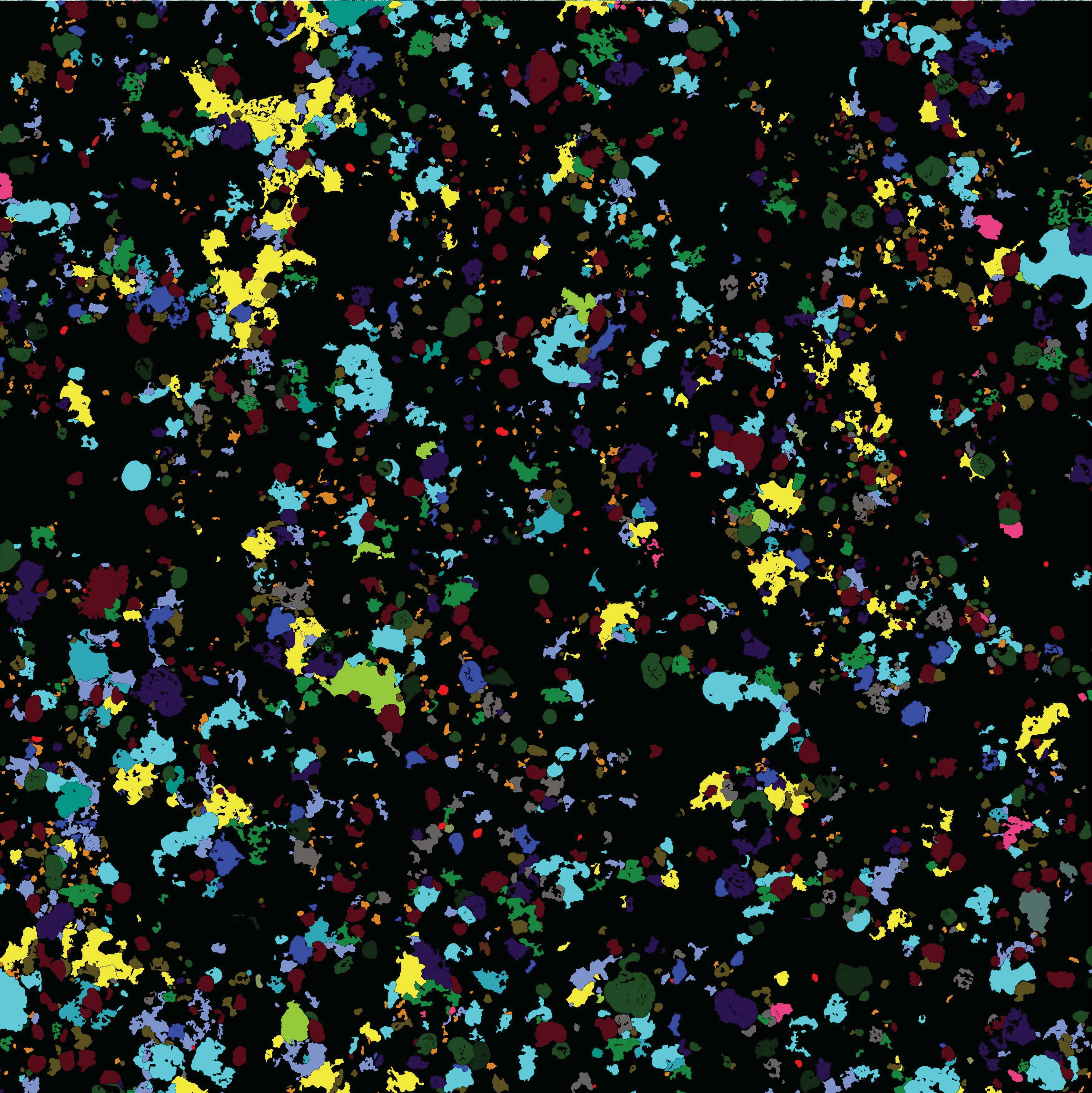


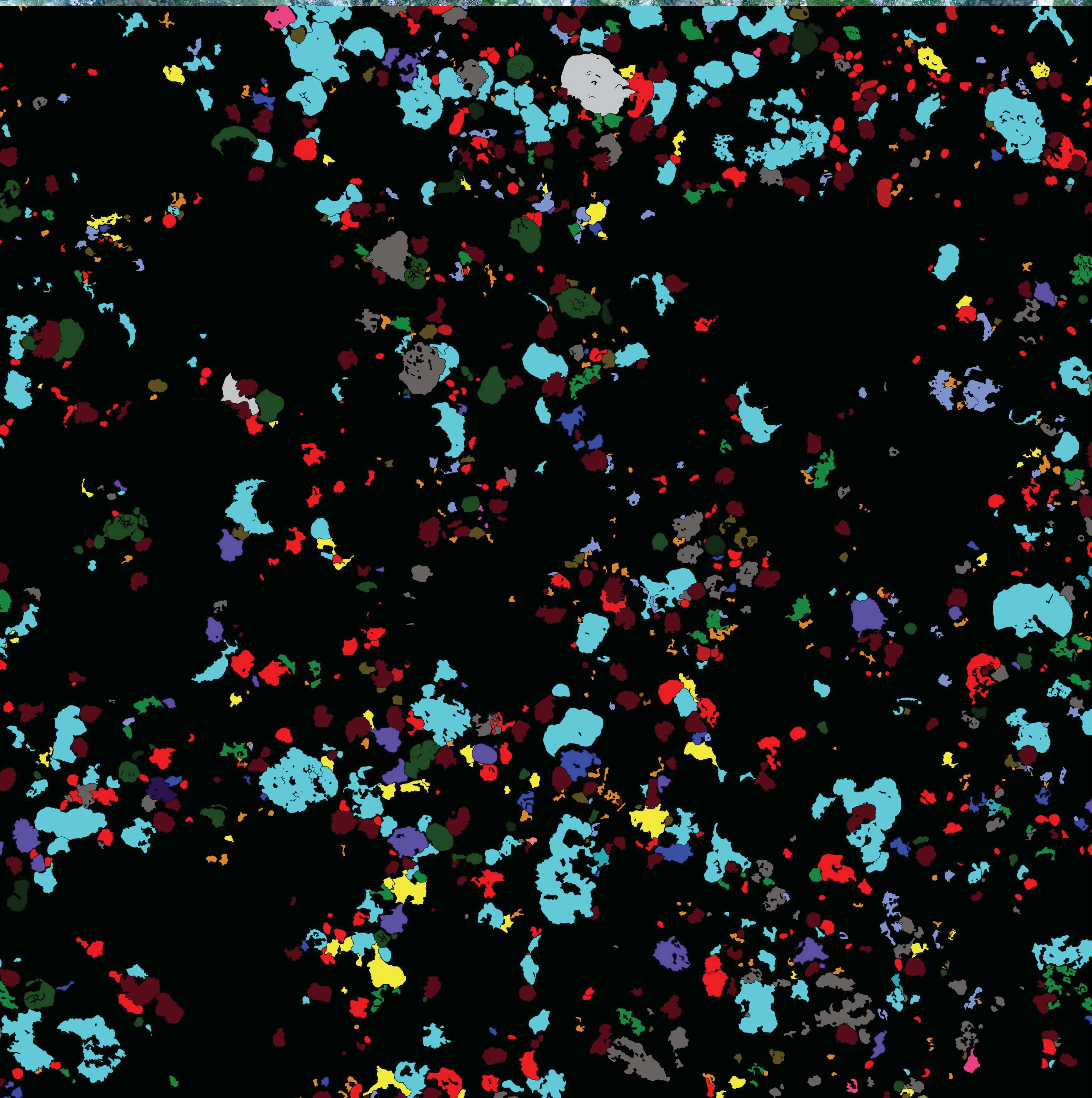


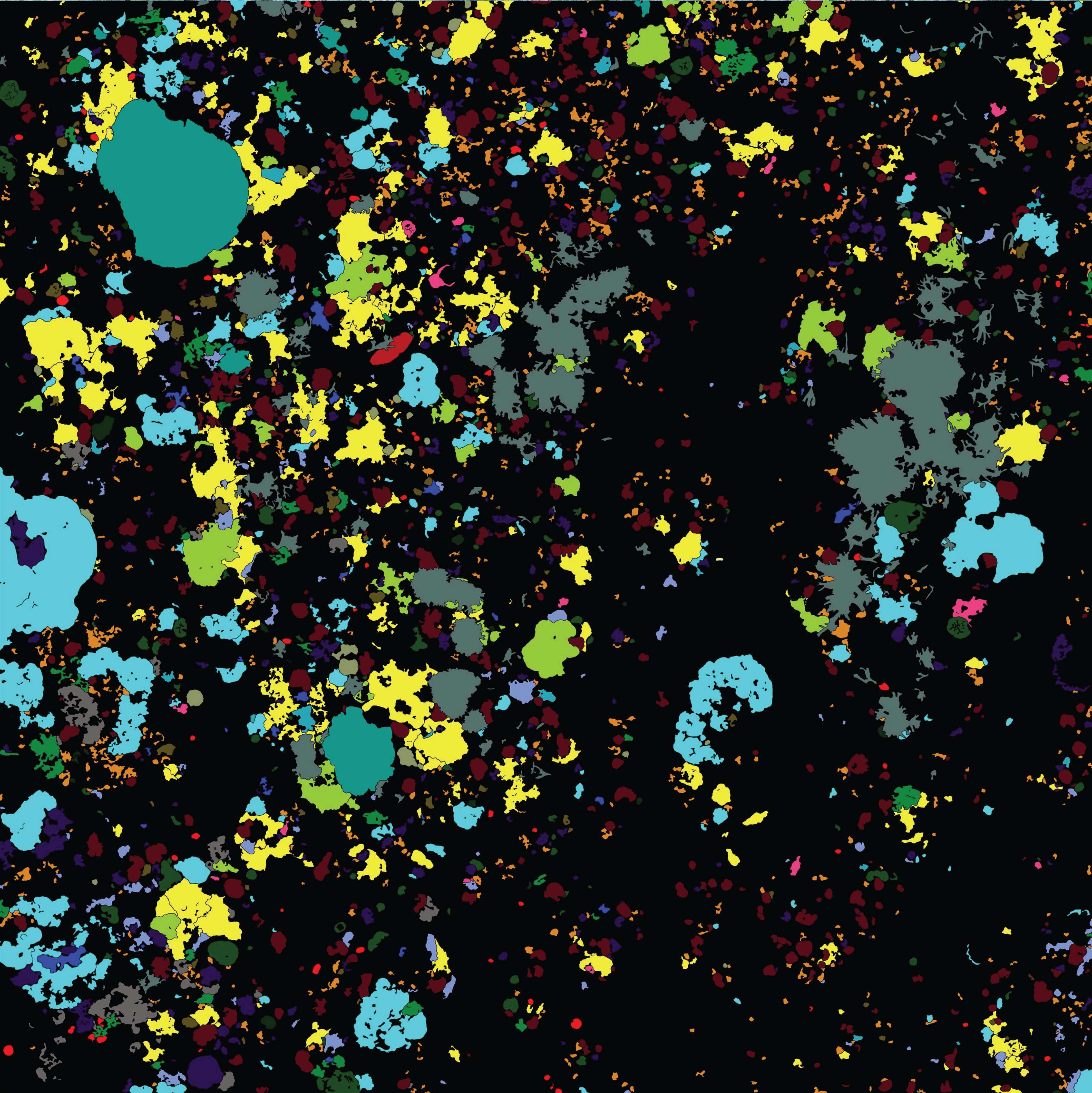
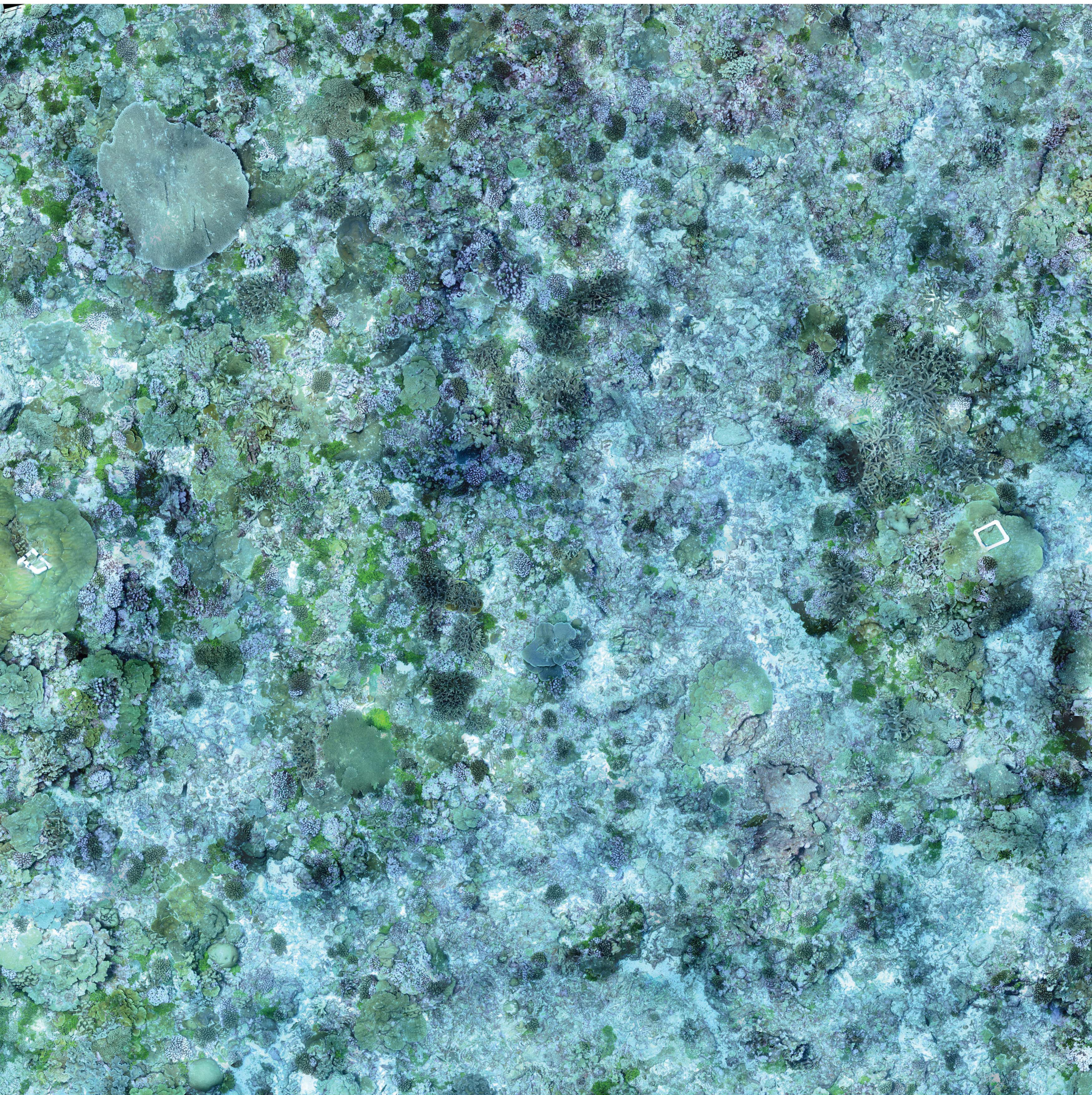


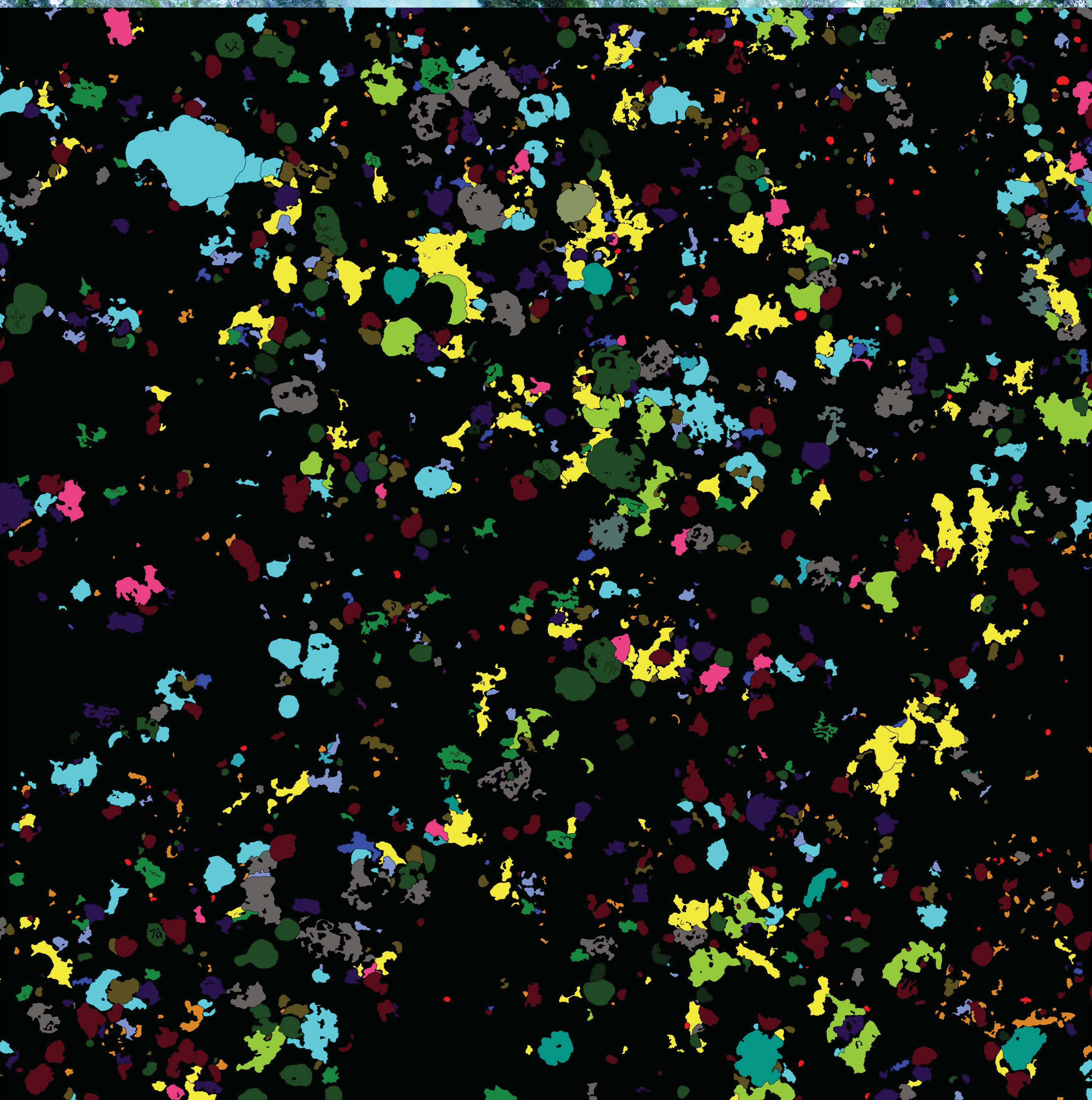
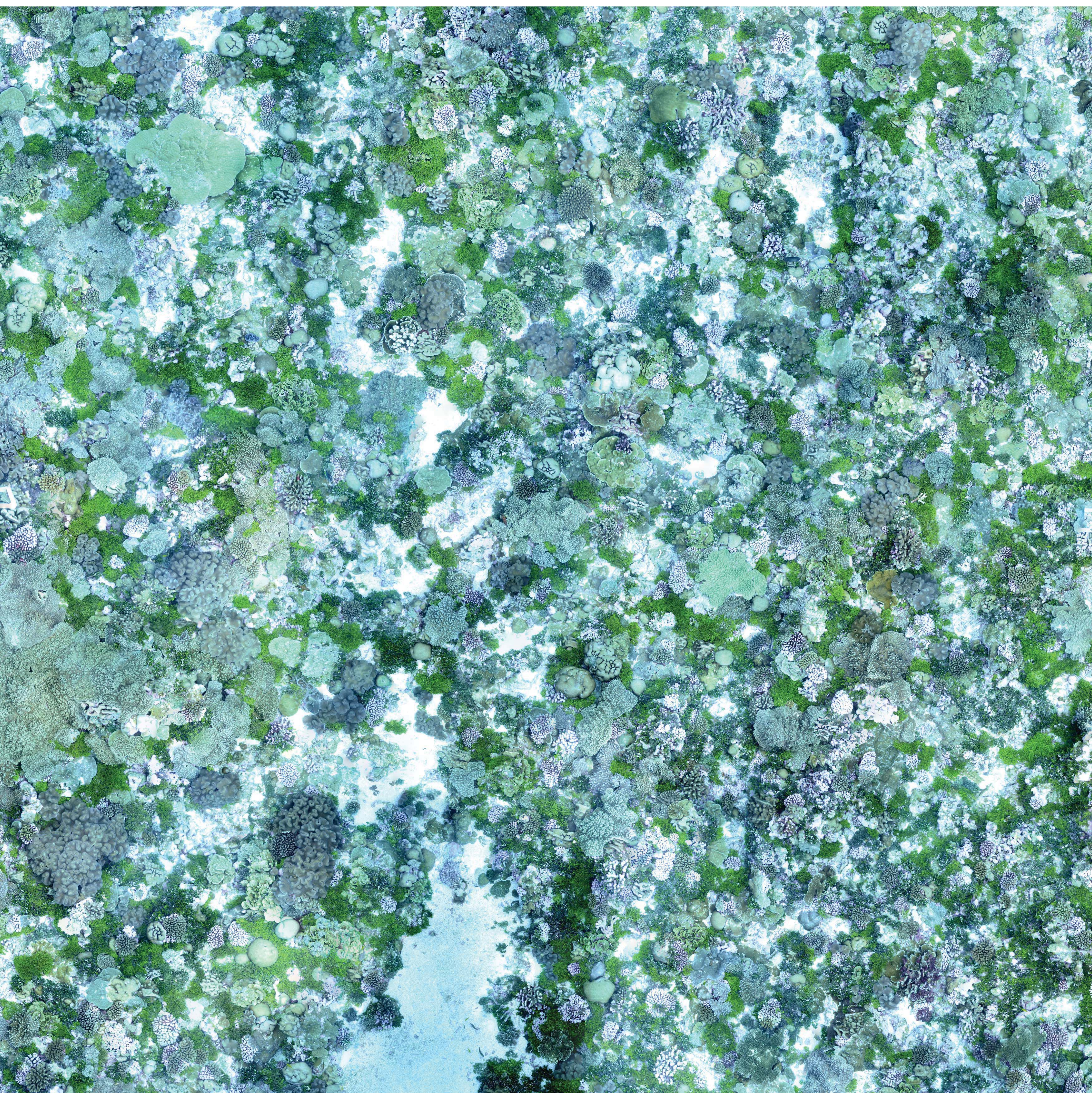


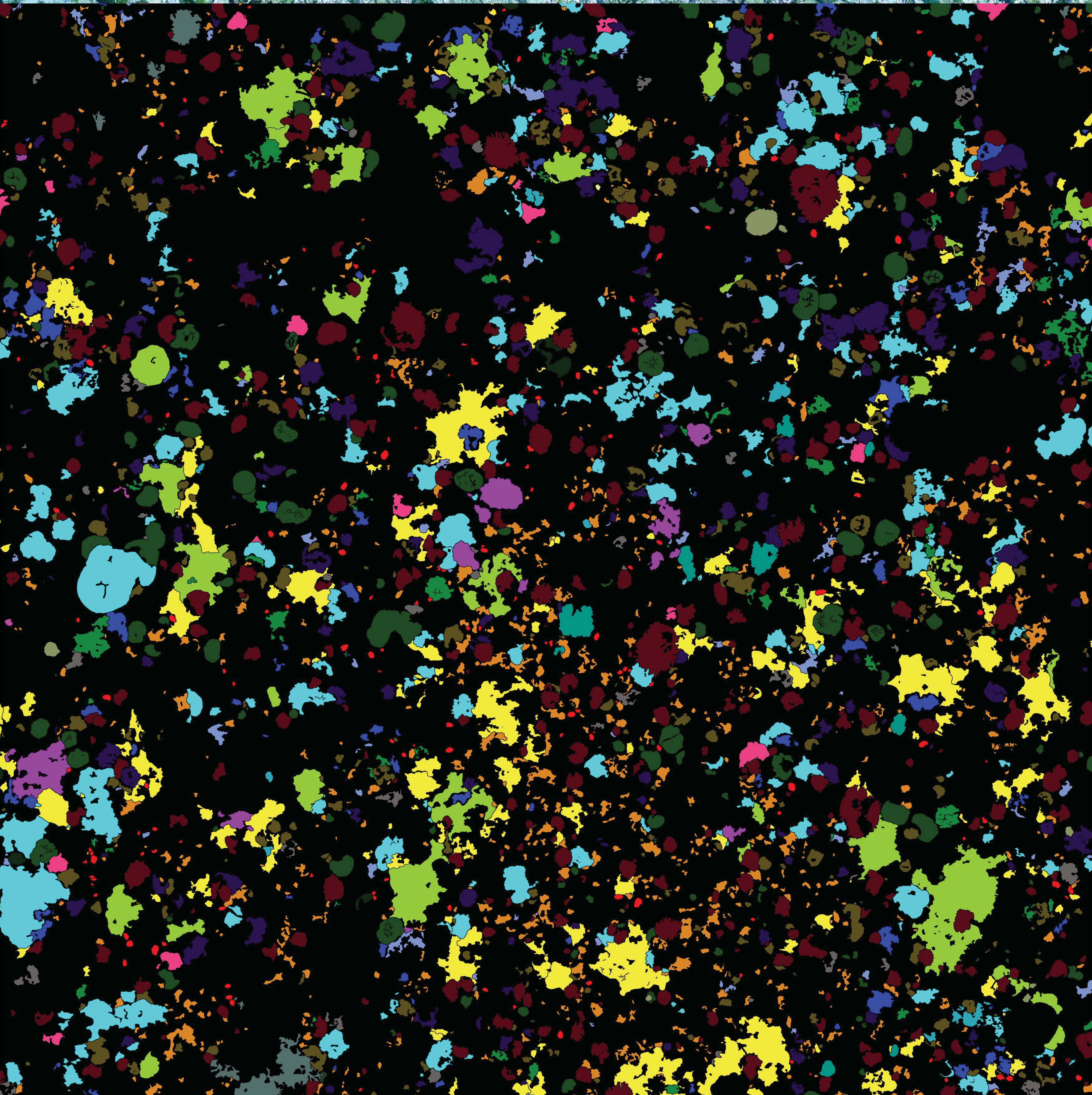
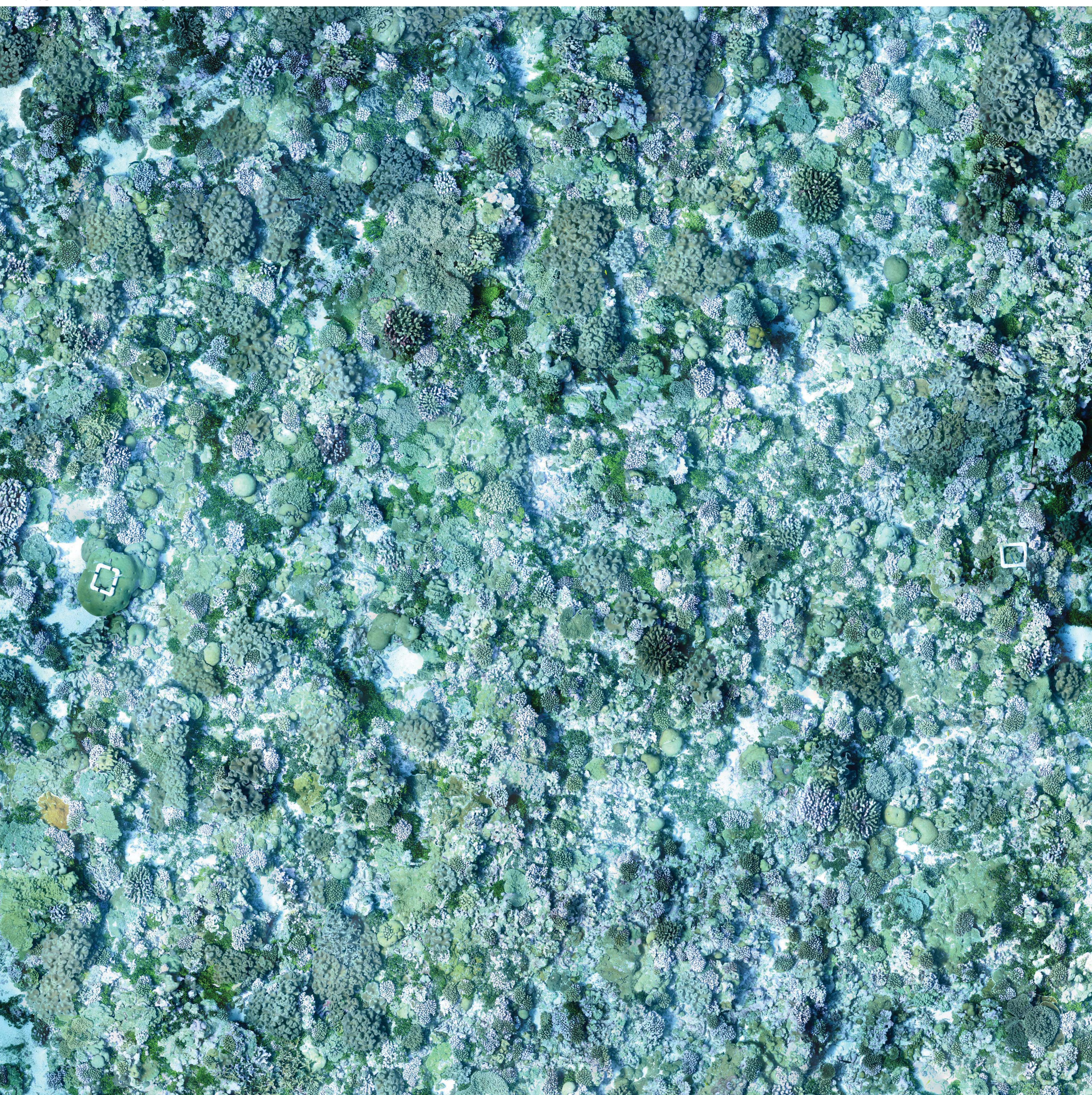


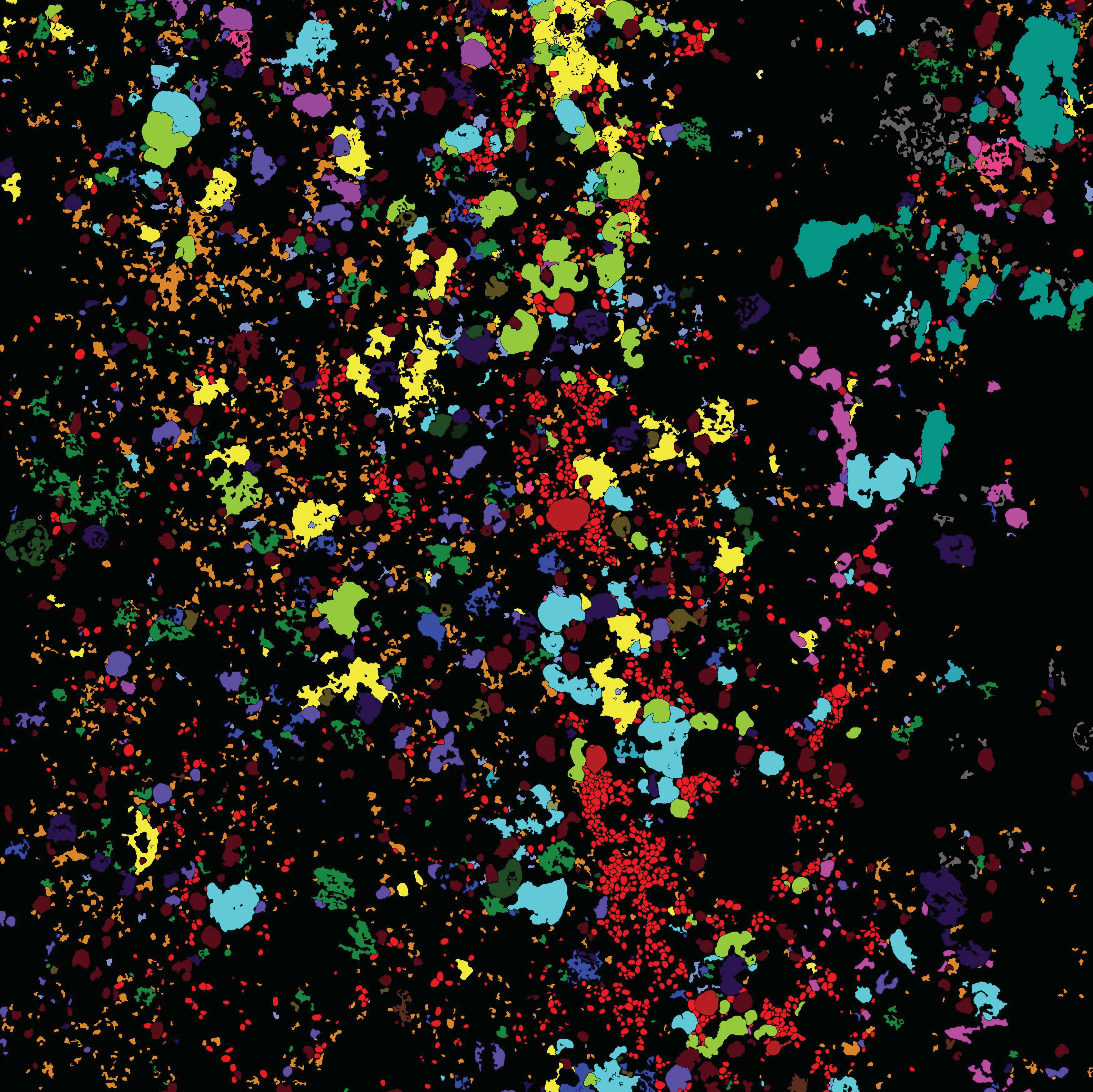


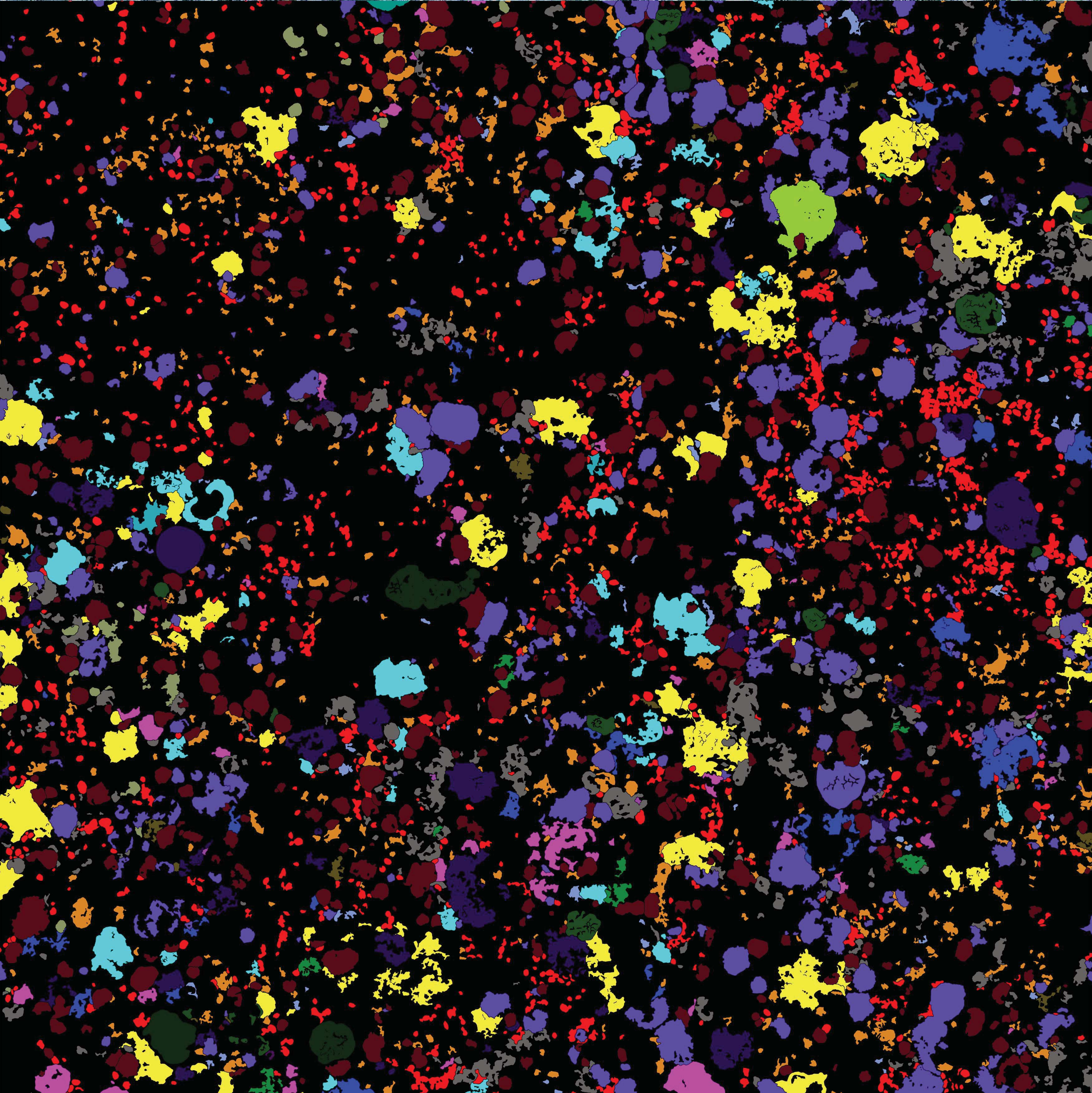
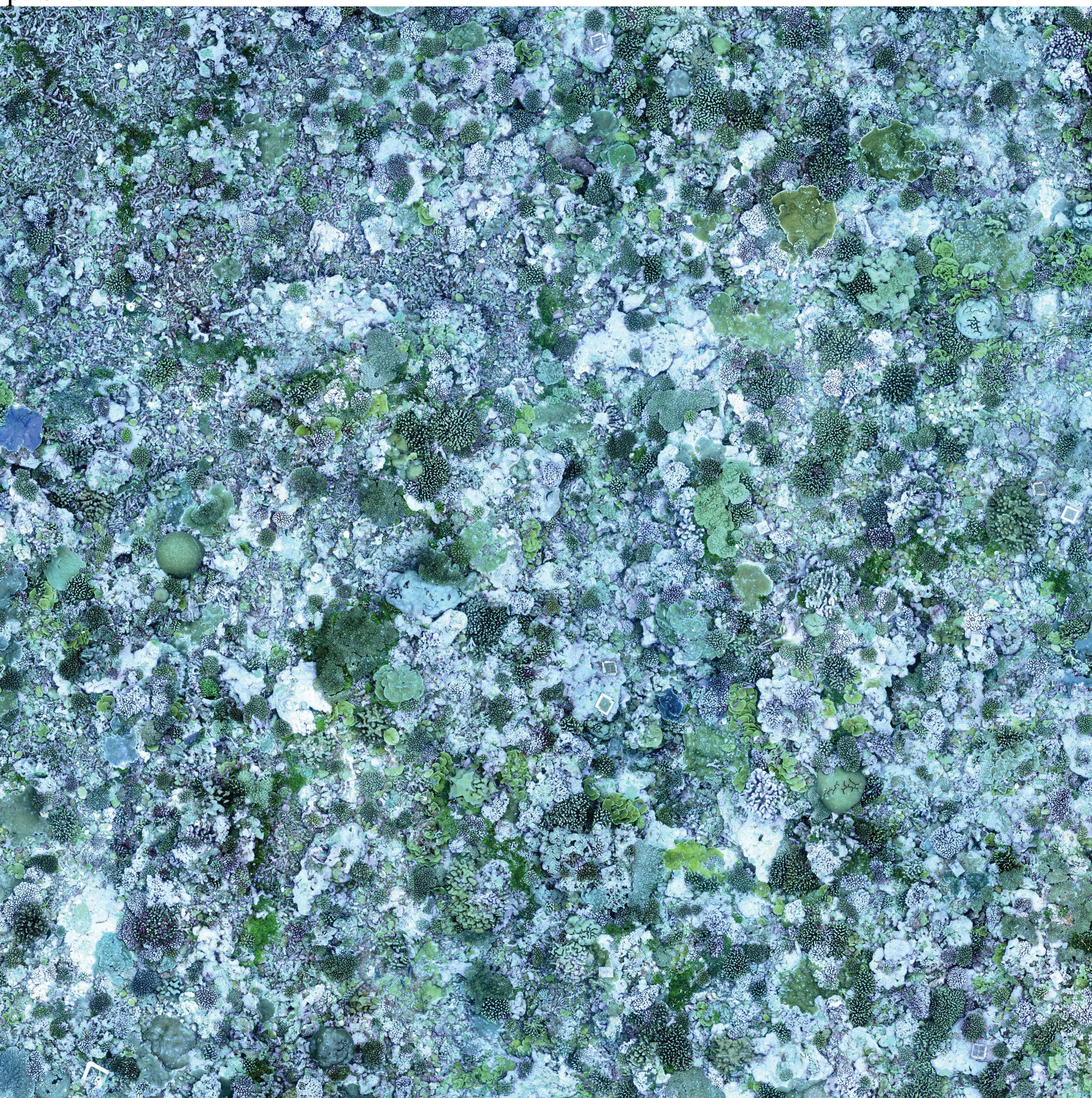












Supplemental Table 1. Palmyra coral species list, adapted from AIMS 2013 and Williams 2008. Functional morphology designations are based on the best available information (Highsmith 1982, Veron 2013) and the expert opinion of the authors. Note, the ‘foliose’ morphology in Veron 2013, has been denoted as ‘plating’ here, but the forms are equivalent.

Family	Genus-Species	Functional Morphology	Source
<i>Acroporidae</i>	<i>Acropora acuminata</i>	Branching	Veron (2013)
<i>Acroporidae</i>	<i>Acropora cerealis</i>	Corymbose	Veron (2013)
<i>Acroporidae</i>	<i>Acropora clathrata</i>	Tabular	Veron (2013)
<i>Acroporidae</i>	<i>Acropora cytherea</i>	Tabular	Veron (2013)
<i>Acroporidae</i>	<i>Acropora elseyi</i>	Branching	Veron (2013)
<i>Acroporidae</i>	<i>Acropora formosa</i>	Branching	Veron (2013)
<i>Acroporidae</i>	<i>Acropora gemmifera</i>	Submassive	Veron (2013)
<i>Acroporidae</i>	<i>Acropora glauca</i>	Tabular	Veron (2013)
<i>Acroporidae</i>	<i>Acropora globiceps</i>	Submassive	Veron (2013)
<i>Acroporidae</i>	<i>Acropora hyacinthus</i>	Tabular	Veron (2013)
<i>Acroporidae</i>	<i>Acropora latistella</i>	Corymbose	Veron (2013)
<i>Acroporidae</i>	<i>Acropora nana</i>	Corymbose	Veron (2013)
<i>Acroporidae</i>	<i>Acropora nasuta</i>	Corymbose	Veron (2013)
<i>Acroporidae</i>	<i>Acropora nobilis</i>	Branching	Veron (2013)
<i>Acroporidae</i>	<i>Acropora palmerae</i>	Encrusting	Veron (2013)
<i>Acroporidae</i>	<i>Acropora retusa</i>	Submassive	Veron (2013)
<i>Acroporidae</i>	<i>Acropora robusta</i>	Branching	Veron (2013)
<i>Acroporidae</i>	<i>Acropora secale</i>	Corymbose	Veron (2013)
<i>Acroporidae</i>	<i>Acropora speciosa</i>	Branching	Veron (2013)
<i>Acroporidae</i>	<i>Acropora spicifera</i>	Tabular	Veron (2013)
<i>Acroporidae</i>	<i>Acropora subulata</i>	Tabular	Veron (2013)
<i>Acroporidae</i>	<i>Acropora valida</i>	Corymbose	Veron (2013)
<i>Acroporidae</i>	<i>Astreopora gracilis</i>	Submassive	Authors
<i>Acroporidae</i>	<i>Astreopora myriophthalma</i>	Submassive	Authors
<i>Acroporidae</i>	<i>Astreopora randalli</i>	Plating	Veron (2013)
<i>Acroporidae</i>	<i>Astreopora suggesta</i>	Submassive	Authors
<i>Faviidae</i>	<i>Barabattoia amicum</i>	Massive	Veron (2013)
<i>Fungiidae</i>	<i>Cycloseris cyclolites</i>	Free-living	Authors
<i>Faviidae</i>	<i>Cyphastrea microphthalma</i>	Massive	Veron (2013)
<i>Echinophyllia</i>	<i>Echinophyllia aspera</i>	Plating	Veron (2013)
<i>Echinophyllia</i>	<i>Echinophyllia sp.</i>	Plating	Veron (2013)
<i>Faviidae</i>	<i>Echinopora gemmacea</i>	Plating	Veron (2013)
<i>Faviidae</i>	<i>Echinopora lamellosa</i>	Plating	Veron (2013)
<i>Faviidae</i>	<i>Favia matthaii</i>	Massive	Veron (2013)
<i>Faviidae</i>	<i>Favia pallida</i>	Massive	Veron (2013)
<i>Faviidae</i>	<i>Favia stelligera</i>	Submassive	Veron (2013)
<i>Faviidae</i>	<i>Favites abdita</i>	Submassive	Authors

<i>Faviidae</i>	<i>Favites flexuosa</i>	Submassive	Veron (2013)
<i>Faviidae</i>	<i>Favites halicora</i>	Massive	Veron (2013)
<i>Faviidae</i>	<i>Favites pentagona</i>	Submassive	Veron (2013)
<i>Faviidae</i>	<i>Favites russelli</i>	Encrusting	Veron (2013)
<i>Fungiidae</i>	<i>Fungia concinna</i>	Free-living	Authors
<i>Fungiidae</i>	<i>Fungia fungites</i>	Free-living	Authors
<i>Fungiidae</i>	<i>Fungia granulosa</i>	Free-living	Authors
<i>Fungiidae</i>	<i>Fungia paumotensis</i>	Free-living	Authors
<i>Fungiidae</i>	<i>Fungia repanda</i>	Free-living	Authors
<i>Fungiidae</i>	<i>Fungia scutaria</i>	Free-living	Authors
<i>Agariciidae</i>	<i>Gardineroseris planulata</i>	Submassive	Authors
<i>Faviidae</i>	<i>Goniastrea pectinata</i>	Submassive	Veron (2013)
<i>Fungiidae</i>	<i>Halomitra pileus</i>	Free-living	Authors
<i>Fungiidae</i>	<i>Herpolitha limax</i>	Free-living	Authors
<i>Fungiidae</i>	<i>Herpolitha weberi</i>	Free-living	Authors
<i>Merulinidae</i>	<i>Hydnophora exesa</i>	Plating	Veron (2013)
<i>Merulinidae</i>	<i>Hydnophora microconos</i>	Massive	Veron (2013)
<i>Merulinidae</i>	<i>Hydnophora pilosa</i>	Encrusting	Veron (2013)
<i>Merulinidae</i>	<i>Hydnophora rigida</i>	Branching	Veron (2013)
<i>Faviidae</i>	<i>Leptastrea pruinosa</i>	Encrusting	Veron (2013)
<i>Faviidae</i>	<i>Leptastrea purpurea</i>	Encrusting	Veron (2013)
<i>Faviidae</i>	<i>Leptastrea transversa</i>	Encrusting	Veron (2013)
<i>Faviidae</i>	<i>Leptoria phrygia</i>	Submassive	Veron (2013)
<i>Agariciidae</i>	<i>Leptoseris explanata</i>	Encrusting	Veron (2013)
<i>Agariciidae</i>	<i>Leptoseris incrustans</i>	Encrusting	Veron (2013)
<i>Agariciidae</i>	<i>Leptoseris mycetoseroides</i>	Plating	Veron (2013)
<i>Agariciidae</i>	<i>Leptoseris scabra</i>	Encrusting	Veron (2013)
<i>Mussidae</i>	<i>Lobophyllia corymbosa</i>	Massive	Veron (2013)
<i>Mussidae</i>	<i>Lobophyllia hemprichii</i>	Massive	Veron (2013)
<i>Merulinidae</i>	<i>Merulina ampliata</i>	Plating	Veron (2013)
<i>Faviidae</i>	<i>Montastrea annuligera</i>	Massive	Veron (2013)
<i>Faviidae</i>	<i>Montastrea curta</i>	Massive	Veron (2013)
<i>Acroporidae</i>	<i>Montipora aequituberculata</i>	Plating	Veron (2013)
<i>Acroporidae</i>	<i>Montipora capitata</i>	Encrusting	Veron (2013)
<i>Acroporidae</i>	<i>Montipora dilatata</i>	Encrusting	Veron (2013)
<i>Acroporidae</i>	<i>Montipora efflorescens</i>	Encrusting	Authors
<i>Acroporidae</i>	<i>Montipora flabellata</i>	Plating	Veron (2013)
<i>Acroporidae</i>	<i>Montipora foveolata</i>	Submassive	Veron (2013)
<i>Acroporidae</i>	<i>Montipora hoffmeisteri</i>	Encrusting	Veron (2013)
<i>Acroporidae</i>	<i>Montipora informis</i>	Encrusting	Veron (2013)
<i>Acroporidae</i>	<i>Montipora monasteriata</i>	Plating	Veron (2013)
<i>Acroporidae</i>	<i>Montipora patula</i>	Plating	Veron (2013)
<i>Acroporidae</i>	<i>Montipora tuberculosa</i>	Plating	Veron (2013)

<i>Acroporidae</i>	<i>Montipora verrilli</i>	Encrusting	Veron (2013)
<i>Acroporidae</i>	<i>Montipora verrucosa</i>	Plating	Veron (2013)
<i>Pectiniidae</i>	<i>Oxypora lacera</i>	Plating	Veron (2013)
<i>Agariciidae</i>	<i>Pachyseris speciosa</i>	Plating	Veron (2013)
<i>Agariciidae</i>	<i>Pavona cactus</i>	Plating	Veron (2013)
<i>Agariciidae</i>	<i>Pavona clavus</i>	Submassive	Veron (2013)
<i>Agariciidae</i>	<i>Pavona duerdeni</i>	Submassive	Veron (2013)
<i>Agariciidae</i>	<i>Pavona explanulata</i>	Submassive	Veron (2013)
<i>Agariciidae</i>	<i>Pavona frondifera</i>	Plating	Veron (2013)
<i>Agariciidae</i>	<i>Pavona gigantea</i>	Massive	Veron (2013)
<i>Agariciidae</i>	<i>Pavona maldivensis</i>	Submassive	Veron (2013)
<i>Agariciidae</i>	<i>Pavona varians</i>	Encrusting	Veron (2013)
<i>Agariciidae</i>	<i>Pavona venosa</i>	Encrusting	Veron (2013)
<i>Faviidae</i>	<i>Platygyra daedalea</i>	Massive	Veron (2013)
<i>Faviidae</i>	<i>Platygyra pini</i>	Massive	Veron (2013)
<i>Faviidae</i>	<i>Platygyra sp</i>	Massive	Authors
<i>Euphyllidae</i>	<i>Plerogyra sinuosa</i>	Massive	Veron (2013)
<i>Pocilloporidae</i>	<i>Pocillopora damicornis</i>	Corymbose	Authors
<i>Pocilloporidae</i>	<i>Pocillopora elegans</i>	Corymbose	Authors
<i>Pocilloporidae</i>	<i>Pocillopora eydouxi</i>	Corymbose	Veron (2013)
<i>Pocilloporidae</i>	<i>Pocillopora ligulata</i>	Corymbose	Authors
<i>Pocilloporidae</i>	<i>Pocillopora meandrina</i>	Corymbose	Authors
<i>Pocilloporidae</i>	<i>Pocillopora molokensis</i>	Corymbose	Authors
<i>Pocilloporidae</i>	<i>Pocillopora verrucosa</i>	Corymbose	Authors
<i>Pocilloporidae</i>	<i>Pocillopora zelli</i>	Branching	Veron (2013)
<i>Poritidae</i>	<i>Porites arnaudi</i>	Plating	Veron (2013)
<i>Poritidae</i>	<i>Porites brighami</i>	Submassive	Veron (2013)
<i>Poritidae</i>	<i>Porites lichen</i>	Plating	Veron (2013)
<i>Poritidae</i>	<i>Porites lobata</i>	Massive	Veron (2013)
<i>Poritidae</i>	<i>Porites lutea</i>	Massive	Authors
<i>Poritidae</i>	<i>Porites rus</i>	Massive	Veron (2013)
<i>Poritidae</i>	<i>Porites sp. (massive)</i>	Massive	Authors
<i>Poritidae</i>	<i>Porites superfusa</i>	Encrusting	Authors
<i>Poritidae</i>	<i>Porites vaughani</i>	Encrusting	Veron (2013)
<i>Siderastreidae</i>	<i>Psammocora digitata</i>	Submassive	Veron (2013)
<i>Siderastreidae</i>	<i>Psammocora haimeana</i>	Encrusting	Authors
<i>Siderastreidae</i>	<i>Psammocora nierstraszi</i>	Submassive	Authors
<i>Siderastreidae</i>	<i>Psammocora profundacella</i>	Submassive	Veron (2013)
<i>Siderastreidae</i>	<i>Psammocora stellata</i>	Submassive	Veron (2013)
<i>Fungiidae</i>	<i>Sandalolitha dentata</i>	Free-living	Veron (2013)
<i>Astrocoeniidae</i>	<i>Stylocoeniella guentheri</i>	Encrusting	Veron (2013)
<i>Pocilloporidae</i>	<i>Stylophora pistillata</i>	Corymbose	Authors
<i>Dendrophylliidae</i>	<i>Turbinaria reniformis</i>	Plating	Veron (2013)

ESM Table 1 References

AIMS (2013) Coral Fact Sheets: Search By Map.

<http://coral.aims.gov.au/info/spatial.jsp>

Highsmith RC (1982) Reproduction by fragmentation in corals. *Mar Ecol Prog Ser*

7:207-226

Veron J (2013) *Corals of the World*. Australian Institute of Marine Science, Townsville,

Australia

Williams GJ, Maragos JE, Davy SK (2008) Characterization of the coral communities at

Palmyra Atoll in the remote Central Pacific Ocean. *Atoll Res Bull* 584:1-29